Fall 12-17-2011

Synthesis and Applications of Luminescent Quantum Dots in Bioassays

Venkata Ramana Kethineedi
University of New Orleans

Synthesis and Applications of Luminescent Quantum Dots in Bioassays

A Dissertation

Submitted to the Graduate Faculty of the
University of New Orleans
in partial fulfillment of the
requirements for the degree of

Doctor of Philosophy
in
Chemistry

by

Venkata Ramana Kethineedi

Bachelor of Science. Andhra University, India, 2000
Master of Science. Andhra University, India, 2002

December, 2011

Dedication

I would like to dedicate this dissertation to my beloved parents Narasimha Rao Kethineedi, Late Samantaka Mani Kethineedi, my wife Naga Vijayalaxmi Abbaraju, and my daughter Shriya Kethineedi.

Acknowledgements

I would like to express my sincere gratitude to my research advisors, Dr. Zeev Rosenzweig and Dr. Matthew A. Tarr for their support, guidance, and encouragement during graduate school. Their invaluable suggestions, guidance helped me a lot throughout my duration here in University of New Orleans.

I would also like to express my gratitude to my advisory committee members Dr. Richard B. Cole, Dr. Gabriel Caruntu, Dr. Ferdinand P. Poudeau, and Dr. John B. Wiley for their valuable comments and suggestions throughout my graduate research.

I thank Dr. Jibao He from Tulane University for the cryo-transmission electron microscopy analysis and Dr. Bob Cao from Dr. Weilie Zhou group for transmission electron microscopy analysis. I thank all my past and present research group members especially Lifang, Ariel and Ashley for their advice, help, and friendship. My sincere thanks to all the faculty and staff in the department of chemistry and the Advanced Materials and Research Institute (AMRI) for their support.

I am thankful to my dear family and friends for always being there for me through thick and thin. I thank my sisters Saraswathi, Syamala, and Sailaxmi; my brother-in-laws Tagore, Sambashiva Rao, and Prasad; my brother Venkata Rao; my sister-in-law Padmavathi; and also my amazing nieces Bharathi, Srivani, Yasaswini, and Hasini. I thank my in-laws Jogeswara Prasad Abbaraju and Hemalatha Abbaraju. Last but not least my best buddies Durga Rao and Sudheer.

I would like to thank my financial support from DOD/DARPA grant HR0011-07-1-0032, NSF grant CHE-0717526, and the LA Board of Regents grant LEQSF (2007-12)-ENH-PKSFI-PRS-04.

Table of Contents

List of Figures

List of Schemes

.

Abstract

Luminescent quantum dot (QD) based probes have gained significance in the last decade for optical imaging of cells, tissues and in bioassays as alternatives to conventional organic fluorophores. The main objective of my PhD dissertation was to develop luminescent quantum dot based bioassays for real time monitoring of enzyme activity and simultaneous detection of several biomarkers. The quantum dot based bioassays developed will be potential tools in identification and diagnosis of several ailments that interfere with normal living conditions of human beings.

In Chapter 2 new liposome encapsulated quantum dot based fluorescence resonance energy transfer (FRET) probes have been fabricated and characterized for monitoring the enzymatic activity of phospholipase A_2. The probes were able to detect the enzyme activity as low as 0.0075 U/mL (PLA_2 = 1500 U/mg) in 30 min. Further these FRET probes were also used to screen the inhibition efficiencies of phospholipase A_2 inhibitors.

Chapter 3 focuses on the first time synthesis and characterization of liposome encapsulated InP/ZnS quantum dots while preserving the integrity of the liposomes. Results from the experiments to assess photostability and effect of pH on the optical properties of InP/ZnS QD-liposomes showed greater advantages over InP/ZnS quantum dots demonstrating their utility as a potential tool in several biological applications such as bio imaging, bioassays and in immunoassays.

Chapter 4 discusses the development of fluorescence based immunoassay for simultaneous detection of the cardiac biomarkers troponin T and troponin I using CdSe/ZnS quantum dots. The assay achieved a detection limit was 0.1 pg/mL for both biomarkers troponin

T and I. The method was highly specific for the both the biomarkers with no observed cross reactivity. The multiplex assay was able to detect two biomarkers simultaneously that will yield a high throughput diagnostic tool for heart attack.

A similar method discussed as above was used in chapter 5 for the simultaneous detection of atherosclerosis biomarkers. The detection limits achieved in this study are comparable to the detection limits of the biomarkers reported so far. Incorporation of QDs in silica beads before conjugation to antibodies might improve detection limits that will also improve risk assessment.

Key words: Quantum dots, Liposomes, FRET, Phospholipase A_2, QD-liposomes, Multiplexing, Myocardial Infarction, Troponins, Atherosclerosis, biomarkers, biosensors, immunoassay.

Chapter 1

Introduction

1.1 Objectives and Aims

The main objective of my PhD dissertation was to develop luminescent quantum dot based bioassays for real time monitoring of enzyme activity and simultaneous detection of several biomarkers. Luminescent quantum dots are potential alternatives to conventional organic fluorophores as they offer several advantages particularly broad absorption range with narrow symmetric emission spectrum. These advantages allows for simultaneous detection of multiple color quantum dots upon illumination with single light source that in turn can be used to analyze several analytes at the same time. My research work was specifically aimed at: i) fabrication and characterization of liposome encapsulated quantum dots and using them as fluorescence resonance energy transfer (FRET) based probes to monitor phospholipase A_2 enzyme activity ii) synthesis and characterization of cadmium free InP/ZnS quantum dots and encapsulating them with liposomes iii) development of a fluorescence immunoassay for the simultaneous detection of heart attack biomarkers troponin T and troponin I, and iv) further use the same method to detect atherosclerosis biomarkers.

1.2 Significance

The majority of studies reported so far for monitoring the enzyme activity of phospholipase A_2 are focused on the use of fluorophores. However the fluorophores are associated with several chemical and photo physical limitations like broad emission spectra, poor photostability, and low quantum yields. As alternatives to conventional organic fluorophores luminescent quantum dots have received great interest in the last decade for optical imaging of

cells, tissues and in bioassays. The first project was to develop liposome encapsulated quantum dot based FRET probes for monitoring phospholipase A_2 enzyme activity and to screen the inhibition efficiencies of phospholipase A_2 inhibitors. This method demonstrates the possibility to multiplex the assay in a 96 well plate and screen a large number of inhibitors simultaneously. Recently, focus has been shifted to the synthesis of cadmium free quantum dots due to cytotoxicity associated with cadmium though they are known to exhibit high quantum yields. InP quantum dots are more popular because they are less cytotoxic and exhibit a wide emission range from UV to NIR range of the electromagnetic spectrum which makes them ideal candidates for *in vivo* applications as opposed to CdSe quantum dots. For the first time InP/ZnS quantum dots were encapsulated with liposomes which not only enhance the optical properties of the quantum dots but also make them biocompatible. The next two projects were aimed at multiplexing quantum dots to develop fluorescence based immunoassays for simultaneous detection of biomarkers that play crucial role in heart attack and atherosclerosis. The ability of detecting the biomarkers simultaneously in a single assay reduces cost, saves time and improves the assessment of risk.

1.3 Quantum Dots

Luminescent semiconductor nanocrystalline particles or quantum dots (QDs) are composed of elements from groups II–VI (CdS, CdSe, CdTe, ZnO, ZnS, ZnSe), III–V (InP, InAs, GaP, GaN, GaAs), and IV-VI (PbS, PbSe, PbTe) of the periodic table. The nanocrystals usually have diameters ranging from 2-10 nm. The exciton Bohr radius defined as the average distance between bound electron-hole pair is confined in quantum dots in all three dimensions. Hence the nanoparticles have characteristics between bulk semiconductors and discrete molecules. This phenomenon is called the quantum-confinement effect. Quantum confinement

causes increased stress on the exciton that result in increased energy of the emitted photon. The smaller the QDs, the less room for exciton separation, and more energy is required to form the exciton and hence they emit at lower wavelengths (Scheme 1.1).

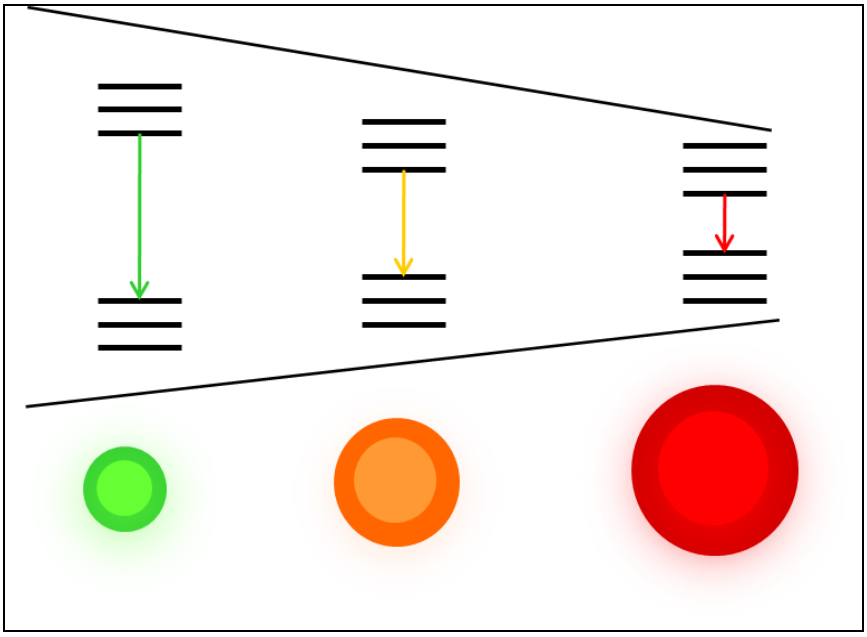

Scheme 1.1 Schematic representation of electronic structure of quantum dots due to quantum confinement.

Because of the quantum confinement effect, QDs exhibit unique optical properties that have several advantages over conventional fluorophores. The exceptional brightness of QDs comes from a combination of efficient light absorption, large extinction coefficient and high quantum yields up to 85%.[1] QDs exhibit high photostability with regard to bleaching compared to conventional fluorophores enabling highly sensitive detection and long observation times in fluorescence microscopy.[2] QDs also have narrow emission spectra and a large Stokes shift, which is the difference between the wavelength of absorbed and emitted light.[3] This large shift allows easy separation of the fluorescence signal of QDs from excitation light source and multi-color imaging without crosstalk between different detection channels in fluorescence

microscope. Additionally, QDs of different emission maxima can be excited by one single wavelength, which eliminates the need for numerous excitation sources in the instrumental setup.[4] Quantum dots enable time-resolved detection as they have relatively long fluorescence lifetime (20–50 ns) that significantly increases the signal-to-background ratio relative to cell auto fluorescence (<5 ns).[5]

1.3.1 Synthesis of quantum dots

Similar to traditional chemical processes colloidal semiconductor nanocrystals are synthesized from precursor compounds dissolved in solutions.[6] The synthesis of colloidal quantum dots is based on a three component system composed of precursors, organic surfactants, and solvents. During synthesis size tuning of QDs is achieved by controlling the relative concentrations, duration, temperature, and ligand molecules used. CdSe is a popularly used semiconductor material because of its tunable absorption energies throughout the visible region, availability of precursors for synthesis, and simple crystallization. The often used method to synthesize CdSe quantum dots is pyrolysis of organometallic precursors CdO, $Cd(Ac)_2$ and $CdCO_3$.[7-9] The excited electron or hole can be trapped by surface defects, such as vacancies, local lattice mismatches, and dangling bonds that lead to the nonradiative recombination, which will result in the low quantum yield.[10] A thin layer of high band gap semiconductor material like ZnS is grown on the surface of quantum dots to decrease the effect of surface defects and to protect surface atoms from oxidation and other chemical reactions.[11-13] This process described as surface passivation improves chemical stability and photostability, increases the emission quantum yield, and reduces the toxicity by preventing leakage of Cd or Se to the surrounding environment.

CdSe/ZnS quantum dots have little future in the biomedical field due to their cytotoxicity, though they have high fluorescence quantum yields.[14, 15] InP quantum dots made from III-V

semiconductor materials are very useful because of low toxicity and greater quantum size effects.[16-18] InP/ZnS core/shell quantum dots can be synthesized to emit into the near infrared region that is ideal for *in vivo* applications. Even though InP/ZnS quantum dots are promising for future applications, the studies of InP/ZnS QDs are less advanced due to their more difficult synthetic chemistry and low quantum yields.[19] Initially the quantum yields of InP nanocrystals were improved from 20–40% by HF etching.[14] In 2007 Peng *et al* reported InP/ZnS core–shell quantum dot synthesis using fatty amine for which the quantum yields reached up to 40%.[20] The synthesis was similar to that for CdSe quantum dots and used relatively low reaction temperatures below 200°C and used indium acetate and myristic acid as precursors. A one step and one pot method for the synthesis of highly luminescent InP with QYs of up to 30% and InP/ZnS QDs with QYs of up to 60% was reported by Nann *et al*.[21] More recently, Reiss *et al* synthesized InP/ZnS QDs in a single step with quantum yield up to 70%.[22]

1.3.2 Bioconjugation of quantum dots

The high quality quantum dots synthesized in organic solvents are insoluble in water, do not have functional groups for bioconjugation and are thus non-biocompatible. In order to make them biocompatible the hydrophobic coating ligands of luminescent quantum dots must be replaced with bifunctional hydrophilic capping ligands or must be further coated with an amphiphilic layer to impart water solubility and potential bioconjugation sites (Figure 1.1). These treatments will facilitate their applications in biological systems. Various methods for the improvement of quantum dot biocompatility and stability have been developed during the past few years. One of the most commonly used methods is ligand exchange that involves the replacement of hydrophobic ligands with bifunctional ligands in which one end binds to the inorganic QD surface and the other end provides hydrophilicity. The hydrophobic capping

ligands are often exchanged with thiol functionalized compounds such as mercaptoalkanoic acids.[23-27] The thiol binding to the ZnS surface is not very strong resulting quantum dots aggregation over time.[28] This instability is the limitation of capping quantum dots with thiol containing ligands.

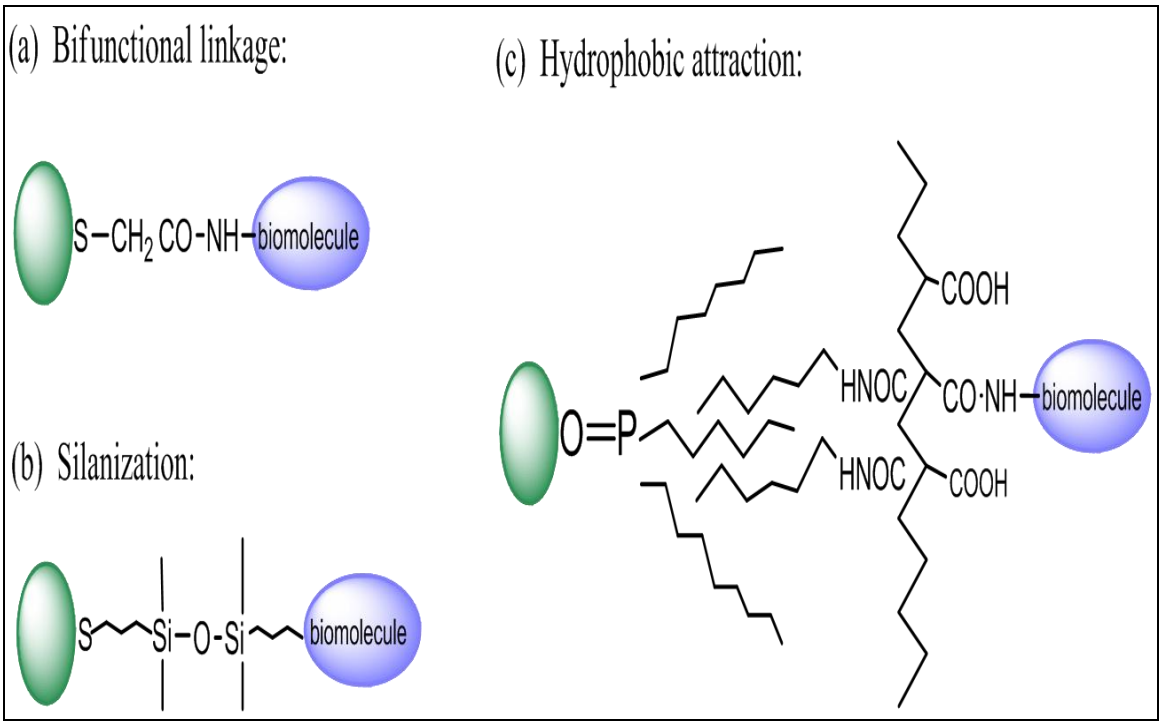

Figure 1.1 Representation of different approaches for conjugation of quantum dots to biomolecules.

Another method is silica encapsulation, which involves the growth of a silica layer on the surface of the quantum dots. Functional groups –SH and $–NH_2$ on the surface of organosilane molecules enable bioconjugation.[29, 30] However, the method is very laborious, difficult to reproduce, and the silica layer may be hydrolyzed.[31] Yet another method is coating QDs with an amphiphilic polymer and phospholipids. This approach is achieved by forming the layer on the QD surface via hydrophobic interactions with the hydrophobic ligands.[32] The polymer has a hydrophilic exterior that makes the quantum dots soluble in aqueous solutions. However, this

method limits many biological applications such as FRET measurements and endocytosis since the size of the coated quantum dots becomes much larger.[31] In addition to the above mentioned methods there are several methods for developing water-soluble, biocompatible quantum dots. Synthesizing high quality water soluble and stable quantum dots still remains an important area of research in quantum dot based nanobiotechnology.

1.3.3 Biological application of quantum dots

Quantum dots are new generation of fluorescent probes that are promising tools in biological applications as an alternative to commonly used organic fluorophores due to their unique optical and chemical properties. Water soluble quantum dots have been extensively used in protein assays,[33-35] hybridization assays,[36-38] and fluorescence resonance energy transfer (FRET) based bioassays.[39-41] They have also been used as labels for *in vitro*[42-44] and *in vivo*[45-47] imaging applications.

1.3.3.1 Quantum dots as FRET donors

Fluorescence resonance energy transfer (FRET) is a non radiative energy transfer from the donor in excited state (D) to an acceptor (A) (Scheme 1.2). The energy transfer is a result of long-range dipole-dipole interactions between the donor and acceptor.[48, 49] Thus the fluorescence intensity and lifetime of the donor is decreased and the acceptor fluorescence intensity is increased. The rate of energy transfer depends on the following three important conditions: (i) spectral overlap between the absorption spectrum of the acceptor and the fluorescence emission spectrum of the donor; (ii) close proximity between the donor and acceptor molecules (typically 0.1-10 nm); and (iii) approximately parallel donor and acceptor transition dipole orientations. FRET with optical microscopy, is a powerful photo-physical technique because of its high sensitivity to changes in distance and relative dipole orientations between donor and acceptor.

FRET has been widely used to study protein-protein interactions, diffusion dynamics, protein conformational changes, and detecting nucleic acids and peptides.[50-52]

Conventional fluorescent organic molecules have been extensively used as FRET pairs due to their small size, compatibility with covalent coupling, and relatively large detectable optical signal. However, organic fluorophores as FRET probes have narrow absorption spectra of the acceptors, broad emission spectra of the donors, and low photo bleaching thresholds. Quantum dots provide a potential solution to the above problems. QDs have been investigated as FRET donors in place of traditional organic dyes because of their high photostability and unique spectral properties.[53-55]

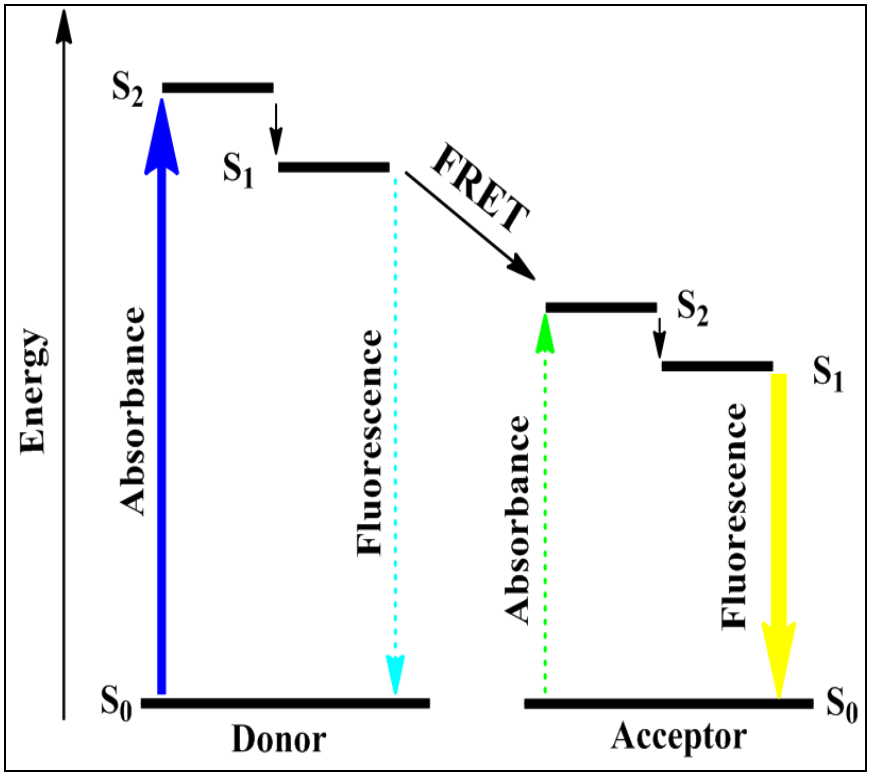

Scheme 1.2 Schematic illustration of fluorescence resonance energy transfer principle.

Several research groups reported FRET between quantum dots and organic dyes.[56-58] Willard *et al* developed quantum dots as FRET donors in a protein-protein binding assay.[59] Quantum dots were conjugated to bovine serum albumin as FRET donors and

tetramethylrhodamine was bound to the protein as the FRET acceptors. In 2003, Medinta *et al* first reported quantum dots based self-assembled nanoscale FRET biosensors for maltose detection by coating CdSe/ZnS quantum dots with maltose binding protein molecules.[60] Since then, quantum dots based FRET biosensors have been reported to detect TNT,[61] toxins,[62] β-lactamase,[63] collagenase,[64] DNA,[65] RNA,[66] and protein.[67]

1.3.3.2 Quantum dots in immunoassays

Immunolabeling is one of the widely explored bioapplications of quantum dots. QDs in this category are more advanced than organic fluorophores due to their unique features like photostability and multiplexing capability. The majority of the studies reported so far demonstrated the use of QDs in target detection of various cancer markers within cells.[68-70] These markers have been of pathological interest because they were either associated with transformations or metastasis and were indicative of both the cancer and its progress. Other uses include monitoring intracellular viruses, typing of blood cell antigens and visualization of drug therapy effects in cellular metabolism.[71, 72] Wilson *et al* used magnetic microspheres encoded with three different quantum dots for the multiplexed detection of three different explosives.[73] Gao *et al* described the use of tri-block copolymer coated quantum dots to perform *in vivo* targeting and imaging of human prostate cancer cells.[74] In 2007 Yezhelyev *et al* used a hetero-bifunctional cross linker to covalently attach multicolored QDs to antibodies that were used to perform in situ molecular profiling of five different breast cancer biomarkers.[75] Zhang *et al* in 2008, synthesized high quality multicolor amphiphilic copolymer coated CdSe/CdS/$Cd_{0.5}Zn_{0.5}S$/ZnS QDs and used them for detecting human and rabbit antigens.[76] Recently, Rauf *et al* developed QD bar coded magnetic microspheres based multiplexed immunoassays via a layer-by-layer technique utilizing unique streptavidin/biotin interaction.[77]

1.4 Liposomes

Liposomes are spherical artificial phospholipid vesicles that are used as models for artificial cells, making them versatile tools in biology, biochemistry and medicine. Liposomes form spontaneously when introduced into aqueous media. Similar to cell membranes, the spherical phospholipids self-assemble to form a bilayer in which the phospholipid head groups point toward the internal and external aqueous phases of the vesicles and the tails are enclosed in a hydrophobic region. The liposomes are classified according to the compartmentalization of aqueous regions between bilayers. In unilamellar liposomes, the aqueous compartment is separated from the external solution by only one membranal bilayer. Unilamellar liposomes are further classified based on the size. Small unilamellar liposomes (SUV) have 100 nm average diameters while large unilamellar liposomes (LUV) have a maximal size of up to 10 μm. Multilamellar liposomes, consist of more than one bilayer each separated by an aqueous compartment. The size, lamellarity (unilamellar or multilamellar) and lipid composition of the bilayers influence many of the important properties like the fluidity, permeability, stability and structure that can be controlled and customized to serve specific needs.

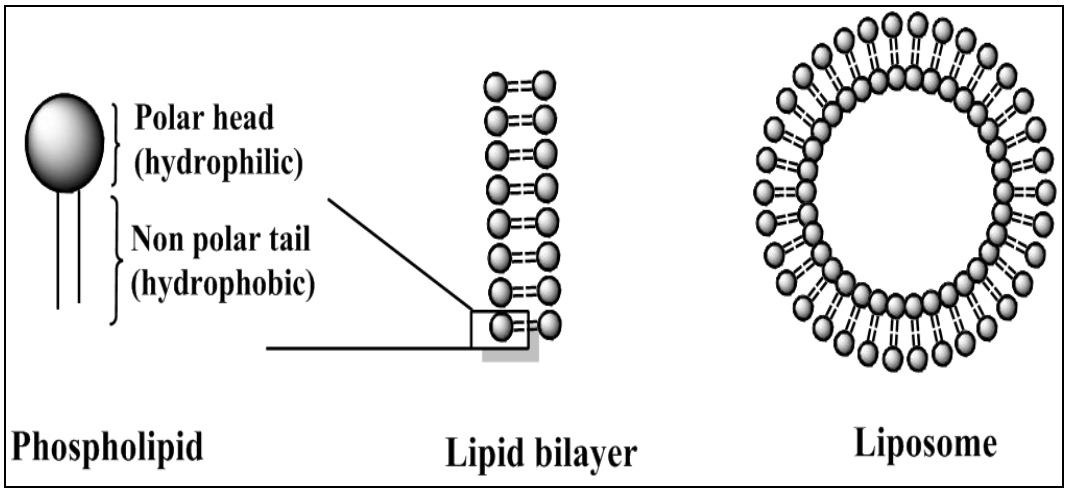

Scheme 1.3 Schematic representation of liposome structure.

There are numerous approaches to prepare liposomes such as the injection method, the dehydration/rehydration method, and the freeze thaw method. The synthesized liposomes are characterized by light scattering, electronic or atomic force microscopy, and capillary electrophoresis. Static and dynamic light scattering measurements are used to characterize the size, size distribution, and shape of vesicles. The morphology of liposomes can be further characterized by transmission electron microscopy (TEM) and atomic force microscopy (AFM).[78] The light scattering techniques provide average values of the physical characteristics of liposome suspensions, while the TEM and AFM approaches provide information on individual liposomes that may or may not represent the entire liposome population. Capillary electrophoresis can also be used to obtain qualitative and quantitative information about the size to charge ratio of liposomes as they are very stable under high electric fields.[79, 80]

Liposomes offer exceptional engineering ability due to their physicochemical characteristics such as vesicle size, structure and surface versatility that can be modified with established methods. They have been used to encapsulate and deliver oral vaccines as well as anti cancer, anti inflammatory and hormonal drugs.[81, 82] Liposomes can entrap large amounts of fluorescent nanoparticles while providing high biocompatibility, and thus enhancing the effectiveness of nanoparticles for detection *in vivo* and *in vitro*.[83] Recently, fabrication of QD-liposome vesicles gained importance as promising tools in nano-biotechnology. QDs have been incorporated into phospholipid liposomes making them biocompatible while retaining photoluminescence. The liposome quantum dot complexes have been applied as fluorescent markers in immunoassays[84] and also to deliver QDs into cytosol of oncogenic brain cells via lipid mediated fusion with the cell membrane.[85] QD-liposomes have also been used for tumor

cell-targeting, imaging, and drug delivery functions in human epidermal growth factor receptor 2 over expressing tumor cells via receptor-mediated endocytosis.[86]

1.5 Phospholipases

Phospholipases are lipolytic enzymes that catalyze the hydrolysis of membrane phospholipids. Their classification is based on cleavage of the bond in phospholipids (scheme 1.4). Phospholipase A_1 and A_2 selectively remove fatty acids from the SN1 and SN2 positions respectively. Phospholipase B cleaves both SN1 and SN2 acyl bonds. Phospholipase C cleaves the bond between glycerol and phosphate and phospholipase D hydrolyzes the amino alcohol moiety from a phospholipid.

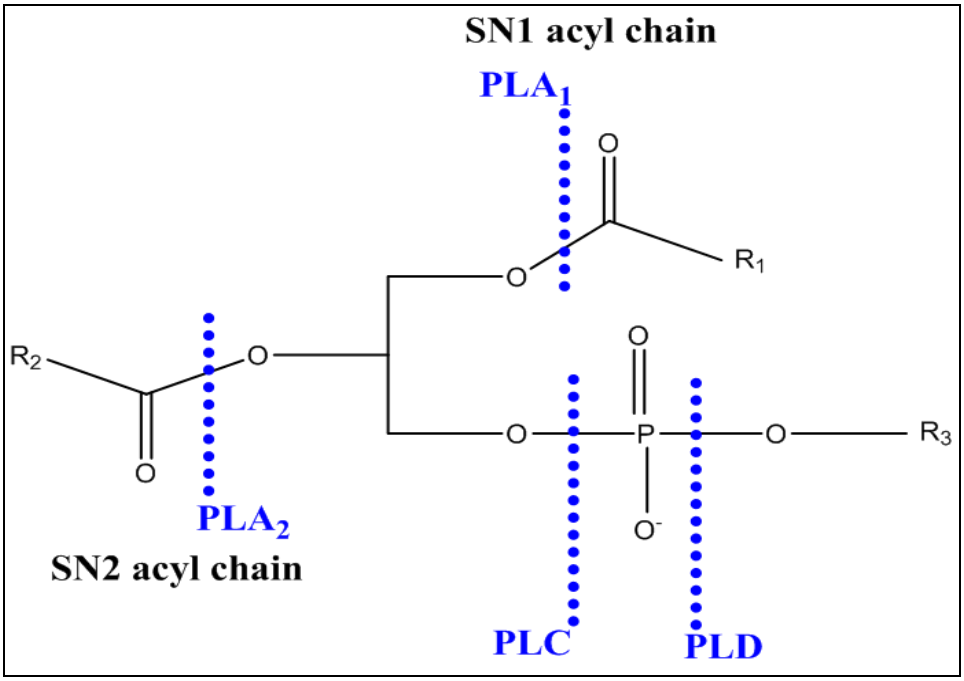

Scheme 1.4 Schematic illustration of phospholipase cleavage sites.

Phospholipase A_2 (PLA_2) are small proteins (ca. 14 kDa) containing multiple disulfide bridges. The water-soluble forms of these extracellular enzymes are the most thoroughly studied and have been used as model systems for the less tractable, membrane-bound forms, as well as for the study of enzyme catalysis at lipid/water interfaces.[87] PLA_2 can be found in membrane-

associated and soluble forms in almost all cell types, where they are believed to play an important role in the normal biosynthesis and turnover of membrane phospholipids,[88, 89] cellular signaling,[90] and protection of membranes from peroxidation damage.[91] In addition, PLA_2 enzymes have also been associated with the pathogenesis of numerous clinical inflammatory processes.[92, 93] PLA_2 catalyzes the hydrolysis of the SN2 fatty acyl ester bond of phospholipids to yield arachidonic acid and lysophospholipid.

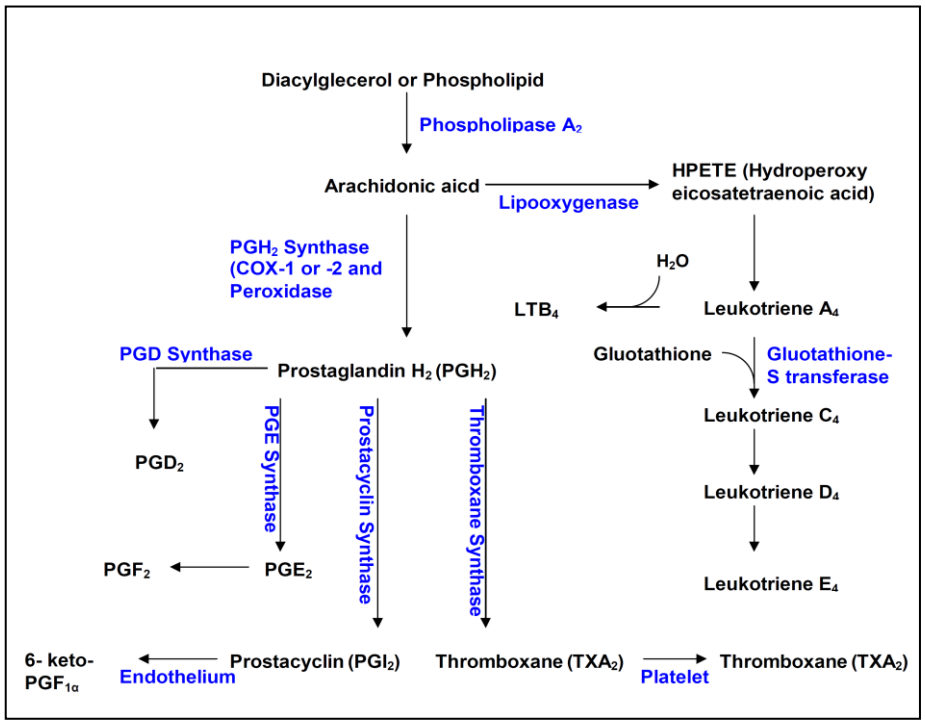

Figure 1.2 Biosynthesis pathways of eicosanoids from arachidonic acid.

Arachidonic acid is converted by the cyclo-oxygenase (COX-1 or -2) pathway to produce a variety of prostaglandins and thromboxanes (Figure 1.2). Specific prostaglandins can cause constriction or dilation in vascular smooth muscle cells, cause aggregation or disaggregation of platelets, control hormone regulation, control cell growth, decrease intraocular pressure, decrease micro vascular permeability and cause platelet aggregation that can influence the course of inflammatory episodes.[94] Thromboxane is a vasoconstrictor, a potent hypertensive agent, and

facilitates platelet aggregation. Leukotrienes play a powerful role in asthma, bronchoconstriction, and other inflammatory responses. Also they play a role in cardiovascular and neuropsychiatric illnesses. Lysophospholipids, another product of PLA_2 enzymatic activity, produce platelet activating factor, which causes a drop in blood pressure and reduced volume of blood pumped by the heart. These effects can lead to shock and possibly death. Thus the inhibition of phospholipase A_2 which in turn blocks the formation of arachidonic acid is of great significance.

1.6 Myocardial Infarction.

Myocardial infarction (MI) or heart attack is the interruption of blood supply to some parts of the heart muscles, causing cell death. This phenomenon occurs due the rupture of a vulnerable atherosclerotic plaque, which is a collection of unstable lipids and white blood cells especially macrophages in the wall of a coronary artery that leads to blockage. The restriction in blood supply and shortage in oxygen can lead to damage or death (*infarction*) of heart muscle tissue (*myocardium*) if left untreated for a long period of time. According to the World Health Organization (WHO), heart attack is the leading cause of death for both men and women worldwide. Every 34 seconds someone in the United States has a heart attack.[95]

The diagnosis of MI has been based on the "two out of three" criteria over several decades as defined by WHO, including typical chest pain symptoms that last for more than 20 minutes, changes in serial electrocardiogram, and increase in the serum level of creatine kinase-MB and troponins.[96] The WHO criteria have been refined in 2000 and recently in 2007 that gave more importance to cardiac biomarkers especially troponins.[97] According to this new criteria cardiac troponin elevation accompanied by any of the typical symptoms are the diagnosis for heart attack. Troponin is a complex of three regulatory muscle proteins troponin T (TnT), troponin I (TnI), and troponin C (TnC) that play crucial role in muscle contraction. Troponin I

binds to actin, troponin T binds to tropomyosin, and the third troponin C binds to calcium ions (Scheme 1.5). When calcium ions bind to troponin C, the troponin changes shape, forcing tropomyosin away from the actin filaments. This causes myosin cross-bridges to attach to actin, and thus enable contractions.[98] In the absence of calcium troponin C does not undergo conformational change and therefore muscles remain intact.

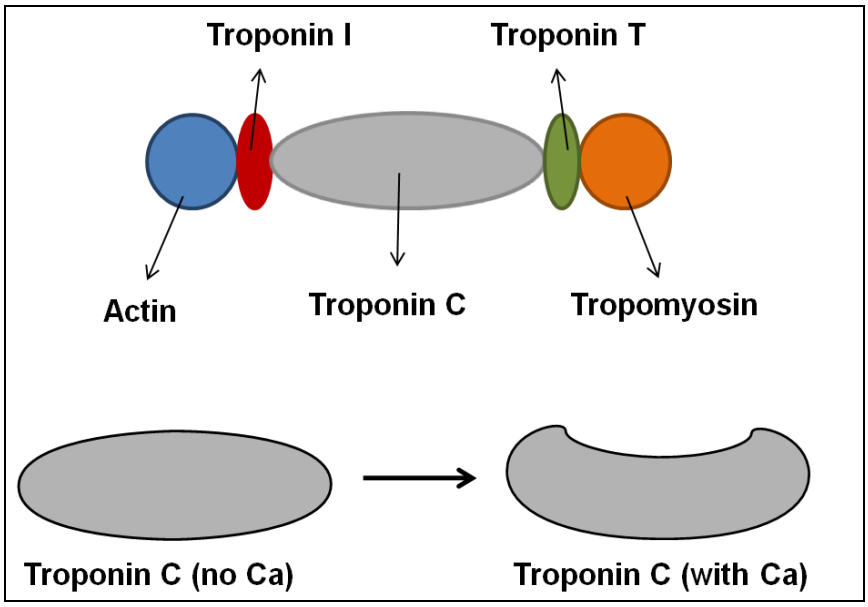

Scheme 1.5 Schematic representation of Troponin complex.

Cardiac and skeletal muscles contain both troponin T and I, however the amino acid sequences of the proteins are different.[99] Troponin C is shared by cardiac and skeletal muscles and therefore does not have cardiac specificity and is not used in assays for the diagnosis of cardiac injury. Under normal conditions troponin T and I levels are very low but the concentrations rise immediately following the heart attack. The release kinetics for both TnT and TnI are similar and release within 4-13 hr following myocardial damage.[100] Currently, several immunoassay methods are available commercially for the detection of troponin I and troponin T separately, most of them are based on ELISA and some of them based on fluoimmunoassay technique.[101-105] However, the current detection limits of troponin assays do not allow

demonstration of normal cardiac troponin in healthy controls.[106] Further lower detection limits with improved assay sensitivity and precision would improve risk assessment.

1.7 Atherosclerosis

Atherosclerosis is a condition that results in accumulation of fatty materials such as cholesterol causing the artery wall to increase in thickness. Atherosclerosis develops from low-density lipoproteins (LDL) that are oxidized by reactive oxygen species (ROS). LDL is in globular shape that carries cholesterol from the liver to cells. A number of reactions occur to repair the damage when oxidized LDL comes in contact with an artery wall, one such reaction is the response of the body's immune system by sending specialized white blood cells (macrophages and T-lymphocytes) to absorb the oxidized-LDL forming the specialized foam cells. Accumulation of foam cells in the artery wall leads to formation of plaque, which can constrict the blood vessels diameter. Although plaque can block blood flow, arteries respond to this blockage by increasing their size. Consequently, plaque formation is not necessarily harmful. However, some plaques become unstable and can rupture. Upon rupture, clot forming compounds can be released, resulting in acute blockage of blood flow that can cause localized tissue death. When such an event occurs in the heart, MI results. Blockages occurring in the brain result in stroke. Plaque can also harden through calcification, resulting in reduction of the blood flow and an increase in blood pressure.

Atherosclerosis is a chronic disease characterized by arterial lesions despite the lack of any symptoms for many years.[107] Atherosclerotic lesions or plaques are categorized as stable and unstable.[108] Stable atherosclerotic plaques are asymptomatic and are rich in extracellular matrix and smooth muscle cells while unstable plaques are rich in macrophages, and foam cells and are usually weak and prone to rupture. For a long time the diagnosis of cardiovascular disease in

humans was based on severe narrowing, stenosis that was detected using angiography and stress testing. Angiography is a conventional method of testing accumulated lipid-containing plaques in the artery or atheroma, which shows motion or still images of inner space of the artery but does not show atheroma within the arterial wall. All these methods are useful for diagnosis at later stages of atheroma i.e. narrowing of arterial walls but do not help early detection. The current most sensitive method, intravascular ultrasound detects and measures atheroma allowing complete and accurate assessment than angiography within living individuals. Due to limitation in cost and the method being body invasive, it is not used until after atheroma begins forming. On the other hand CT scans have been the most effective method for detecting calcification present in plaque however atheroma has to be advanced enough to have relatively large areas of calcification within them.

Recent research efforts have repeatedly shown the use of biomarkers involved in different stages of atherosclerosis like molecular proinflammatory biomarkers, plaque destabilization and plaque rupture biomarkers to predict future cardiovascular occurrences not only in healthy individuals, but also in patients with acute coronary syndrome.[109] Therefore testing patients for several of these markers will provide important information useful for predicting future occurrence of atherosclerosis. Thus my fourth project aims at detecting the three biomarkers monocyte chemoattractant protein-1 (MCP-1), interleukin 15 (IL-15), and interleukin 18 (IL-18) that play a significant role in two important stages of atherosclerosis, fatty streaks and plaque destabilization. MCP-1 is an important chemokine that is involved in regulated migration and infiltration of monocytes/macrophages whose effects are mainly mediated through β-chemokine receptors 2. In response to various cytokines, growth factors, and oxLDL[110] monocytes express MCP-1 and thus increase expression of MCP-1 in atherosclerotic lesions, particularly in

macrophage-rich areas.[111] In animal models, the extent of atherosclerosis and macrophage infiltration into the atherosclerotic lesion is evaluated based on the expression of MCP-1.[112] Interleukin 15 is another biomarker associated with atherosclerosis, it is a cytokine with structural similarity to IL-2. IL-15 is found in high levels in plasma of patients with coronary artery disease.[113] The expression of IL-15 is found exclusively in fibrolipid and lipid-rich plaques in complex foam cells.[114] The up regulation of IL-15 in atherosclerotic lesions, stimulates T lymphocytes.[115] IL-18, is another biomarker and proinflammatory cytokine that is widely expressed in various cell types. IL-18 enhances the expression of matrix metalloproteases (MMPs)[116-118] along with interferon eliciting helper T cell (Th1) immune response and these two abilities of IL-18 characterize it as a crucial and potent mediator of atherosclerotic plaque destabilization. In human atherosclerotic plaques, increased expression of IL-18 is seen in lesions prone to rupture, and is localized mainly in plaque macrophages.[119] In animal models, inhibition of IL-18 by IL-18 binding protein reduced atherosclerotic plaque development and progression supporting a proatherogenic role of IL-18.[120]

1.8 References

1) Peng, Z. A.; Peng, X. *J. Am. Chem. Soc.* **2001**, 123, 183–184.

2) Smith, A. M.; Nie, S. *Analyst* **2004**, 129, 672-677.

3) Bruchez Jr., M.; Moronne, M.; Gin, P.; Weiss, S.; Alivisatos, A. P. *Science* **1998**, 281, 2013–2016.

4) Jaiswal, J. K.; Mattoussi, H.; Mauro, J. M.; Simon, S. M. *Nat. Biotechnol.* **2003**, 21, 47–51.

5) Dahan, M.; Laurence, T.; Pinaud, F.; Chemla, D.S.; Alivisatos, A. P.; Sauer, M.; Weiss, S. *Opt. Lett.* **2001**, 26, 825–827.

6) Murphy, C. J. *Analytical Chemistry* **2002**, 520A-526A.

7) Murray, C. B.; Norris, D. J.; Bawendi, M. G. *J. Am. Chem. Soc.* **1993**, 115, 8701-8715.

8) Peng, Z. A.; Peng, X.; *J. Am. Chem. Soc.* **2001,** 123(1), 183-184.

9) Yu, W. W.; Qu, L.; Guo, W.; Peng, X. *Chem. Mater.* **2003,** 15(14), 2854-2860.

10) Dabbousi, B. O.; Rodriguez-Viejo, J.; Mikulec, F. V.; Heine, J. R.; Mattoussi, H.; Ober, R.; Jensen, K. F.; Bawendi, M. G. *J. Phys. Chem*. B **1997**, 101, 9463-9475.

11) Li, J. J.; Wang, Y. A.; Guo, W.; Keay, J. C.; Mishima, T. D.; Johnson, M. B.; Peng, X. *J. Am. Chem. Soc*. **2003**, 125, 12567-12575.

12) Mekis, I.; Talapin, D. V.; Kornowski, A.; Haase, M.; Weller, H. *J. Phys. Chem*. B **2003**,107, 7454-7464.

13) Malik, M. A.; O'Brien, P.; Revaprasadu, N. *Chem. Mater*. **2002**, 14, 2004-2010.

14) Talapin, D.; Gaponik, N.; Borchert, H.; Rogach, A.; Hasse, M.; Weller, H. *J. Phys. Chem. B* **2002,** 106, 12659-12663.

15) Xie, R.; Battaglia, D.; Peng, X. *J. Am. Chem. Soc.* **2007,** 129, 15432-15433.

16) Lucey, D. W.; MacRae, D. J.; Furis, M.; Sahoo, Y.; Cartwright, A. N.; Prasad, P. N. *Chem. Mater.* **2005,** 17, 3754-3762.

17) Bharali, D. J.; Lucey, D. W.; Jayakumar, H.; Pudavar, H. E.; Prasad, P. N. *J. Am. Chem. Soc.* **2005,** 127, 11264-11371.

18) Borchert, H.; Haubold, S.; Haase, M.; Weller, H. *Nano Letters* **2002,** 2, 151-154.

19) Battaglia, D.; Peng, X. G. *Nano Lett.* **2002**, 2, 1027-1030.

20) Xie, R. G.; Battaglia, D.; Peng, X. G. *J. Am. Chem. Soc.* **2007**, 129, 15432-15433.

21) Xu, S.; Ziegler, J.; Nann, T. *J. Mater. Chem.* **2008**, 18, 2653–2656.

22) Li, L.; Reiss, P. *J. Am. Chem. Soc.* **2008**, 130, 11588–11589.

23) Chan, W. C.; Nie, S. M., *Science* **1998,** 281, 2016-2018.

24) Qian, J.; Yong, K.-T.; Roy, I.; Ohulchanskyy, T. Y.; Bergey, E. J.; Lee, H. H.; Tramposch, K. M.; He, S.; Maitra, A.; Prasad, P. N. *The Journal of Physical Chemistry B* **2007,** 111, 6969-6972.

25) Chen, D.; Wang, G.; Li, J. *The Journal of Physical Chemistry C* **2007,** 111, 2351-2367.

26) Mattoussi, H.; Mauro, J. M.; Goldman, E. R.; Anderson, G. P.; Sundar, V. C.; Mikulec, F. V.; Bawendi, M. G, *J. Am. Chem. Soc.* **2000,** 122, 12142-12150.

27) Pathak, S.; Choi, S. K.; Arnheim, N.; Thompson, M. E., *J. Am. Chem. Soc.* **2001,** 123, 4103-4104.

28) Aldana, J.; Wang, Y. A.; Peng, S. *J. Am. Chem. Soc.* **2001,** 123, 8844-8850.

29) Gerion, D.; Pinaud, F.; Williams, S. C.; Parak, W. J.; Zanchet, D.; Weiss, S.; Alivisatos, A. P. *J. Phys. Chem. B* **2001,** 105, 8861-8871.

30) Nann, T.; Mulvaney, P. *Angew. Chem. Int. Ed.* **2004,** 43, 5393-5396.

31) Alivisatos, A. P.; Gu, W. W.; Larabell, C. *Annu. Rev. Biomed. Eng.* **2005,** 7, 55-76.

32) Pellegrino, T.; Manna, L.; Kudera, S.; Liedl, T.; Koktysh, D.; Rogach, A. L.; Keller, S.; Raedler, J.; Natile, G.; Parak, W. J. *Nano. Lett.* **2004,** 4, 703-707.

33) Goldman, E. R.; Balighian, E. D.; Mattoussi, H.; Kuno, M. K.; Mauro, J. M.; Tran, P. T.; Anderson, G. P. *J. Am. Chem. Soc.* **2002,** 124(22), 6378-6382.

34) Lingerfelt, B. M.; Mattoussi, H.; Goldman, E. R.; Mauro, J. M.; Anderson, G. P. *Anal. Chem.* **2003**, 75(16), 4043-4049.

35) Zhang, Y.; So, M.; Loening, A. M.; Yao, H.; Gambhir, S. S.; Rao, J. *Angewandte Chemie, International Edition* **2006,** 45(30), 4936-4940.

36) Medintz, I. L.; Goldman, E. R.; Lassman, M. E.; Mauro, J. M. *Bioconj. Chem.* **2003**, 14, 909-918.

37) Zhang, C. Y.; Yeh, H. C.; Kuroki, M. T.; Wang, T. H. *Nature Materials* **2005**, 4, 826-831.

38) Gill, R.; Willner, I.; Shweky, I.; Banin, U. *J. Phys. Chem. B* **2005**, 109, 23715-23719.

39) Patolsky, F.; Gill, R.; Weizmann, Y.; Mokari, T.; Banin, U,; Willner, I. *J. Am. Chem. Soc.* **2003**, 125, 13918-13919

40) Medintz, I. L.; Clapp, A. R.; Melinger, J. S.; Deschamps, J. R.; Mattoussi, H. *Adv. Mat.* **2005**, 17, 2450-2455.

41) Pons, T.; Medintz, I. L.; Wang, X.; English, D. S.; Mattoussi, H. *J. Am. Chem. Soc*. **2006**, 128(47), 15324-15331.

42) Dubertret, B.; Skourides, P.; Norris, D. J.; Noireaux, V.; Brivanlou, A. H.; Libchaber, A. *Science* **2002**, 298(5599), 1759-1762.

43) Wu, X.; Liu, H.; Liu, J.; Haley, K. N.; Treadway, J. A.; Larson, J. P.; Ge, N.; Peale, F.; Bruchez, M. P. *Nature Biotechnology* **2003**, 21(1), 41-46

44) Smith, A. M.; Dave, S.; Nie, S.; True, L.; Gao, X. *Expert Review of Molecular Diagnostics* **2006**, 6(2), 231-244.

45) Larson, D. R.; Zipfel, W. R.; Williams, R. M.; Clark, S. W.; Bruchez, M. P.; Wise, F. W.; Webb, W. W. *Science* **2003**, 300(5624), 1434-1437.

46) So, M. K.; Xu, C.; Loening, A. M.; Gambhir, S. S.; Rao, J. *Nature Biotechnology* **2006**, 24(3), 339-343.

47) Cai, W.; Shin, D. W.; Chen, K.; Gheysens, O.; Cao, Q.; Wang, S..; Gambhir, S. S.; Chen, X. *Nano Letters* **2006**, 6(4), 669-676.

48) Lakowicz, J. R. Principles of Fluorescence Spectroscopy, 3nd Edition; Springer: New York, **2006.**

49) Haugland, R. P. Handbook of Fluorescent Probes and Research Products, 9th Edition**, 2002.**

50) Bensin, D. E., Conrad, D. W., de Lorimer, R. M., Tranmel, S. A., Hllinga, H. W. *Science* **2001**, 293, 1641-1644.

51) Looger, L. L.; Dwyer, M. A.; Smith, J. J.; Hellinga, H. W. *Nature* **2003**, 423, 185-190.

52) Jares-Erijman, E. A.; Jovin, T. M. *Nat. Biotechnol.* **2003**, 21, 1387-1395.

53) Clapp, A. R.; Medintz, I. L.; Mauro, J. M.; Fisher, B. R.; Bawendi, M. G.; Mattoussi, H. *J. Am. Chem. Soc.* **2004**, 126(1); 301-310.

54) Willard, D. M.; Van Orden, A. *Nat. Mater.* **2003**, 2 (9): 575-576.

55) Gao, X.; Cui, Y.; Levenson, R.M.; Chung, L. W.; Nie, S. *Nat. Biotechnol.* **2004**, 22, 969-976.

56) Kagan, C. R.; Murray, C. B.; Nirmal, M, Bawendi, M. G. *Phys. Rev. Lett.* **1996,** 76, 1517-1520.

57) Finlayson, C. E.; Ginger, D. S.; Greenham, N. C. *Chem. Phys. Lett.* **2001**, 338, 83-87.

58) Mamedova, N. N.; Kotov, N. A.; Rogach, A. L.; Studer, J. *Nano Lett.* **2001,** 1, 281-286.

59) Willard, D. M.; Carillo, L. L.; Jung, J.; Orden, A. V. *Nano Lett.*, **2001,** 1, 469-474.

60) Medintz, I. L.; Clapp, A. R.; Matoussi, H.; Goldman, E. R.; Fisher, B.; Mauro, J. M. *Nat. Mater.* **2003**, 2, 630-638.

61) Goldman, E. R.; Medinta, I. L.; Whitley, J. L. *J. Am. Chem. Soc.* **2005,** 127, 6744-6751.

62) Goldman, E. R.; Clapp, A. R.; Anderson, G. P.; Uyeda, H. T.; Mauro, J. M.; Medintz, I. L.; Mattoussi, H. *Anal. Chem.* **2004,** 76(3), 684-688.

63) Xu, C.; Xing, B.; Rao, J.; *Biochem. Biophys. Res. Commun.* **2006,** 344, 931-935.

64) Chang, E.; Miller, J. S.; Sun, J., *et al. Biochem. Biophys. Res. Commun.* **2005,** 334(4), 1317-1321.

65) Zhang, C. Y.; Yeh, H. C.; Kuroki, M. T.; Wang, T. H. *Nat. Mater.* **2005,** 4, 826-831.

66) Bakalova, R.; Zhelev, Z., Ohba, D.; Baba, Y. *J. Am. Chem. Soc.* **2005**, 127,11328-11335.

67) Medintz, I. L.; Konnert, J. H.; Clapp, A. R. *Proc. Natl. Acad. Sci. U.S.A.* **2004**, 101, 9612-9617.

68) Wu, X.; Liu, H.; Liu, J.; Haley, K. N.; Treadway, J.; Larson, P.; Ge, N.; Peale, F.; Bruchez, M. P. *Nature Biotechnol.* **2003**, 21, 41-46.

69) Wang, H.; Wang, H.; Liang, R.; Ruan, K. C. *Acta Biochim Biophys Sin* **2004**, 36(10), 681-686.

70) Hu, F.; Ran, Y.; Zhou, Z.; Gao, M. *Nanotechnology* **2006**, 17, 2972-2977.

71) Bentzen, E. L.; House, F.; Utley, T. J.; Crowe, J. E.; Wright, D. W. *Nano Letters* **2005**, 5, 591-595.

72) Bocsi, J.; Lenz, D.; Mittag, A.; Varga, V. S.; Molnar, B.; Tulassay, Z.; Sack, U.; Tárnok, A. *Cytometry Part A* **2006**, 69A(3), 131-134.

73) Wilson, R.; Spiller, D. G.; Prior, I. A.; Bhatt, R.; Hutchinson, A. *Journal of Materials Chemistry* **2007,** 17, 4400-4406.

74) Gao, X. H.; Yang, L.; Petrsos, J. A.; Marshall, F. F.; Simons, J. W.; Nie, S. M. *Curr. Opin. Biotechnol.* **2005,** 16, 63-72.

75) Yezhelyev, M. V.; Al-Hajj, A.; Morris, C.; Marcus, A. I.; Liu, T.; Lewis, M.; Cohen, C.; Zrazhevskiy, P.; Simons, J. W.; Rogatko, A.; Nie, S.; Gao, X.; O'Regan, R. M. *Adv. Mater.* **2007**, 19, 3146.

76) Zhang, B. B.; Liu, X. H.; Li, D. N.; Tian, H.; Ma, G. P.; Chang, J. *Chinese Science Bulletin* **2008**, 53, 2077.

77) Rauf, S.; Glidle, A.; Cooper, J. M. *Chem. Commun.* **2010**, 46, 2814.

78) Schubert, R.; and Stauch, O. *Biomacromolecules* **2002**, 3, 565-578.

79) Robert, M. A.; Locasscio-Brown, L.; MacCrehan, W. A.; Durst, R. A. *Anal. Chem.* **1996**, 68, 3434-3440.

80) Wiedmer, S. K.; Hautala, J.; Holopainen, J. M.; Kinnunen, P. K. J.; Riekkola, M. L. *Electrophoresis* **2001**, 22, 1305-1313.

81) Li, L.; Reiss, P. *J. Am. Chem. Soc.* **2008**, 130, 11588–11589.

82) Barber, K.; Mala, R. R.; Lambert, M. P.; Qiu, R. Z.; MacDonald, R. C.; Klein, W. L. *Neurosci. Lett.* **1996**, 207, 17-20.

83) Xu, S.; Ziegler, J.; Nann, T. *J. Mater. Chem.* **2008**, 18, 2653–2656.

84) Williams, D. M.; Carter, K. C.; Baillie, A. J. *J. Drug Targeting* **1995**, 3, 1–7.

85) Ruckmani, K.; Jayakar, B.; Ghosal, S. K. *Drug Dev. Ind. Pharm.* **2000**, *26*, 217–222.

86) Veronica, D.; Melissa, R.; Gilchrist, M. L.; Holland, E. C. Vazquez, M. *J. Nanosci. Nanotechnol.* **2008**, 8, 2293-2300.

87) Dennis, E. A. *The Enzymes* **1983**, 56, 307-353.

88) Van den Bosch, H. *Biochim. Biophys. Acta* **1980**, 604, 191–246.

89) Waite, M. *Plenum Publishing Corp., New York* **1987**, 332.

90) Dennis, E. A.; Rhee, S. G.; Billah, M. M.; Hannun, Y. A. *FASEB J.* **1991**, 5, 2068–2077.

91) Van Kuijk, G. M.; Sevenian, A.; Handelman, G. J.; Dratz, E. A. *Trends Biochem. Sci.* **1987**, 12, 31–34.

92) Nevalainen, T. J. *Clin. Chem.* **1983**, 39, 2453–2459.

93) Vadas, P.; Pruzanski, W. *Lab. Invest.* **1986**, 55, 391–404.

94) Dennis, E. A. *J. Biol. Chem.* **1994**. 269, 13057-13060.

95) Robert, B. *et al. The World Health Report 2004–Changing History* **2004**, 120–124.

96) World Health Organization task force on standardization of clinical nomenclature. *Circulation* **1979**, 59, 607-609.

97) Alpert, J. S.; Thygesen, K.; Antman, E.; Bassand, J. P. *J Am Coll Cardiol* **2000**, 36(3), 959–969.

98) Filatov, V. L.; Katrukha, A. G.; Bulargina, T. V.; Gusev, N.B. *Biochemistry (Moscow)* **1999**, 64, 969-985.

99) Mair, J.; Dworzak, E. A.; Lechleitner, P.; Smidt, J.; Wagner, I.; Diensti, F. *Clin Chem* **1991**, 37, 845-852.

100) Cantor, W. J.; Newby, L. K.; Christenson, R. H.; Tuttle, R. H.; Hasselblad, V.; Armstrong, P. W. *J Am Coll Cardiol* **2002**, 39, 1738-1744.

101) Hugo, A. K.; Siegfried, L.; Klaus, H.; Andrew, R.; Thomas, S.; Anneliese, B.; Ulrich, E.; Ursula, G. *Clinical Chemistry* **1992**, 38(3), 386-393.

102) Sheila, A. G.; Darcy, J. L.; Mary, E. P.; Lisa, B.; Orthan, S. *Sensor Lett.* **2004**, 2(1), 58-63.

103) Stacy, E. F.; Melanson, M. J.; Tanasijevic.; Petr, J. *Circulation* **2007**, 116, e501-e504.

104) Sergiy, M.; Meike, A. K.; Michael, W.; Andrey, L.; Thomas, A. K.; Alfons, N.; Konrad, K.; Fernando, D. S.; Jochen, F. *Nano Lett.* **2009**, 9(12), 4558-4563.

105) Angelo, C.; Elisabetta, D.; Francesco, R.; Domenico, D. B.; Fosco, P.; Valter, S.; Vittorio, C. *Clinical Chemistry* **2009**, 55(1), 196-198.

106) Morrow, D. A.; Antman, E. M. *Clinical Chemistry* **2009**, 55(1), 5-8,

107) Ross, R. *Nature* **1993**, 362(6423), 801-809.

108) Ross, R. *New England Journal of medicine* **1999**, 340(2), 115-126.

109)Stary, H. C.; Chandler, A. B.; Dinsmore, R. E.; Fuster, V.; Glagov, S.; Insull, W.; Rosenfeld, M. E.; Schwartz, C. J.; Wagner, W. D.; Wissler, R. W. *Circulation* **1995**, 92, 1355–1374.

110)Mach, F. *Curr. Atheroscler. Rep*. **2001**, 3, 243–251.

111)Yla-Herttula, S.; Lipton, B. A.; Rosenfeld, M. E.; Sarkioja, T.; Yoshimura, T.; Leonard, E. J. *PNAS* **1991**, 88, 5252–5256.

112)Yamamoto, T.; Eckes, B.; Mauch, C.; Hartmann, K.; Krieg, T. *J Immunol*. **2000**, 164, 6174–6179.

113)Elhage, R.; Jawien, J.; Rudling, M.; Ljunggren, H. G.; Takeda, K.; Akira, S.; Bayard, F.; Hansson, G. K. *Cardiovasc Res.* **2003**, 59, 234–240.

114)Wuttge, D. M.; Eriksson, P.; Sirsjö, A.; Hansson, G. K.; Stemme, S. *Am. J. Pathol.* **2001**, 159, 417-23.

115)Masaharu, K.; Mitsuru, O.; Norihisa, I. *Am. J. Hypertens.* **2005**, 18, 1019-25.

116)Namiki, M.; Kawashima, S.; Yamashita, T.; Ozaki, M.; Hirase, T.; Ishida, T.; Inoue, N.; Hirata, K.; Matsukawa, A.; Morishita, R.; Kaneda, Y.; Yokoyama, M. Arterioscler Thromb Vasc Biol. **2002**, 22, 115–120.

117)Ishida, Y.; Migita, K.; Izumi, Y.; Nakao, K.; Ida, H.; Kawakami, A.; Abiru, S.; Ishibashi, H.; Eguchi, K.; Ishii, N. *FEBS Lett.* **2004**, 69, 156 –160.

118)Mallat, Z.; Corbaz, A.; Scoazec, A.; Besnard, S.; Leseche, G.; Chvatchko, Y.; Tedgui, A. *Circulation* **2001**, 104, 1598 –1603.

119)Mallat, Z.; Corbaz, A.; Scoazec, A.; Graber, P.; Alouani, S.; Esposito, B.; Humbert, Y.; Chvatchko, Y.; Tedgui, A. *Circ Res.* **2001**, 89, e41– e45.

120)Houtkamp, M. A.; Van der Wal, A. C.; De Boer, O. J. *Arterioscler Thromb Vasc Biol* **2001**, 21, 1208-13.

Chapter 2

Quantum dot-liposome complexes as fluorescence resonance energy transfer probes to monitor phospholipase A_2 enzyme activity

2.1 Abstract

In the current chapter new liposome encapsulated quantum dot (QD) based fluorescence resonance energy transfer (FRET) probes for monitoring the enzymatic activity of phospholipase A_2 have been fabricated and characterized. Luminescent CdSe/ZnS quantum dots in the lipid bilayer acted as donor and the lipid bound membrane dye NBD acted as acceptor. As the quantum dots were not attached covalently to the phospholipids they did not affect the enzyme activity of phospholipase A_2. The addition of phospholipase A_2 to QD-liposomes demonstrated changes in FRET signals due to cleavage of the SN2-acyl bond and release of NBD fluorophores from the membrane. The changes in FRET signals were found to be dependent on phospholipase A_2 enzyme activity. The probes were able to detect enzyme activity as low as 0.0075 U/mL (PLA_2 = 1500 U/mg) in 30 min. The FRET format thus enables real time monitoring of the enzyme activity. Further these FRET probes were also used to screen the inhibition efficiencies of phospholipase A_2 inhibitors. It is also possible to multiplex the assay in a 96 well plate and screen large number of inhibitors simultaneously. Thus, the developed *in vitro* bioassay is sensitive, reliable and can be easily performed to provide valuable information about phospholipase A_2 and its inhibitors for both medical and pharmacological fields.

2.2 Introduction

Luminescent quantum dot (QD) based probes have been effectively utilized in the last decade for optical imaging of cells and tissues and in bioassays as alternatives to conventional organic flurophores.[1,2] QDs have unique size-dependent chemical and physical properties offering advantages like brightness, greater photostability, broad excitation wavelength range, and size-tunable narrow, and symmetric emission spectra ranging from 400 to 2000 nm.[3-8] However, quantum dot applications in bio-medical and clinical fields have been limited by the disadvantage of QDs being capped with hydrophobic coating ligands.[9,10] To overcome this limitation, focus has been made on several synthetic strategies over the past several years to make QDs water soluble and biocompatible. The attempts towards solubilization involved the exchange of the hydrophobic surface ligands with hydrophilic thiol containing molecules like mercaptoalkanoic acids.[4,11-13] Some studies used other exchange ligands like dendrons,[14] peptides,[15,16] silica,[17] block copolymers[18, 19] or encapsulated QDs in water miscible phospholipid micelles.[20]

Recently, fabrication of QD-liposome vesicles gained importance as a promising tool in nano-biotechnology. QDs have been incorporated into phospholipid liposomes making them biocompatible while retaining photoluminescence. Liposomes are concentric bilayered vesicles consisting of a hydrophobic phospholipid bilayer surrounding a hydrophilic aqueous phase. Liposomes offer exceptional engineering ability due to their physicochemical characteristics such as vesicle size, structure and surface versatility that can easily be modified with established methods. Liposomes can entrap large amount of fluorescent nanoparticles providing high biocompatibility, thus they enhance the effectiveness of nanoparticles for detection *in vivo* and *in vitro*.[21] They have been used to encapsulate and deliver oral vaccines as well as anti cancer, anti

inflammatory and hormonal drugs.[22-24] Liposome quantum dot complexes have been applied as fluorescent markers in immunoassays[25] and also to deliver QDs into cytosol of oncogenic brain cells via lipid mediated fusion with the cell membrane.[26] Further, QD-liposomes were also used for tumor cell-targeting, imaging, and drug delivery functions in human epidermal growth factor receptor 2-overexpressing tumor cells via receptor-mediated endocytosis.[27]

Phospholipase A_2 (EC 3.1.1.4) is a family of lipolytic extracellular enzymes that are relatively small proteins (ca. 14 kDa) containing multiple disulfide bridges. Phospholipase A_2 can be found in membrane-associated and soluble forms in almost all cell types, where they are believed to play an important role in the normal biosynthesis[28-31] and pathogenesis of various inflammatory processes.[32, 33] Phospholipase A_2 catalyzes the hydrolysis of the SN2 fatty acyl ester bond of phospholipids to yield arachidonic acid, and a lysophospholipid. Arachidonic acid produces leukotrienes by the lipooxygenase pathway that play powerful role in asthama, broncho-constriction, cardiovascular and neuropsychiatric illnesses. Lysophospholipids, another product of phospholipase A_2 enzymatic activity, produce platelet activating factor which causes a drop in blood pressure and reduced pumping of blood by the heart, which leads to shock and potentially death. Thus the measurement of phospholipase A_2 enzyme activity can be of major medical importance in drug discovery.

Phospholipase activity was monitored using traditional methods including titrimetry, colorimetry, fluorometry and radiometry.[34] Most of the methods are limited in terms of sensitivity with the exception of fluorometry and radiometry. Radiometric methods are most sensitive and most widely used but they are expensive, hazardous, laborious, and impractical when dealing with large scale samples. Many of the initial fluorescence assays were discontinuous and require phase separations to separate substrate and products. Wilton *et al* have

described a continuous fluorescence displacement assay for PLA_2 that involves monitoring the loss of fluorescence when the fatty acid probe 11-(dansylamino)undecanoic acid is displaced from liver fatty-acid-binding protein as a result of PLA_2 activity.[35] The assay detected enzyme activity down to ~10 pmol/mL. Prestwich *et al* reported a fluorogenic assay for the detection of PLA_2 activity in real time using FRET with substrates having SN1-acyl chain labeled with Dabcyl and SN2-acyl labeled with BODIPY fluorophore.[36] Perez-Gilabert *et al* described a spectrophotometric assay for the continuous and indirect measurement of PLA_2 activity.[37] The activity of PLA_2 is measured by the increase in absorbance at 234 nm due to the formation of hydrogen peroxide from linoleic acid released from hydrolyses of dilinoleoyl phosphatidylcholine. Recently, a fluorescence assay for PLA_2 was reported by Whitten *et al* where cationic poly(phenyleneethynylene) PPE derivatives physically adsorbed onto solid nonporous borosilicate microspheres were subsequently coated with 1,2-dimyristoyl-sn-glycero-3-[phospho-rac-(1-glycerol)] (DMPG).[38] The lipid bilayer acts as a substrate for PLA_2 and also shields the fluorescence of PPE from quenching by 9,10-anthraquinone-2,6-disulfonic acid (AQS). The amplified quenching of the polymer fluorescence by AQS is restored, as the DMPG is digested by PLA_2.

Many research labs including ours have recently developed quantum dot based fluorescence resonance energy transfer based assays.[39-44] Chang *et al* developed solution based FRET assays using QDs as donors and gold nanoparticles as acceptors for proteolytic activity measurements.[44] Shi *et al* from our lab have covalently linked molecular fluorescent acceptors to the surface of single quantum dot and used the FRET probes for real-time monitoring of protease activity in solution.[42] Most of the developed quantum dot based FRET assays were focused on measuring the proteolytic activity. In the current study, a quantum dot based FRET assay was

employed for lipase activity measurements. The quantum dot encapsulated liposome based FRET probes were synthesized and characterized to monitor the enzymatic activity of phospholipase A_2. The phospholipid bilayer in QD encapsulated liposomes were also labeled with acyl NBD fluorophores. The addition of phospholipase A_2 to QD-liposomes showed changes in FRET signals due to cleavage of SN2-acyl bond and release of NBD fluorophores from the membrane (scheme 2.1). These changes in FRET signals were found to be phospholipase A_2 concentration dependent. Further the FRET probes were also used to screen the inhibition efficiencies of phospholipase A_2 inhibitors. This method demonstrates the possibility to multiplex the assay in a 96 well plate and screen a large number of inhibitors simultaneously.

2.3 Experimental Methods

2.3.1 Materials and reagents. Technical grade (90%) trioctylphosphine oxide (TOPO), technical grade (90%) trioctylphosphine (TOP), cadmium oxide (99.99%), selenium powder (99.5%), lauric acid (98%), technical grade (90%) hexadecylamine (HDA), diethyl zinc ($Zn(Et)_2$) solution 1.0 M in heptane, hexamethyldisilathiane ($(TMS)_2S$), methanol anhydrous (99.8%), chloroform (99.5%), cholesterol, and phospholipase A_2 from honey bee venom were purchased from Sigma Aldrich. 1,2-dioleoyl-sn-glycero-3-phosphocholine (DOPC), and 1,2-dioleoyl-sn-glycero-3-phosphoglycerol (DOPG) were purchased from Avanti Polar Lipids. N-(fluorescein-5-thiocarbamoyl)-1,2-dihexadecanoyl-*sn*-glycero-3-phosphoethanolamine triethyl ammonium salt (DHPE-fluorescein), 2-(6-(7-nitrobenz-2-oxa-1,3-diazol-4-yl)amino)hexanoyl-1-hexadecanoyl-*sn*-glycero-3-phosphocholine (NBD C_6-HPC) were purchased from Invitrogen. All reagents were used as received without further purification.

2.3.2 Synthesis of TOPO capped luminescent quantum dots. TOPO-capped CdSe/ZnS quantum dots were prepared following a method first proposed by Peng[6] with a slight

modification.[45] Briefly, 12-13 mg of cadmium oxide and 160-180 mg of lauric acid were mixed under nitrogen atmosphere. The mixture was heated in a 100 mL three neck flask to slightly above 200°C to fully dissolve the cadmium oxide (clear solution). Then, 2 g of TOPO and 2 g HDA were added to the solution with constant stirring. Temperature was raised to 280°C before being cooled down slowly. Upon reaching the desirable temperature 80 mg selenium powder dissolved in 2 mL solution of TOP was rapidly injected into the solution under vigorous stirring. For shell coating, a 2 mL TOP solution containing 250 μL $(TMS)_2S$ and 1 mL $Zn(Et)_2$ was injected drop-wise into the solution. The reaction mixture was kept at 180°C for one hour before it was cooled to room temperature, washed three times with methanol, centrifuged at 4000 rpm for 10 minutes each, and redispersed in chloroform. The concentration of this solution was found to be 1 μM. The solution was stored at room temperature.

2.3.3 Encapsulation of quantum dots with liposomes. A 20 mM lipid stock solution was prepared with 1:1:0.4 molar ratios of DOPC, DOPG, and cholesterol in chloroform. The phospholipid stock solution was stored in a sealed vial at -10°C until use. A 100 μL aliquot of the lipid stock solution was added to 75 μL of 1 μM TOPO coated quantum dots and dried under nitrogen in a glass vial until all the chloroform was removed. A thin film formed at the bottom of the glass tubes. 1 mL of 10 mM pH 7.4 PBS buffer was added to the above formed thin film followed by sonication for 10 minutes and vortexing for 2 minutes. Unilamellar liposomes containing quantum dots in the membrane were thus formed.

2.3.4 Fabrication of QD-NBD-liposome based FRET probes. A 100 μL aliquot of 20 mM lipid stock solution was added to 75 μL of 1 μM TOPO coated quantum dots and then mixed with varying volumes 0, 25, 50, 100, 200, and 500 μL of 100 μM NBD C_6-HPC lipid molecules dissolved in chloroform. These mixtures were further dried under nitrogen in a glass vial until all

the chloroform was removed. A thin film formed at the bottom of the glass tubes. 1 mL of 10 mM pH 7.4 PBS buffer was added to the above formed thin film followed by sonication for 10 minutes and vortexing for 2 minutes. The corresponding NBD concentrations in the fabricated QD-NBD-liposome based FRET probes are 0, 2.5, 5, 10, 20, and 50 μM respectively. Another two fold dilution was performed on these samples to measure changes in FRET signals.

2.3.5 Enzyme activity and inhibition assays. A 100 μL aliquot of QD-NBD-liposome FRET based probes with 20 μM NBD was dissolved in PBS buffer pH 8.0, following which varying volumes of 0.5 mg/mL phospholipase A_2 in PBS buffer containing 1 mM of $CaCl_2$ were added to make a final volume of 200 μL. Time-dependent spectral measurements were carried out following the addition of phospholipase A_2 using a fluorescence spectrometer or a digital fluorescence spectral imaging system. Inhibition assays were monitored using fluorescence spectroscopy. To carry out the inhibition assays, 50 μL of 100 μg/mL phospholipase A_2 was added to various concentrations of inhibitors to a total volume of 100 μL. Following 30-min incubation, 100 μL of 75 nM QD-liposome FRET-based probes was added to the mixture and FRET measurements were carried out to monitor to enzymatic reaction.

2.3.6 Fluorescence spectroscopy measurements. Excitation and emission spectra were measured using a spectrofluorometer (Perkin Elmer), equipped with a 75-W continuous Xenon arc lamp as a light source. The samples with DHPE-fluorescein were excited at 480 nm. For the FRET assay all the samples were excited at minimum absorption wavelength of 375 nm to reduce interference from direct excitation of NBD molecules. All other samples were excited at 400 nm. Emission scans were measured from 425-700 nm.

2.3.7 Digital fluorescence imaging microscopy. Luminescence images were obtained using a digital inverted fluorescence microscope (Olympus IX71) equipped with a 100 W mercury lamp

as a light source. The fluorescence images were collected via a 20 X microscope objective with numerical aperture = 0.5. A filter cube containing a 380±20 nm band-pass excitation filter, a 425 nm dichroic mirror, and a 450 nm long pass emission filter was used to ensure spectral imaging purity. Digital point controller (DP72) was used for digital imaging. An exposure time of 100 ms was typically used to acquire the fluorescence images of QD based probes.

2.3.8 Cryo-transmission electron microscopy measurements. Sample preparation for cryo-transmission electron microscopy was carried out in a temperature and humidity controlled chamber. A specimen grid was dipped into a suspension and withdrawn, and excess liquid was blotted away. Thin films were formed between the bars of the grids. To vitrify these thin films, the grid was shot into melting ethane. The grids with vitrified thin films were analyzed with a JEM2010 high resolution transmission electron microscope (JEOL, Tokyo) at -170°C using a Gatan-626 cryo-specimen holder and cryotransfer system (Gatan, Warrendale, PA). The micrographs were collected at 120 kV. This microscope is equipped with a Gatan 2048- 2048 CCD camera and a Gatan energy filter.

2.4 Results and Discussion

2.4.1 Characterization of QD-liposomes. Luminescent CdSe/ZnS quantum dots were successfully encapsulated into DOPC, DOPG, Chol (1:1:0.4) liposomal bilayer membranes rendering the quantum dots water soluble. During the encapsulation process the hydrophobic coating on the surface of QDs interacts with hydrophobic regions of liposomes via hydrophobic interactions while the hydrophilic region of liposome is exposed to the water phase.

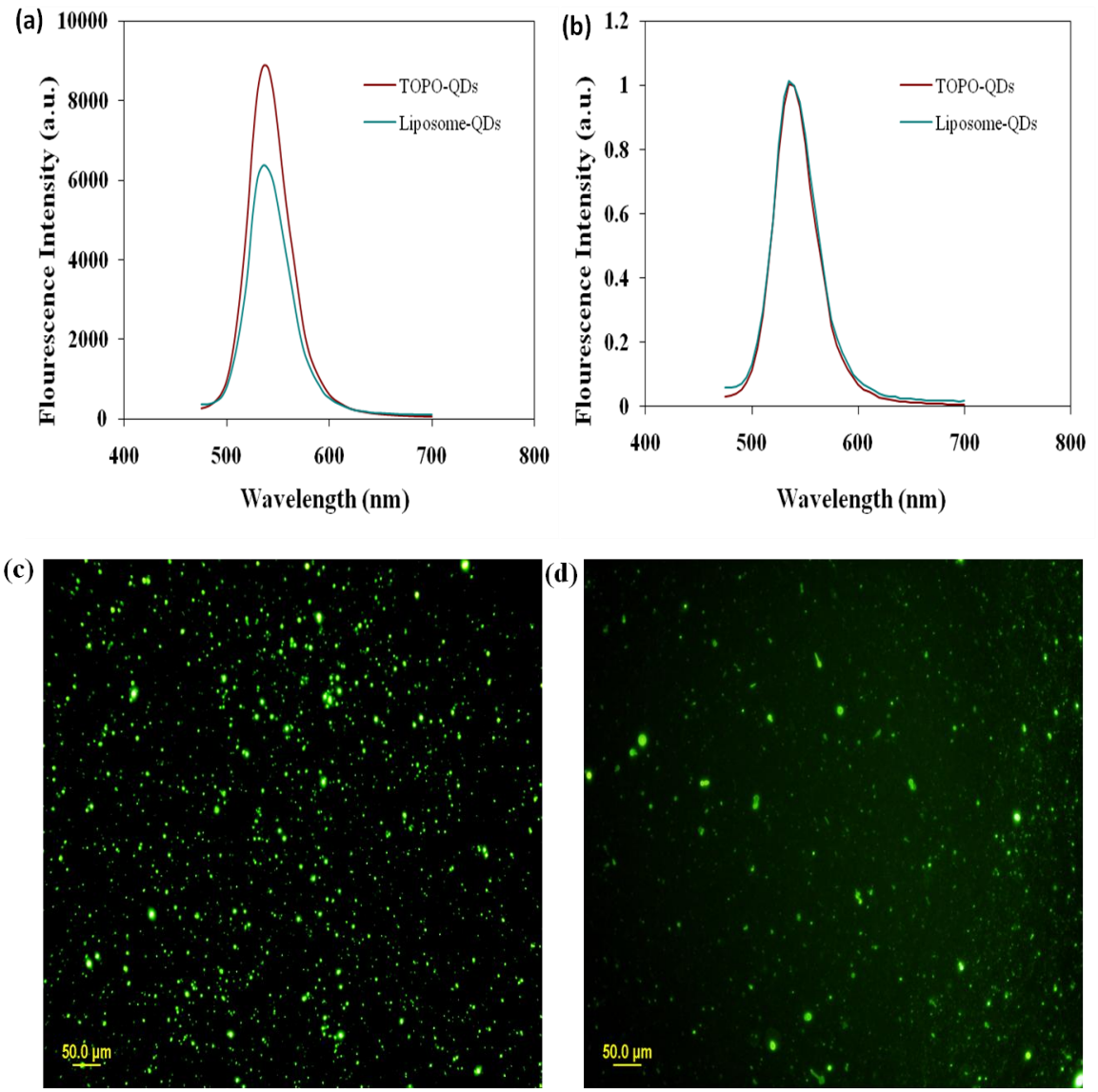

Figure 2.1 (a) Emission spectra, and (b) normalized emission spectra of TOPO coated quantum dots in chloroform (red line) and liposome encapsulated quantum dots in PBS pH 7.2 buffer (green line) at 50 nM concentration of quantum dots. Digital fluorescence microscopic images of (c) liposome encapsulated quantum dots with exposure time of 100 ms, and (d) liposome encapsulated fluorescein with exposure time of 100 ms.

The liposome encapsulated quantum dots were characterized for optical properties using a spectrofluorometer and digital fluorescence imaging microscopy. Figure 2.1 (a, b) are the emission and normalized spectra of TOPO coated quantum dots and liposome encapsulated quantum dots respectively, at the same concentration of quantum dots. The normalized spectra show that the optical properties of CdSe/ZnS quantum dots were well preserved even after encapsulation with liposomes. Figure 2.1 (c, d) are the fluorescence microscopic images of QD-liposomes and fluorescein (lipid membrane dye)-liposomes. It is evident from these images that the QD-liposomes are brighter than fluorescein-liposomes and also had low background noise compared to fluorescein-liposomes. Also the photo bleaching of the fluorescein containing liposomes can be seen (Figure 2.1d) while the QD-liposomes were pretty stable under light.

Cryo-transmission electron microscopy was employed to study the structural characteristics of the liposome encapsulated quantum dots. The results as depicted in figure 2.2a show that the quantum dots are concentrated in the liposome bilayer membrane that are seen as a dense bilayer. The microscopic image 2.2b is a control without quantum dots inside the liposomal membrane that do not show dense bilayers as QD-liposomes. Also at lower concentrations of quantum dots, the structures of the QD-liposomes were almost spherical in shape where as at the higher concentration of QDs, some degree of deformation of the vesicle structures was observed, visualized as elongated and deformed vesicular structures in the images (figure 2.2d). The cryo-TEM results were in agreement with the previous work by Al Jamal *et al*.[29]

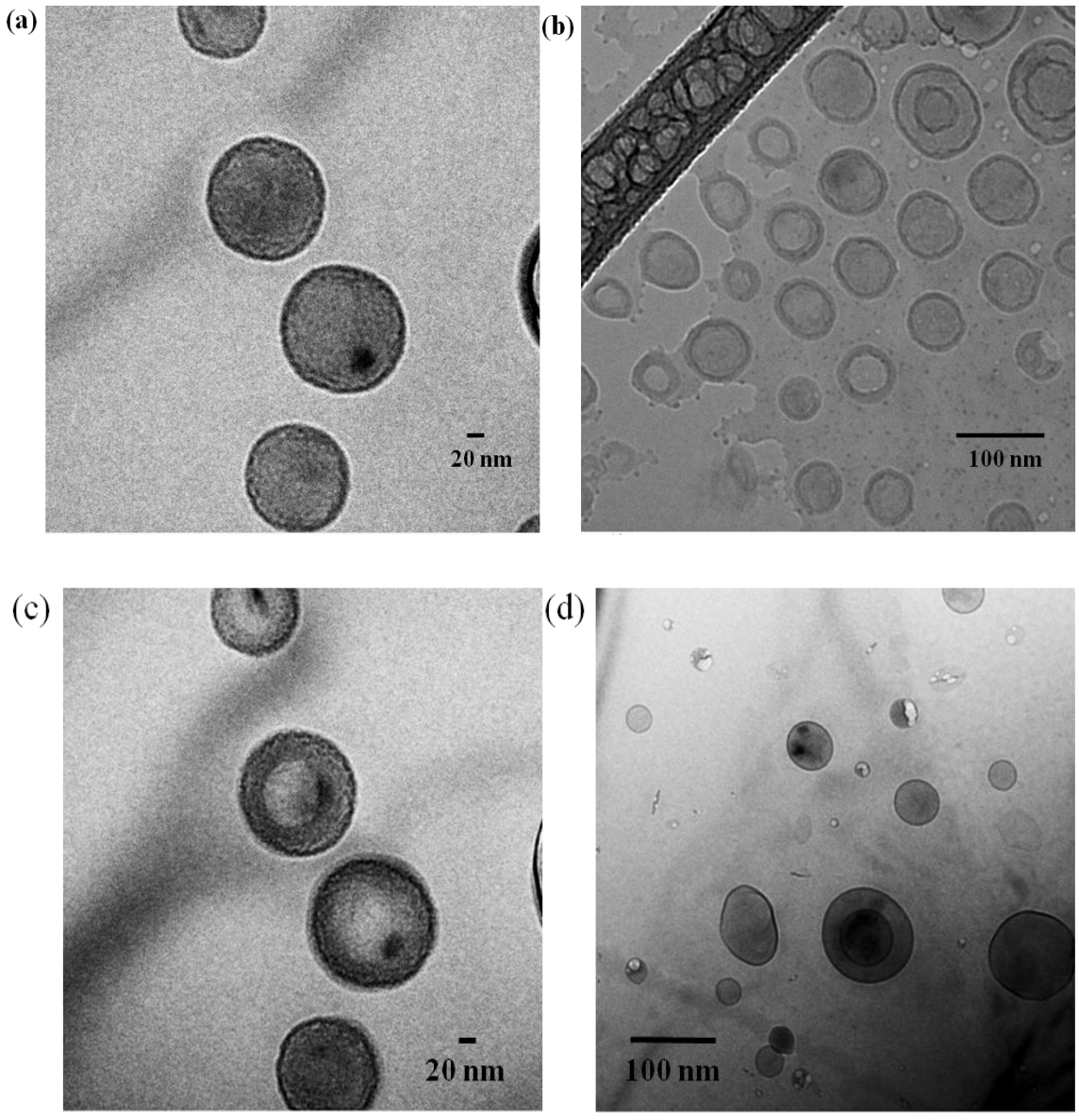

Figure 2.2 Cryo-transmission electron microscopy images of quantum dot containing liposomes at 50 nM (a, c), at 500 nM QD concentration (d), and liposomes without quantum dots (b).

2.4.2. Fabrication of FRET probes. After characterization of QD-liposomes, the complexes were used as fluorescence resonance transfer energy based probes to monitor enzyme activity of phospholipase A_2. The composition of the QD-liposomes in 1:1:0.4 molar ratio of DOPC:DOPG:chol provides the negative charge and the unsaturation on the liposome membrane that is necessary for phospholipase A_2 enzyme activity.

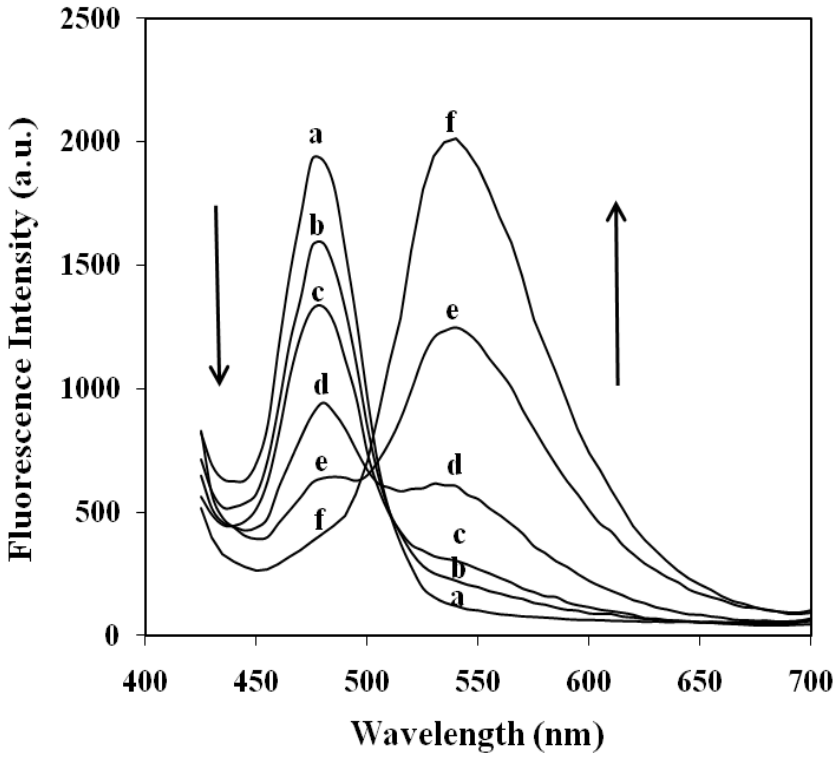

Figure 2.3 Emission spectra of QD-NBD-liposome based FRET probes at (a) 0, (b) 1.25, (c) 2.5, (d) 5, (e) 10, and (f) 25 μM of NBD C_6-HPC lipid molecule concentration. λ_{ex}: 375nm.

Quantum dots present in the lipid bilayer will act as donor and the lipid membrane dye NBD will act as acceptor. Different concentrations of NBD C_6-HPC lipid molecules of final concentrations ranging from 0 to 25 μM were incorporated into QD-liposomes and the probes were characterized using spectrofluorometer and digital fluorescence microscope. When excited at 375 nm, the absorbance minimum of NBD, to avoid direct excitation of NBD, it was observed that the fluorescence resonance energy was transferred from the quantum dot emitting at 480 nm to the NBD molecule emitting at 540 nm. This result is represented in figure 2.3 as increased NBD intensities and decreased QD intensities at increasing concentrations of NBD.

2.4.3. Enzyme activity of phospholipase A_2. FRET based probes were used to monitor the enzymatic activity of the phospholipase A_2. Phospholipase A_2 is an enzyme that hydrolyzes

phospholipids into fatty acids and other lipophilic substances. NBD is labeled on the acyl chain of phospholipids as shown in scheme 2.1. The enzyme phospholipase A_2 specifically recognizes the SN2 acyl bond of phospholipids and breaks away NBD from the lipid membrane. As a result energy transfer can no longer takes place as demonstrated by a decreased FRET signal.

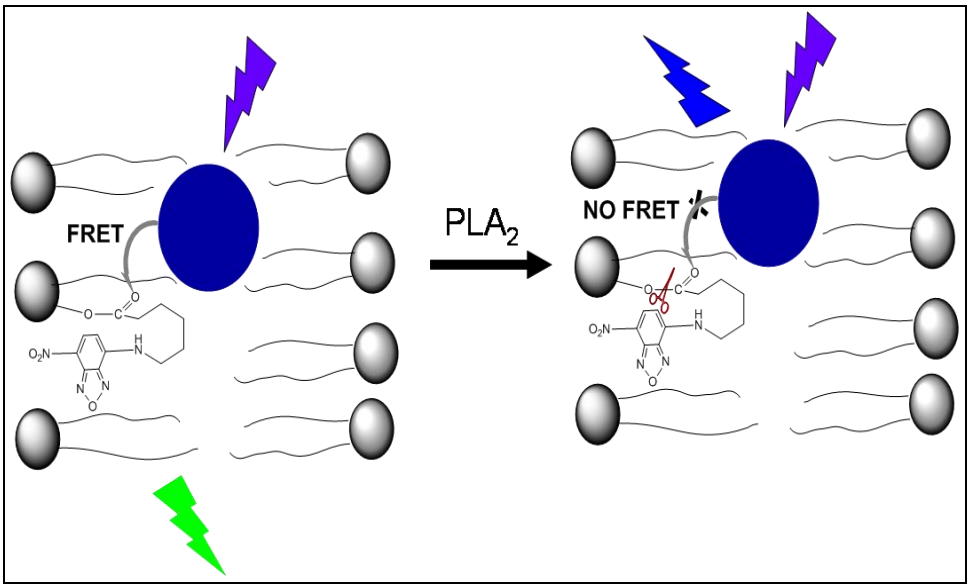

Scheme 2.1 Schematic representation of QD-liposome based FRET probes for monitoring phospholipase A_2 enzyme activity.

Figure 2.4 shows the emission spectra of QD-liposome based FRET probes at increasing phospholipase A_2 enzyme activities from 0-75 U/mL. The spectra were recorded 30 min after the addition of phospholipase A_2 to the QD-liposome solution. An increase in the quantum dot emission intensities at 480 nm and a decrease in the NBD emission intensities at 540 nm were clearly observed, suggesting a significant decrease in the FRET efficiency with increase in phospholipase A_2.

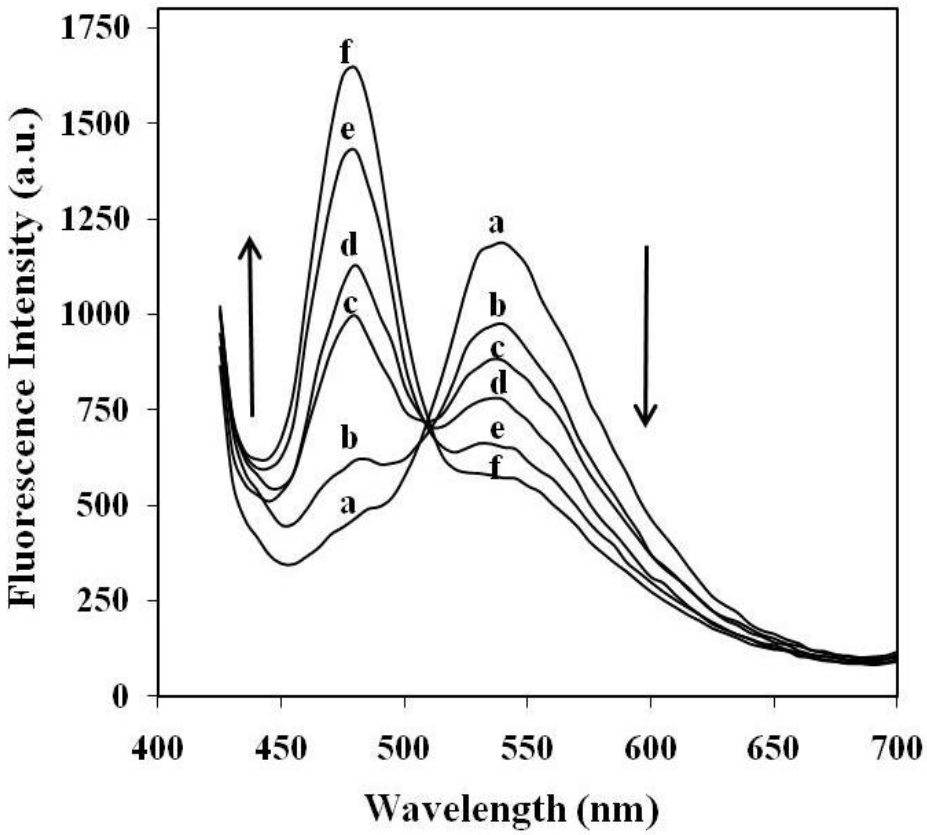

Figure 2.4 Emission spectra of QD-NBD-liposome based FRET probes with 10 μM NBD and at increasing phospholipase A_2 enzyme activities: (a) 0, (b) 1.5, (c) 7.5, (d) 15, (e) 37.5, and (f) 75 U/mL. λ_{ex}: 375nm.

A non-linear dependence of normalized F_d/F_a on phospholipase A_2 was observed where, F_d and F_a are the emission intensities of the quantum dot FRET-based probes at 480 nm (quantum dot donors) and 540 nm (NBD acceptors) respectively, when excited at 375 nm. F_d/F_a values were normalized to $(F_d/F_a)_0$; the ratio of F_d/F_a prior to adding phospholipase A_2 to the QD-liposome solutions. The dependence of FRET signal on phospholipase A_2 concentration was attributed to the enzymatic cleavage of the phospholipid molecules that release NBD molecules from the lipid molecule into the solution. The NBD molecule is hydrophilic in nature and preferentially releases into aqueous phase after cleavage decreasing the FRET efficiency.

Control experiments were performed with QD-liposomes without NBD labeling and NBD-liposomes without quantum dots. Adding phospholipase A_2 did not result in a significant change of the emission intensities. These measurements ruled out the possibility of nonspecific adsorption of phospholipase A_2 on quantum dots surface that might alter resulting emission intensities. Also the possibility that the decrease in the fluorescence intensity of NBD during FRET enzymatic assays resulted from a change in the chemical environment of the NBD molecules during the enzymatic cleavage by phospholipase A_2 was precluded.

Figure 2.5 shows the temporal dependence of the ratio F_d/F_a at increasing phospholipase A_2 enzyme activities ranging from 0 to 75 U/mL (ex: 375 nm). F_d/F_a increases with increase in incubation time and with the increase in phospholipase A_2 enzyme activity. It was possible to detect the enzymatic activity as low as 0.0075 U/mL (PLA_2 = 1500 U/mg) in 30 min at room temperature. Control experiments using QD-liposome based probes in the absence of phospholipase A_2 showed almost no changes in the FRET signal which clearly indicate that the changes in FRET signals associated with QD-liposome probes are due to the enzymatic activity of phospholipase A_2.

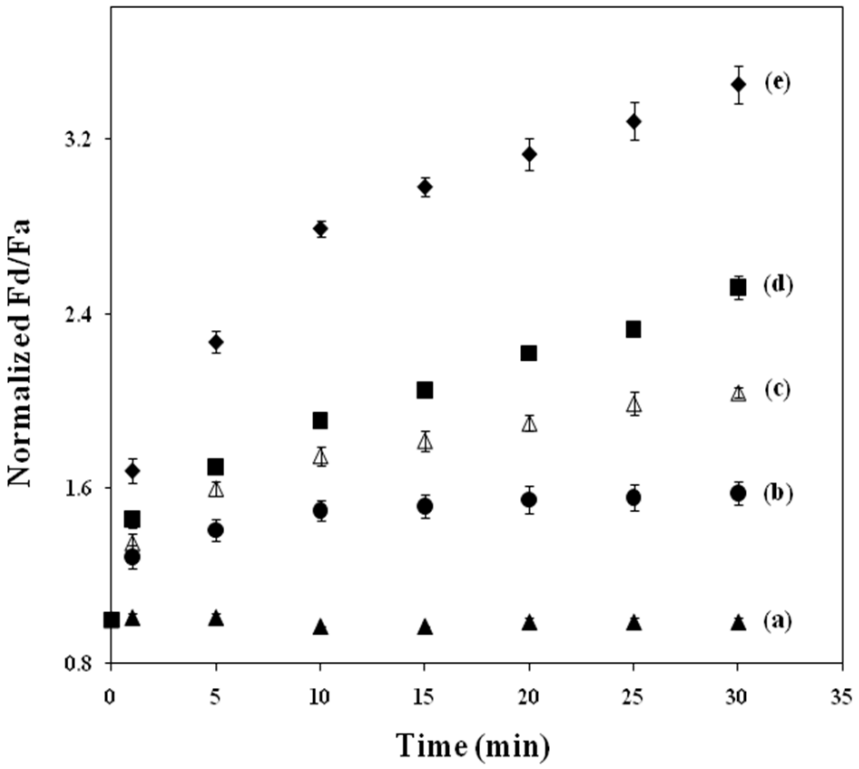

Figure 2.5 Time dependence of QD-NBD-liposome probes with 10 μM NBD and at increasing phospholipase A_2 enzyme activities: (a) 0, (b) 0.075, (c) 1.5, (d) 15, and (e) 75 U/mL. λ_{ex}: 375nm. The ratio F_d/F_a was normalized to $(F_d/F_a)_0$; the ratio of F_d/F_a prior to adding phospholipase A_2 to the QD-liposome solutions.

Images 2.6a and 2.6b are the digital fluorescence microscopic images of QD-liposomes and QD-liposomes labeled with NBD respectively. QD-liposomes show their characteristic blue emission while the QD-liposomes labeled with NBD emit bluish green light due to FRET between the quantum dots and NBD molecules. Image 2.6c shows the fluorescence image of the quantum dot FRET-based probes 30 min following the addition of 75 U/mL phospholipase A_2. It was seen that the emission color of the quantum dots turned blue due to enzymatic cleavage of the phospholipid molecule that released NBD molecules to the solution and restored the blue emission color of the quantum dots.

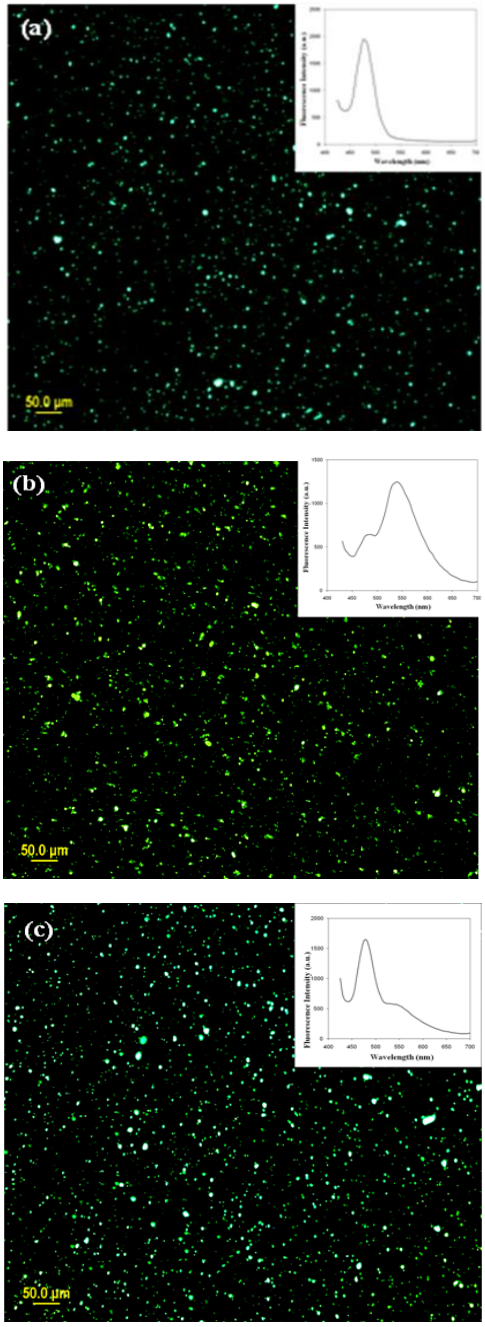

Figure 2.6 Digital fluorescence microscopic images of (a) only QD-liposomes showing blue emission (b) QD-NBD-liposomes with 10 µM NBD showing green emission due to FRET between quantum dots and NBD (c) QD-NBD-liposome based probes with 10 µM NBD after incubating for 30 min with 75 U/mL phospholipase A_2 enzyme activity. Emission spectra are provided as insets.

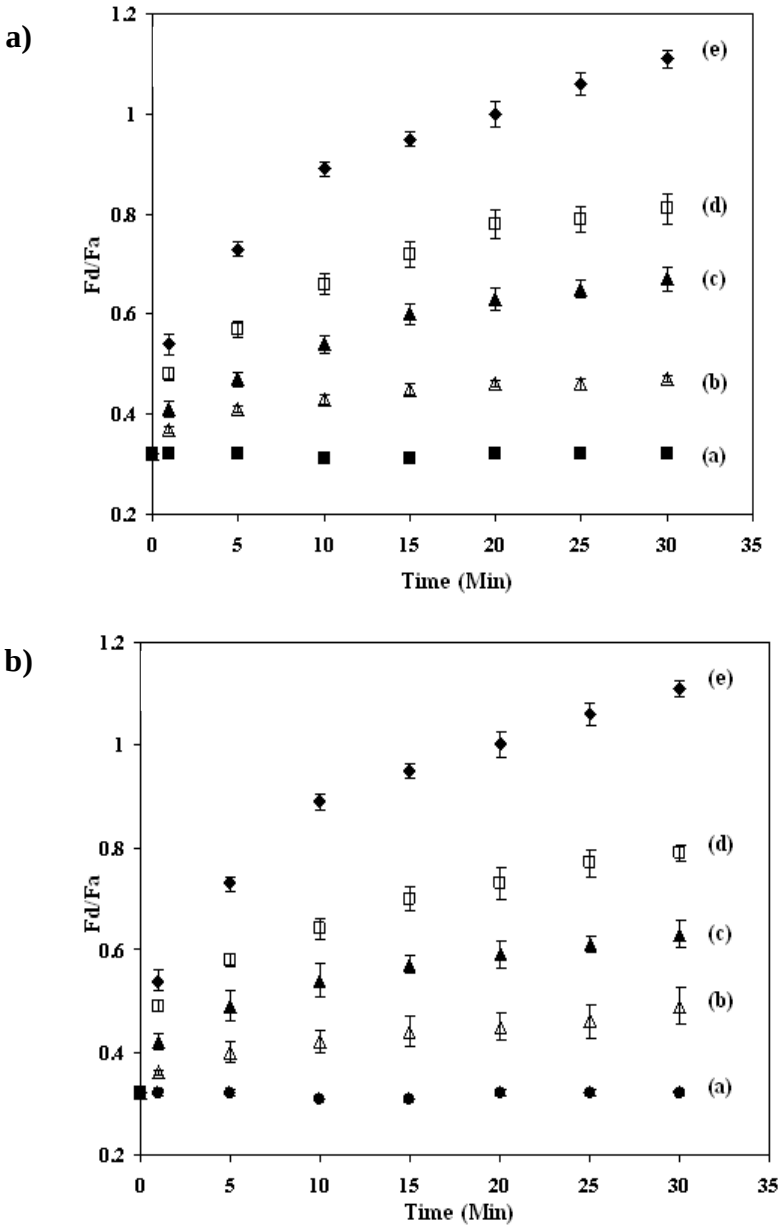

Figure 2.7 a) Time dependence of F_d/F_a at 75 U/mL of phospholipase A_2 activity and increasing concentrations of its inhibitor MJ33. (a) control in the absence of phospholipase and inhibitor, (b) 50 μg/mL, (c) 1 μg/mL, (d) 0.1 μg/mL, and (e) 0 μg/mL. b) time dependence of F_d/F_a at 75 U/mL of phospholipase A_2 activity and increasing concentrations of its inhibitor OBAA. (a) control in the absence of phospholipase and inhibitor, (b) 125 μg/mL, (c) 50 μg/mL, (d) 25 μg/mL, and (e) 0 μg/mL.

2.4.4. Screening enzyme inhibitors. The QD-liposome probes were used to screen the inhibition efficiencies of two phospholipase A_2 inhibitors: 1-hexadecyl-3-(trifluoroethyl)-sn-glycero-2-phosphomethanol (MJ33) and 3(4octadecyl) benzoylacrylic acid (OBAA). Figure 2.7a shows the temporal dependence of the ratio, F_d/F_a of quantum dot based probes with increasing concentrations of inhibitor MJ33 from 0 to 50 μg/mL at 75 U/mL of phospholipase A_2 activity. Figure 2.7b shows the temporal dependence of the ratio F_d/F_a with increasing concentrations of OBAA from 0 to 125 μg/mL at 75 U/mL of phospholipase A_2 activity. The rate of increase of F_d/F_a was found to be dependent on the concentration of the enzyme inhibitors. The trend towards decreasing phospholipase A_2 enzyme activity with increase in concentrations of enzyme inhibitors was observed for both MJ33 as well as OBAA. However, it was seen that the inhibition efficiency of MJ33 was higher than the inhibition efficiency of OBAA at 50 μg/mL.

2.4.5. Advantages offered by QD based FRET probes. The unique feature of this work is the platform of liposome encapsulated QDs that can be prepared using commercially available substrates. Since the quantum dots are not attached covalently to the phospholipids they do not affect the enzyme activity of phospholipase A_2. The FRET format enables real time monitoring of the enzyme activity. The QD based FRET probes were able to detect the enzyme activity as low as 0.0075 U/mL (PLA_2 = 1500 U/mg) in 30 min at room temperature which is the best detection limit attained so far in comparison to 0.05 U/mL of commercially available detection kit. These FRET probes were further used to screen the inhibition efficiencies of PLA_2 inhibitors. QD based FRET probes allow for multiplexing and screening large number of inhibitors simultaneously. The method is also suitable for both kinetic analysis and large-scale screening using automated readers for 96-well plates.

2.5 Conclusions

Liposome encapsulated CdSe/ZnS quantum dots have been synthesized successfully making the quantum dots water soluble and biocompatible. The optical characterization revealed that the properties of quantum dots were well preserved even after encapsulation with liposomes. Structural characterization using cryo-TEM was in accordance with previous work showing dense bilayers for QDs encapsulated liposomes. Further to fabricate QD liposome based FRET probes, NBD bound to acyl chain of phospholipids was incorporated into QD liposomes. These complexes were then used as FRET based probes to monitor the enzyme activity of phospholipase A_2. The FRET signal changes were found to be phospholipase A_2 enzyme activity dependent. Since the quantum dots were not attached covalently to the phospholipids, they did not affect the enzyme activity of phospholipase A_2. The probes were able to detect the enzymatic activity as low as 0.0075 U/mL (PLA_2 = 1500 U/mg) in 30 min. Therefore, the FRET format enables real time monitoring of the enzyme activity. Further these FRET probes were also used to screen the inhibition efficiencies of two phospholipase A_2 inhibitors 1-hexadecyl-3-(trifluoroethyl)-sn-glycero-2-phosphomethanol and 3(4octadecyl)benzoylacrylic acid. It is also possible to multiplex the assay in a 96 well plate and screen a large number of inhibitors simultaneously. Thus the developed *in vitro* bioassay is sensitive, reliable and can be easily performed to provide valuable information about phospholipase A_2 and its inhibitors to both the medical and pharmacological fields.

2.6 References

(1) Michalet, X.; Pinaud, F.; Bentolila, L. A.; Tsay, J. M.; Doose, S.; Li, J. J.; Sundaresan, G.; Wu, A. M.; Gambhir, S. S.; Weiss, S. *Science* **2005**, 307, 538-44.

(2) Jaiswal, J. K.; Simon, S. M. *Trends Cell Biol.* **2004**, 14, 497-504.

(3) Bruchez Jr, M.; Moronne, M.; Gin, P.; Weiss, S.; Alivisatos, A. P. *Science* **1998**, 281, 2013-2016.

(4) Chan, W. C.; Nie, S. *Science* **1998**, 281, 2016-2018.

(5) Peng, X. G.; Manna, L.; Yang, W. D.; Wickham, J.; Scher, E.; Kadavanich, A.; Alivisatos, A. P. *Nature* **2000**, 404, 59-61.

(6) Peng, Z. A.; Peng, X. G. *J. Am. Chem. Soc.* **2001**, 123, 183-184.

(7) Qu, L. H.; Peng, X. G. *J. Am. Chem. Soc.* **2002**, 124, 2049-2055.

(8) Medintz, I. L.; Uyeda, H. T.; Goldman, E. R.; Mattoussi, H. *Nat. Mater.* **2005**, 4, 435-446.

(9) Reiss, P.; Bleuse, J.; Pron, A. *Nano Lett.* **2002**, 2, 781-784.

(10) Malik, M. A.; O'Brien, P.; Revaprasadu, N. *Chem. Mater.* **2002**, 14, 2004-2010.

(11) Mattoussi H. H.; Mauro, J. M.; Goldman, E. R.; Anderson, G. P.; Sundar, V.C.; Mikulec, F. V.; Bawendi, M. G. *J. Am. Chem. Soc.* **2002**, 122, 12142–12150.

(12) Pathak, S.; Choi, S. K.; Arnheim, N.; Thompson, M. E. *J. Am. Chem. Soc.* **2001**, 123, 4103–4104.

(13) Gaponik, N.; Talapin, D. V.; Rogach, A. L.; Hoppe, K.; Shevchenko, E.V.; Kornowski, A.; Eychmuller, A.; Weller, H. *J. Phys. Chem. B* **2002**, 106, 7177–7185.

(14) Guo, W.; Li, J. J.; Wang, Y. A.; Peng, X. G. *Chem. Mater.* **2003**, 15, 3125–3133.

(15) Pinaud, F.; King, D.; Moore, H. P.; Weiss, S. *J. Am. Chem. Soc.* **2004**, 126, 6115–6123.

(16) Mattoussi, H.; Mauro, J. M.; Goldman, E.R.; Anderson, G.P.; Sundar, V.C; Mikulec, F.V.; Bawendi, M.G. *J. Am. Chem. Soc.* **2000**, 122, 12142–12150.

(17) Gerion, D.; Pinaud, F.; Williams, S.C.; Parak, W. J.; Zanchet, D.; Weiss, S.; Alivisatos, A. P. *J. Phys. Chem. B* **2001**, 105, 8861–8871.

(18) Wu, X.; Liu, H.; Liu, J.; Haley, K.N.; Treadway, J.A.; Larson, J. P.; Ge, N.; Peale, F.; Bruchez, M.P. *Nat. Biotechnol.* **2003**, 21, 41–46.

(19) Gao, X.; Cui, Y.; Levenson, R.M.; Chung, L.W.; Nie, S. *Nat. Biotechnol.* **2004**, 22, 969–976.

(20) Dubertret, B.; Skourides, P.; Norris, D. J.; Noireaux, V.; Brivanlou, A. H.; Libchaber, A. *Science* **2002**, 298, 1759–1762.

(21) Barber, K.; Mala, R. R.; Lambert, M. P.; Qiu, R. Z.; MacDonald, R. C.; Klein, W. L. *Neurosci. Lett.* **1996**, 207, 17-20.

(22) Udupa, N.; Chandraprakash, K. S.; Umadevi, P.; Pillai, G. K. *Drug De*v. *Ind. Pharm.* **1993**, 19, 1331–1342.

(23) Williams, D. M.; Carter, K. C.; Baillie, A. J. *J. Drug Targeting* **1995**, 3, 1–7.

(24) Ruckmani, K.; Jayakar, B.; Ghosal, S. K. *Drug De*V. *Ind. Pharm.* **2000**, 26, 217–222.

(25) Shan, G. Y.; Li, D.; Feng, L. Y.; Kong, X. G.; Liu, Y. C.; Bai, Y.B.; Li, T. J.; Sun, J. Z. *Chinese Journal of Chemistry* **2005**, 23, 1688-1692.

(26) Veronica, D.; Melissa, R.; Gilchrist, M. L.; Holland, E. C. Vazquez, M. *J. Nanosci. Nanotechnol.* **2008**, 8, 2293-2300.

(27) Weng, K. C.; Noble, C.; Papahadjopoulos-Sternberg, B.; Chen, F. F.; Drummond, D. C.; Kirpotin, D. B.; Wang, D.; Hom, Y. K.; Hann, B, Park, J. W. *Nano Lett.* **2008**, 8(9), 2851-2857.

(28) Van den Bosch, H. *Biochim. Biophys. Acta.* **1980**, 604, 191–246.

(29) Waite, M. Plenum Publishing Corp., New York. **1987**, 332.

(30) Dennis, E. A.; Rhee, S. G.; Billah, M. M.; Hannun, Y. A. *FASEB J.* **1991**, 5, 2068–2077.

(31) Van Kuijk, G. M.; Sevenian, A.; Handelman, G. J.; Dratz, E. A. *Trends Biochem. Sci.* **1987**, 12, 31–34.

(32) Nevalainen, T. J. *Clin. Chem.* **1983**, 39, 2453–2459.

(33) Vadas, P.; Pruzanski, W. *Lab. Invest.* **1986**, 55, 391–404.

(34) Reynolds, L. J.; Washburn, W. N.; Deems, R. A.; Dennis, E. A. *Methods Enzymol.* **1991**, 197, 3-23.

(35) Wilton, D. C. *Biochem. J.* **1990**, 266, 435-439.

(36) Feng, L.; Manabe, K.; Shope, J. C.; Widmer, S.; DeWald, D. B.; Prestwich, G. D. *Chem. Biol.* **2002**, 9, 795-803.

(37) Jimenez, M.; Cabanes, J.; Gandia-Herrero, F.; Escribano, J.; Garcia-Carmona, F.; Perez-Gilabert, M. *Anal. Biochem.* **2003**, 319, 131-137.

(38) Chemburu S.; Ji, E.; Casana Y.; Wu Y.; Buranda T.; Schanze K. S.; Lopez G. P.; Whitten D. G. *J Phys Chem B.* **2008,** 112, 14492–1449.

(39) Medintz, I. L.; Clapp, A. R.; Mattoussi, H.; Goldman, E. R.; Fisher, B.; Mauro, J. R. *Nat. Mater.* **2003**, 2, 630-639.

(40) Clapp, A. R.; Medintz, I. L.; Mauro, J. M.; Fisher, B. R.; Bawendi, M. G.; Mattoussi, H. *J. Am. Chem. Soc.* **2004**, 126, 301-310.

(41) Shi, L.; De Paoli, V.; Rosenzweig, N.; Rosenzweig, Z. J. *Am. Chem. Soc.* **2006**, 128, 10378-10379.

(42) Shi, L.; Rosenzweig, N.; Rosenzweig, Z. *Anal. Chem.* **2007**, 79, 208–214.

(43) Crivat, G.; Da Silva, S. M.; Reyes, D. R.; Locascio, L. E.; Gaitan, M.; Rosenzweig, N.; Rosenzweig, Z. *J. Am. Chem. Soc.* **2010**, 132, 1460–1461.

(44) Chang, E.; Miller, J. S.; Sun, J.; Yu, W. W.; Colvin, V. L.; Drezek, R.; West, J. W. L. *Biochem. Biophys. Res. Commun.* **2005**, 334, 1317–1321.

(45) Wang, D.; He, J.; Rosenzweig, N.; Rosenzweig, Z. *Nano Lett.* **2004**, 4, 409-413.

(46) Al-Jamal, W. T.; Al-Jamal, K. T.; Tian, B.; Lacerda, L.; Bomans, P. H.; Frederik, P.M.; Kostarelos, K. *ACS Nano* **2008**, 2(3), 408-418.

Chapter 3

Synthesis and characterization of liposome encapsulating InP/ZnS quantum dots

3.1 Abstract

InP quantum dots (QDs) are popular III-V semiconductor nanocrystals, however, studies of InP quantum dots are less advanced in comparison to II-VI semiconductor nanocrystals because of their difficult synthetic chemistry and low quantum yield. This work for the first time focuses on the synthesis and characterization of liposome encapsulated InP/ZnS quantum dots. InP/ZnS-liposome complexes were successfully synthesized preserving the integrity of the liposomes. A comparative photostability study of InP/ZnS QD-liposomes with 16-mercaptohexadecanoic acid (MHDA) coated QDs and InP/ZnS QDs showed enhanced stability of InP/ZnS QDs after encapsulation. After 60 min of continuous irradiation, the fluorescence intensity of InP/ZnS QDs decreased to 57% of the original intensity, whereas MHDA coated QDs and InP/ZnS QD-liposomes decreased by only 30% and 27% respectively. Further the effect of pH on the emission of InP/ZnS-liposome complexes was also studied, showing only 10% variation in the PL intensity of InP/ZnS QDs. Thus InP/ZnS-liposomes exhibit greater advantages over InP/ZnS quantum dots demonstrating their utility as a potential tool in several biological applications such as bioimaging, bioassays and immunoassays.

3.2 Introduction

Quantum dot based probes have received great interest in the last two decades for optical imaging of cells, tissues and in bioassays as an alternative to conventional organic flurophores.[1,2] The majority of the research has focused on the use of II/VI luminescent quantum dots such as CdSe or CdSe/ZnS as probes in several biological applications.[3-8] Also there are studies that reported the use of CdTe quantum dots for near infrared bioimaging.[9] Despite several advantages offered by II/VI type QDs, complete replacement of organic fluorophores is limited due to cytotoxicity associated with the individual ions present in the quantum dots.[10-12] The limitation is overcome by the growth of thick ZnS shell on top of the CdSe or CdTe nanoparticles making them less toxic. The ZnS shell inactivates the non-radiative recombination sites on the core surface of the quantum dots to improve the quantum yield; it also acts as a barrier preventing the contact of CdSe with the surrounding solvent avoiding dissolution. However, the ZnS shell does not provide permanent and complete protection; therefore, the quantum dots are not completely safe for biological applications.

The main advantage of III-V semiconductor nanocrystals over II-VI quantum dots is the robustness of the covalent bond as opposed to the ionic bond. The more covalent bond is much less likely to allow ionization and subsequent dissolution of the ions, making the particles less cytotoxic. Among III-V semiconductor materials InP is popular, due to its bulk band gap of 1.35 eV that enables quantum dots to have photoluminescence emission wavelengths ranging from blue to the near infrared. Thus InP quantum dots serve as alternatives to the frequently used CdSe quantum dots for several applications including bio-labeling, light emitting devices, photovoltaic cells, quantum dot lasers.[1,13-15] However, quantum yield (QY) of III-V quantum dots is less than 1% due to surface traps and dangling bonds in the crystal lattice and high activation

barrier for de-trapping as compared to II-VI semiconductors.[16-18] Initially the quantum yields of InP NCs were improved to 20–40% by HF etching.[19] Recently Peng *et al* reported InP/ZnS core–shell quantum dots synthesis using fatty amine for which the quantum yields reached up to 40%.[20] A one step and one pot method for the synthesis of highly luminescent InP with QYs of up to 30% and InP/ZnS QDs with QYs of up to 60% was reported by Nann *et al*.[21] More recently, Reiss *et al* synthesized InP/ZnS QDs in a single step with quantum yield up to 70%.[22]

Liposomes are concentric bilayered vesicles consisting of a hydrophobic phospholipid bilayer surrounding a hydrophilic aqueous phase. Liposomes offer exceptional engineering ability because of their physicochemical characteristics such as lipid vesicle size, lipid vesicle structure and surface versatility that can be easily modified with established methods. Liposomes can entrap large amounts of fluorescent nanoparticles while providing high biocompatibility and thus enhancing the effectiveness of nanoparticles for detection *in vivo* and *in vitro*.[23] Therefore they have been used to encapsulate and deliver oral vaccines as well as anticancer, antiinflammatory and hormonal drugs.[24-26] Recently, research involving the fabrication of liposome-quantum dot vesicles gained more importance as a promising tool in nano-biotechnology. Liposomes and nanoparticles together are used as novel tools extensively in pharmacological profile to retain biocompatibility and physio-chemical characteristics of lipid bilayer and luminescent characteristics of QDs for therapeutic and diagnostic applications. Cationic liposomes were used to deliver non-targeted CdSe/ZnS quantum dots into the cytosol of oncogenic brain cells via lipid mediated fusion with the cell membrane.[27] In another study, researchers were able to internalize cationic lipid QDs in human epithelial lung tumor cells *in vitro* and human cervical carcinoma xenografts *in vivo* and showed that they were able to monitor intracellular trafficking inside the cells.[28] Recently, it was seen that QD-immuno

liposomes were capable of tumor cell-targeting, imaging, and drug delivery functions by synthesizing QD-immuno liposomes that selectively and efficiently internalized in human epidermal growth factor receptor 2 over expressing tumor cells via receptor-mediated endocytosis.[29] Furthermore, Yang *et al* demonstrated the targeting and imaging ability of folate receptor targeted liposomes containing CdTe QDs in the human uterine cervix cancer cell line.[30]

In the current study, for the first time, liposome encapsulating InP/ZnS quantum dots were successfully synthesized. The structure and optical properties were characterized using cryogenic transmission electron microscopy, dynamics scattering light measurements and spectroflourometry. A comparative photostability study of InP/ZnS QD-liposomes with 16-mercaptohexadecanoic acid (MHDA) coated QDs and InP/ZnS QDs was performed. Further the effects of pH and quantum dot concentration on the emission intensity of QD-liposomes were also studied. The results suggest greater advantages of InP/ZnS-liposome complexes than the InP/ZnS quantum dots and thus allowing wide range of biological applications such as bioimaging, bioassays and immunoassays.

3.3 Experimental Methods

3.3.1 Materials and reagents. Indium acetate (99.99%), myristic acid (99%), 1-dodecanethiol (98%), 1-octylamine (99%), 1-octadecene (90%), sulfur (99.9%), zinc stearate (90%), methanol anhydrous (99.8%), chloroform (99.5%), 16-mercaptohexadecanoic acid, dihexadecyl phosphate, cholesterol were purchased from Sigma Aldrich. Tris(trimethylsilyl)phosphine ($P(TMS)_3$, 95%) was purchased from Alfa Aesar. Dimyristoylphospatidylcholine (DMPC) was purchased from Avanti Polar Lipids. N-(fluorescein-5-thiocarbamoyl)-1,2-dihexadecanoyl-*sn*-glycero-3-phospho-ethanolamine triethyl ammonium salt (DHPE-fluorescein) was purchased from Invitrogen. All reagents were used as received without further purification.

3.3.2 Synthesis of luminescent InP/ZnS quantum dots. InP/ZnS quantum dots were synthesized by following the procedure of Peng *et al*.[20] Briefly, 0.4 mmol of indium acetate, 1.2 mmol of myristic acid, and 5ml of octadecene were loaded into a three-neck flask. The mixture was heated to 180ºC under argon flow, for 30 min. Then a solution containing 0.2 mmol of $P(TMS)_3$ and 2.4 mmol 1-octylamine made in glove box was injected rapidly into the hot reaction mixture and allowed 60 min to react. For the growth of ZnS shell, the reaction solution was cooled down to 150ºC. Zinc stearate and sulfur precursors were added consecutively to the reaction flask with the InP nanocrystals, waiting for 10 min between each injection at 150ºC. After that, the temperature was increased to 230ºC for 20 min to allow the growth of the ZnS shell. The reaction was cooled down to room temperature and the nanocrystals were precipitated with methanol and centrifuged at 4000 rpm for 20 minutes three times. The precipitate was then redispersed in chloroform.

3.3.3 Encapsulation of InP/ZnS quantum dots into liposomes. A 20 mM lipid stock solution was prepared with a 5:4:1 molar ratio of dimyristoylphospatidylcholine, cholesterol, and dihexadecyl phosphate in chloroform. This phospholipid composition provides maximum structural stability of liposomes stored at room temperature.[31] The phospholipid solution was stored in a sealed vial at -10°C until use. A 100 μL aliquot of the stock solution was added to 100 μL of 2 μM InP/ZnS quantum dots and dried under nitrogen in a glass vial until all the chloroform was removed. A thin film was formed at the bottom of the glass tubes. 1 mL of 10 mM pH 7.4 PBS buffer was added to the above formed thin film. The sample was sonicated for 5-10 minutes and vortexed for 2 minutes resulting in the formation of unilamellar liposomes.

3.3.4 Fluorescence spectroscopy measurements. Excitation and emission spectra were measured using a spectrofluorometer (Molecular Probes, SpetraMax M2), equipped with a with a

75-W continuous Xenon arc lamp as a light source. The samples with DHPE-fluorescein were excited at 480nm. Samples having QDs were excited at 400nm. Emission scans were measured from 450-700nm.

3.3.5 Digital fluorescence imaging microscopy. Luminescence images were obtained using a digital luminescence imaging microscopy system. The system consisted of an inverted fluorescence microscope (Olympus IX71) equipped with a 100 W mercury lamp as a light source. The fluorescence images were collected via a 20 X microscope objective with numerical aperture = 0.5. A filter cube containing a 420 ±10 nm band-pass excitation filter, a 450 nm dichroic mirror, and a 480-nm long pass emission filter was used to ensure spectral imaging purity.

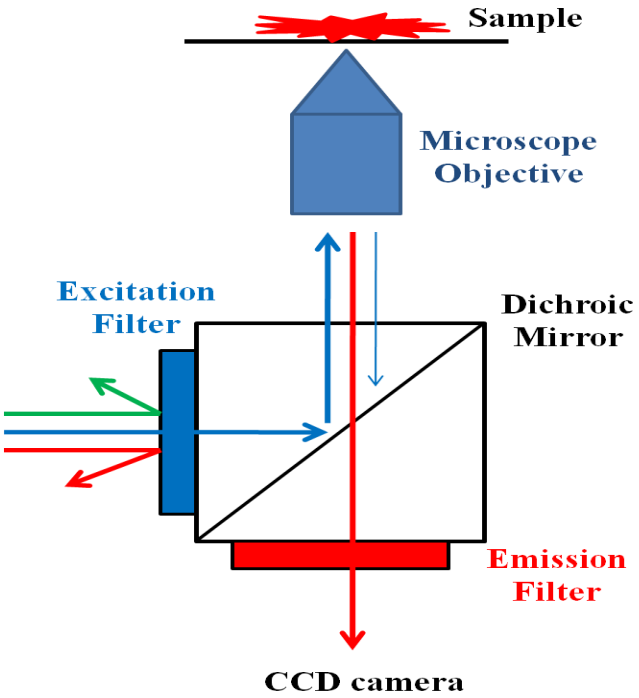

Scheme 3.1 Schematic illustration of light path through filter cube in an inverted fluorescence microscope.

Schematic representation of typical light path through filter cube of an inverted fluorescence microscope was shown in scheme 3.1. The filter cube consists of three types of filters: excitation filter, emission filter and dichromatic beam splitter (dichroic mirror). Excitation filter permits only selected wavelengths from the illuminator to pass through on the way toward the specimen. Emission filter is designed to suppress or absorb the excitation wavelengths and permit only selected emission wavelengths to pass toward the eye or other detector. A dichroic mirror is a specialized filter which is designed to efficiently reflect excitation wavelengths and pass emission wavelengths. It is positioned in the light path after the excitation filter but before the emission filter. Dichroic mirror is oriented at a 45 degree angle to the light passing through the excitation filter and at a 45 degree angle to the emission filter as illustrated in Scheme 3.1.

3.3.6 Transmission electron microscopy. Transmission electron microscope images were taken on JEOL 2000EX microscope at an accelerating voltage of 200 kV. One drop of InP/ZnS quantum dots (emitting at 520 nm) in chloroform solution was deposited on a copper grid covered by an amorphous carbon film and allowed to dry overnight.

3.3.7 Dynamic light scattering measurements. The average particle size and size distribution were determined by dynamic light scattering with a Malvern Zetasizer Nano ZS (Malvern Instruments Ltd., U.K.) at 25°C. About 0.2 mL of each liposome suspension was diluted with 2.5 mL of water immediately after preparation. Each experiment was repeated three times. The zeta potential was also measured by using a the Zetasizer ZS instrument. Zeta limits ranged from-150 to 150 V. Strobing parameters were set as follows: strobe delay -1.00, on time 200.00 ms, and off time 1.00 ms.

3.4 Results and Discussion

InP/ZnS quantum dots were synthesized as described by Peng *et al*.[20] Different sizes of InP/ZnS quantum dots with emission maxima ranging from 450 nm to 680 nm were prepared by varying the molar ratios of In and P precursors (Figure 3.1). The synthesized InP/ZnS quantum dots were characterized using spectrofluorometer and transmission electron microscopy.

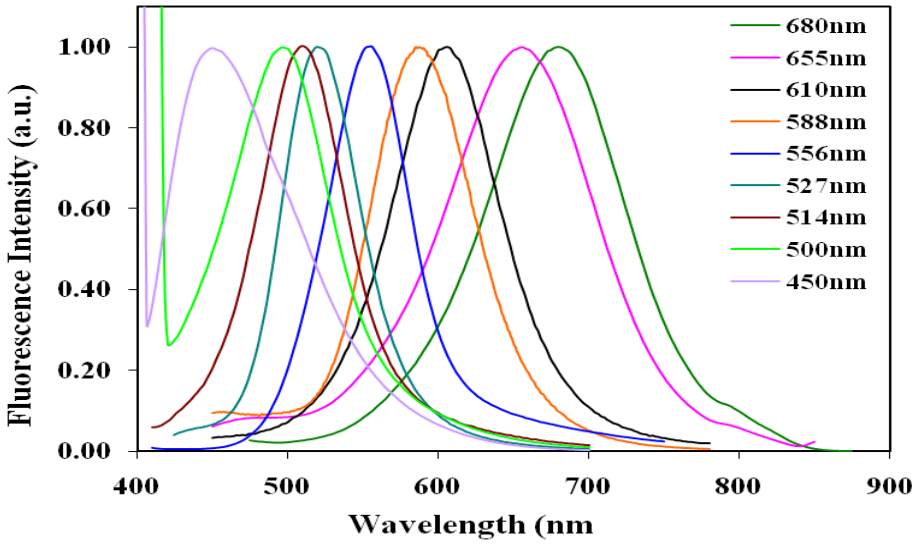

Figure 3.1 Normalized emission spectra of different InP/ZnS quantum dots in chloroform emitting from 450nm to 680nm.

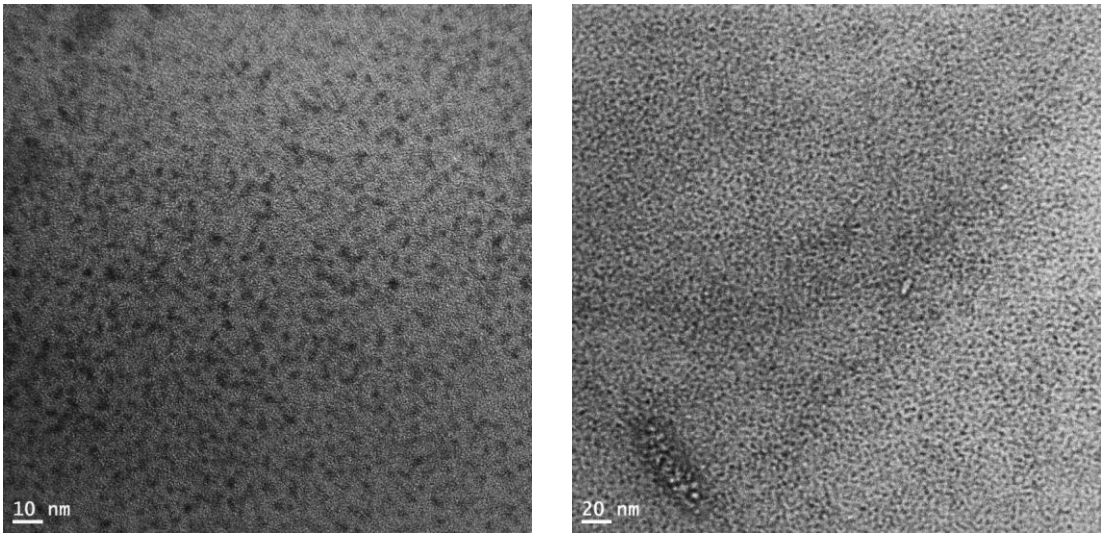

Figure 3.2 Transmission electron microscopic images of InP/ZnS QDs emitting at 556 nm.

(a)

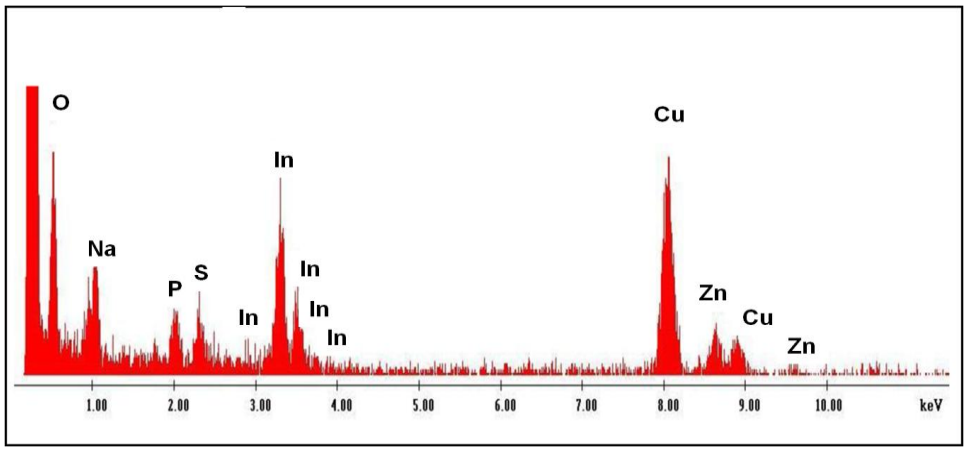

(b)

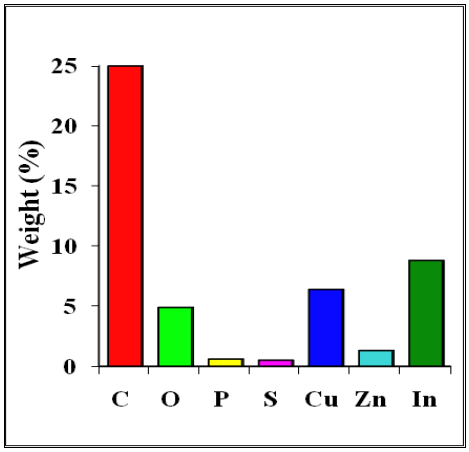

Element	Weight %	Atomic %
C K	77.6	92.3
O K	4.9	4.4
P K	0.6	0.4
S K	0.5	0.2
Cu K	6.4	1.4
Zn K	1.3	0.3
In L	8.8	1.0

Figure 3.3 (a) EDS spectrum of InP/ZnS QDs showing the individual peaks of In, P, Zn, and S elements. (b) elemental analysis showing a molar ratio of 1:0.4 for In: P in InP/ZnS QDs.

Figure 3.2 shows the transmission electron microscopic images at different magnifications of InP/ZnS quantum dots emitting at 556 nm. The corresponding EDS spectrum, shown in Figure 3.3 indicates the presence of individual peaks of In, P, Zn, and S elements confirming the composition of InP/ZnS quantum dots. Also, elemental analysis confirmed a molar ratio of 1:0.4 for In: P in InP/ZnS quantum dots comparable to the starting material ratio of In: P 1:0.5.

InP/ZnS quantum dot encapsulated in liposomes have been successfully prepared DMPC, Chol, DP (5:4:1) liposomal bilayer membrane rendering water solubility to the quantum dots.

This phospholipid composition provides maximum structural stability to liposomes stored at room temperature. During the encapsulation process, the surface of QDs interacts with hydrophobic regions of the liposomes via hydrophobic interactions and the hydrophilic region of the liposome is exposed to the water phase. The liposome encapsulated quantum dots were further characterized for optical properties using spectroflourometry and digital fluorescence imaging microscopy.

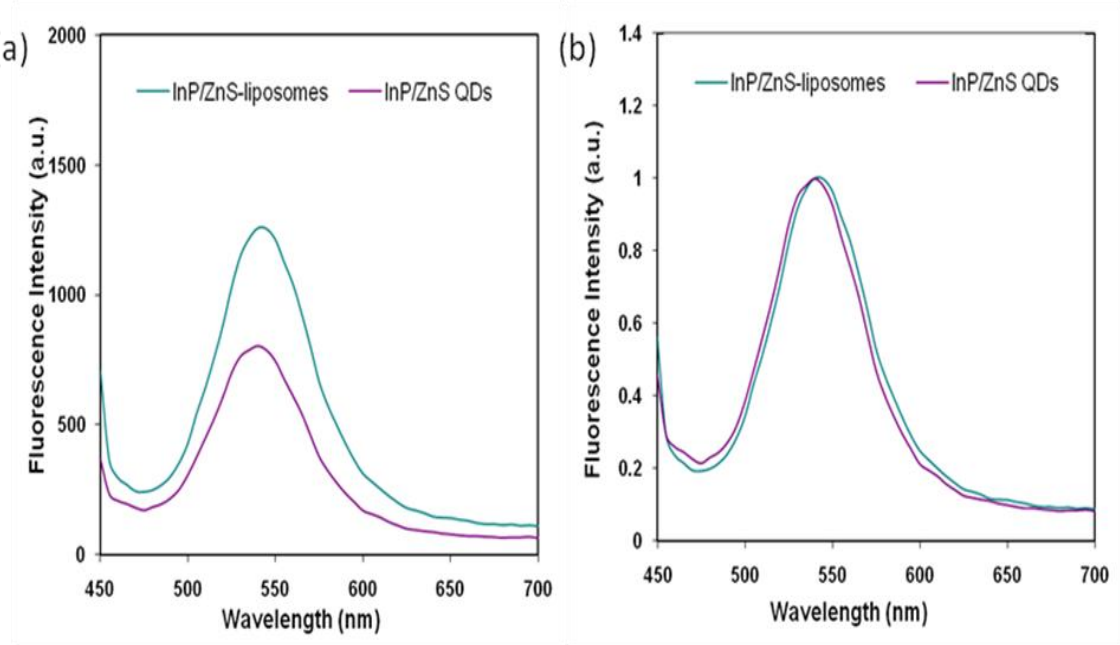

Figure 3.4 (a) Emission spectra and (b) normalized emission spectra of InP/ZnS quantum dots in chloroform (red) and liposome encapsulated InP/ZnS quantum dots (green) in pH 7.2 PBS buffer at the same concentration of quantum dots.

Figure 3.4 (a, b) are the emission and normalized emission spectra of InP/ZnS quantum dots in chloroform and liposome encapsulated InP/ZnS quantum dots in pH 7.2 PBS buffer with the same concentration of quantum dots. As quantum dots are surrounded by two different solvent environments in TOPO coated QDs and in liposome encapsulated QDs there might be some difference in the emission intensities as observed in Figure 3.4a. The normalized spectra

show that the optical properties of InP/ZnS quantum dots were well preserved even after encapsulation with liposomes.

The structural characteristics of these InP/ZnS QD-liposomes were studied by dynamic light scattering. The mean diameter of these QD-liposomes was found to be 102.7±6.8 nm, similar with the liposomes consisting of the equivalent lipids alone (100.9±3.0 nm). In particle size analysis system, the polydispersity index is used to describe the spread in particle diameters produced in a sample of particles. As the index approaches zero, the size range produced becomes narrower. The polydispersity index of the liposomes and QD-liposomes were 0.17±0.04 and 0.290±0.01 respectively indicating narrow size distribution. The surface charge characteristics measured using zeta potential was found to be -30 mV for liposomes and -29 mV for QD-liposome vesicles. The measurements thus revealed that the integrity of liposomes was well preserved even after incorporation with InP/ZnS quantum dots.

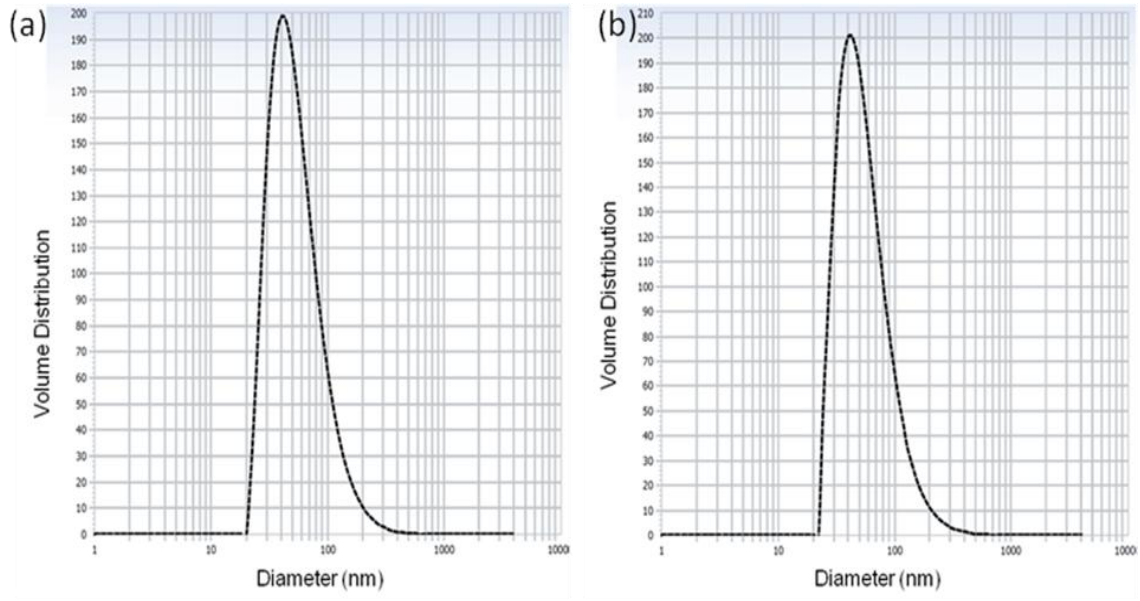

Figure 3.5 Particle size distributions of (a) liposomes and (b) InP/ZnS QD-liposomes.

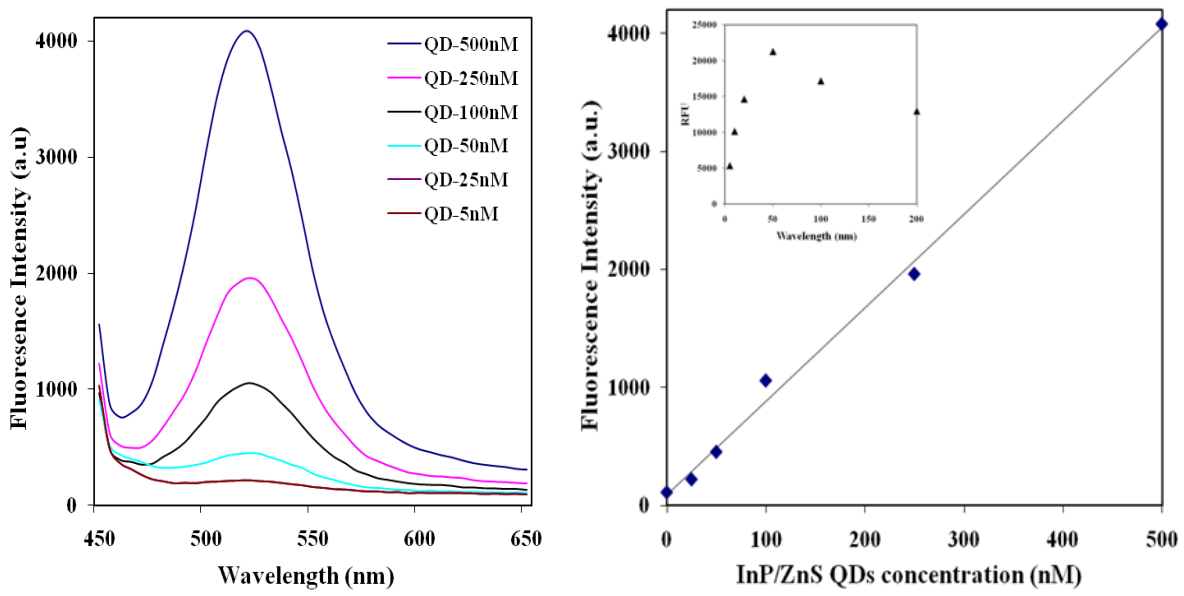

Figure 3.6 (a) Emission spectra, and (b) normalized graph of liposome encapsulated quantum dots in PBS pH 7.2 buffer at various concentrations from 0 nM to500 nM of quantum dots.

The effect of quantum dot concentration on emission intensity of QD-liposomes was studied and compared to that of fluorescein-liposomes (Figure 3.6). It was observed that the emission intensity of QD-liposomes increased with an increase in concentrations of quantum dots from 0 to 500 nM (Figure 3.6a) and the fluorescence intensity plotted as a function of QDs concentration showed a linear regression (Figure 3.6b). On the other hand, the emission intensity of fluorescein-liposomes increased with increase in concentration of fluorescein from 0-50 μM and then decreased (Figure 3.6b insert). This behavior can be attributed to self-quenching of fluorescein.

The photostability of InP/ZnS QD-liposomes was studied and compared with the MHDA capped quantum dots and InP/ZnS quantum dots for 60 min. For demonstration of photostability, all the samples were illuminated continuously with a mercury lamp of 60 W/cm^2 for 1 hr. The fluorescence intensity of the InP/ZnS QDs decreased by 57% of the initial intensity (Figure 3.7). On the other hand fluorescent intensity of MHDA capped QDs and QD-liposomes decreased to

30% and 27% of the initial intensities after 60 min of continuous illumination. This suggests that the encapsulation of InP/ZnS QDs into liposomes further enhances the photostability of the InP/ZnS quantum dots.

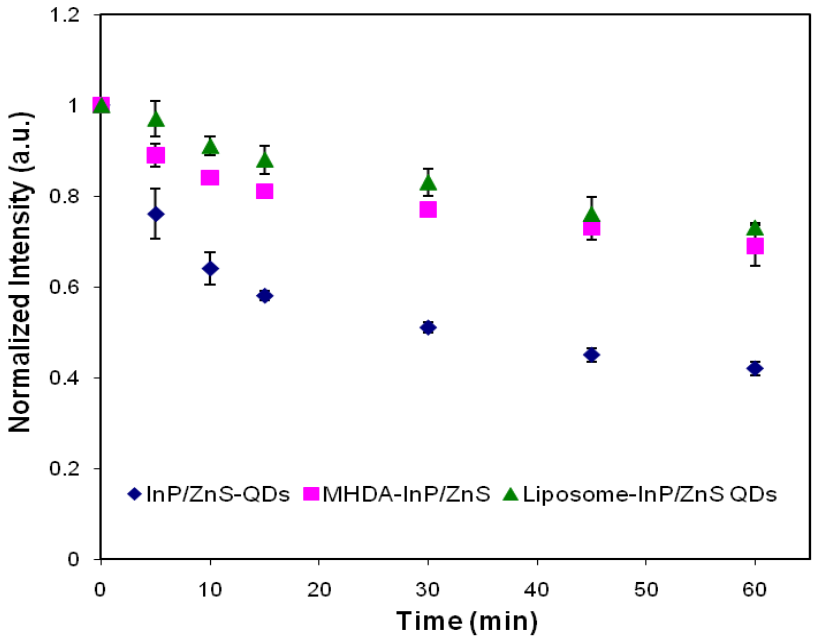

Figure 3.7 Photostability studies of lnP/ZnS quantum dots (♦), 16-mercaptohexadecanoic acid (MHDA) coated InP/ZnS QDs (■), and liposome encapsulated InP/ZnS quantum dots (▲) in PBS pH 7.2 buffer.

The effect of pH on the optical properties of InP/ZnS quantum dots encapsulated in liposomes as demonstrated in Figure 3.8 showed that the PL intensity of the InP/ZnS quantum dots was independent on the pH of the buffer. When changing the pH of the buffer from 4.2 to 11.2, less than 10% variation in the PL intensity of InP was observed as opposed to ~40% variation in PL intensity of InP/ZnS coated with mercaptosuccinic acid reported by Yong *et al*.[32] The bilayer surrounding the quantum dots is believed to have contributed to greater stability of QD-liposomes when altering the pH from 4.2 to 11.2.

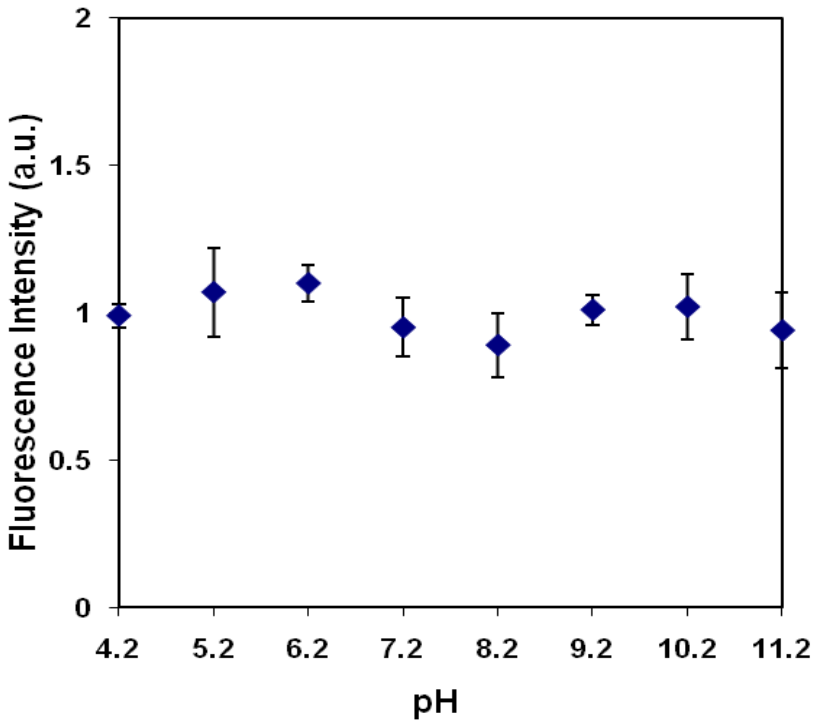

Figure 3.8 InP/ZnS PL intensity dependence on pH.

3.5 Conclusions

For the first time InP/ZnS quantum dots were incorporated into liposomes, making the InP/ZnS quantum dots water soluble and biocompatible. The structural characterization of InP/ZnS quantum dots demonstrated well preserved integrity of liposomes even after incorporation of InP/ZnS quantum dots. The photostability studies of InP/ZnS QD-liposomes compared with the MHDA capped quantum dots and InP/ZnS quantum dots showed that indeed encapsulation enhanced the photostability of the InP/ZnS quantum dots. The effect of pH on the optical properties of InP/ZnS quantum dots showed < 10% variation in the PL intensity of InP as opposed to ~40% variation in PL intensity of InP/ZnS coated with mercaptosuccinic acid reported previously by Yong *et al*.[32] The results show greater advantages of InP/ZnS QD-liposomes over InP/ZnS quantum dots. The InP/ZnS-liposome complexes thus synthesized will find a wide range of biological applications such as bioimaging, bioassays and immunoassays.

Thus InP/ZnS-liposome complexes can aid as potential tools in identification and diagnosis of several ailments associated with human pathology.

3.6 References

(1) Michalet, X.; Pinaud, F.; Bentolila, L. A.; Tsay, J. M.; Doose, S.; Li, J. J.; Sundaresan, G.; Wu, A. M.; Gambhir, S. S.; Weiss, S. *Science* **2005**, 307, 538-44.

(2) Jaiswal, J. K.; Simon, S. M. *Trends Cell Biol.* **2004**, 14, 497-504.

(3) Bruchez Jr, M.; Moronne, M.; Gin, P.; Weiss, S.; Alivisatos, A. P. *Science* **1998**, 281, 2013-2016.

(4) Chan, W. C.; Nie, S. *Science* **1998**, 281, 2016-2018.

(5) Peng, X. G.; Manna, L.; Yang, W. D.; Wickham, J.; Scher, E.; Kadavanich, A.; Alivisatos, A. P. *Nature* **2000**, 404, 59-61.

(6) Peng, Z. A.; Peng, X. G. *J. Am. Chem. Soc.* **2001**, 123, 183-184.

(7) Qu, L. H.; Peng, X. G. *J. Am. Chem. Soc.* **2002**, 124, 2049-2055.

(8) Medintz, I. L.; Goldman, E. R.; Mattoussi, H. *Nat. Mater.* **2005**, 4, 435-446.

(9) Kim, S.; Lim, Y. T.; Soltesz, E. G.; De Grand, A. M.; Lee, J.; Nakayama, A.; Parker, J. A.; Mihaljevic, T.; Laurence, R. G.; Dor, D. M.; Cohn, L. H.; Bawendi, M. G.; Frangioni, J. V. *Nat. Biotechnol.* **2004**, 22, 93-97.

(10) Hoshino, A.; Fujioka, K.; Oku, T.; Suga, M.; Sasaki, Y. F.; Ohta, T.; Yasuhara, M.; Suzuki, K.; Yamamoto, K. *Nano Lett.* **2004**, 4, 2163-2169.

(11) Kirchner, C.; Liedl, T.; Kudera, S.; Pellegrino, T.; Javier, A. M.; Gaub, H. E.; Stolzle, S.; Fertig, N.; Parak, W. J. *Nano Lett.* **2005**, 5, 331-338.

(12) Derfus, A. M.; Chan, W. C. W.; Bhatia, S. N. *Nano Lett.* **2004**, 4, 11-18.

(13) Yoffe, A. D. *Adv. Phys.* **2001**, 50, 1, 1-208.

(14) Pearton, S. J.; Abernathy, C. R.; Overberg, M. E.; Thaler, G. T.; Norton, D. P.; Theodoropoulou, N.; Hebard, A. F.; Park, Y. D.; Ren, F.; Kim, J.; Boatner, L. A. *J. Appl. Phys.* **2003**, 93, 1, 1-13.

(15) Bosi, M.; Pelosi, C. *Prog. Photovoltaics.* **2007**, 15, 51-68.

(16) Kim, S. H.; Wolters, R. H.; Heath, J. R. *J. Chem. Phys.* **1996**, 105, 7957-7963.

(17) Kortan, A. R.; Hull, R.; Opila, R. L.; Bawendi, M. G.; Steigerwald, M. L.; Carroll, P. J.; Brus, L. E. *J. Am. Chem. Soc.* **1990**, 112, 1327-1332.

(18) Battaglia, D.; Peng, X. G. *Nano Lett.* **2002**, 2, 1027-1030 .

(19) Talapin, D. V.; Gaponik, N.; Borchert, H.; Rogach, A. L.; Haase, M.; Weller, H. *J. Phys. Chem. B.* **2002**, 106, 12659-12663.

(20) Xie, R. G.; Battaglia, D.; Peng, X. G. *J. Am. Chem. Soc.* **2007**, 129, 15432-15433.

(21) Xu, S.; Ziegler, J.; Nann, T. *J. Mater. Chem.* **2008**, 18, 2653–2656.

(22) Li, L.; Reiss, P. *J. Am. Chem. Soc.* **2008**, 130, 11588–11589.

(23) Barber, K.; Mala, R. R.; Lambert, M. P.; Qiu, R. Z.; MacDonald, R. C.; Klein, W. L. *Neurosci. Lett.* **1996**, 207, 17-20.

(24) Udupa, N.; Chandraprakash, K. S.; Umadevi, P.; Pillai, G. K. *Drug De*v. *Ind. Pharm.* **1993**, 19, 1331–1342.

(25) Williams, D. M.; Carter, K. C.; Baillie, A. J. *J. Drug Targeting* **1995**, 3, 1–7.

(26) Ruckmani, K.; Jayakar, B.; Ghosal, S. K. *Drug Dev. Ind. Pharm.* **2000**, 26, 217–222.

(27) Veronica, D.; Melissa, R.; Gilchrist, M. L.; Holland, E. C. Vazquez, M. *J. Nanosci. Nanotechnol.* **2008**, 8, 2293-2300.

(28) Al-Jamal, W. T.; Al-Jamal, K. T.; Tian, B.; Lacerda, L.; Bomans, P. H.; Frederik, P.M.; Kostarelos, K. *ACS Nano* **2008**, 2(3), 408-418.

(29) Weng, K. C.; Noble, C.; Papahadjopoulos-Sternberg, B.; Chen, F. F.; Drummond, D. C.; Kirpotin, D. B.; Wang, D.; Hom, Y. K.; Hann, B, Park, J. W. *Nano Lett.* **2008**, 8(9), 2851-2857.

(30) Yang, C.; Ding, N.; Xu, Y.; Qu, X.; Zhang, J.; Zhao, C.; Hong, L.; Lu, Y.; Xiang, G. *J Drug Target.* **2009**, 17, 7, 502-511.

(31) Park, K. Ed. *Controlled Drug Delivery: Challenges and Strategies*; American Chemical Society: Washington, DC, **1997**.

(32) Yong, K; Ding, H; Roy, I; Law, W; Bergey, E.J.; Maitra, A.; Prasad, P.N. *ACS Nano*, **2009**, 3 (3), 502-510.

Chapter 4

CdSe/ZnS quantum dot based immunoassay for simultaneous detection of myocardial infarction biomarkers

4.1 Abstract

Myocardial infarction or heart attack is the leading cause of death worldwide for both men and women. Sensitive and selective measurement of cardiac biomarkers is crucial in assisting diagnosis of heart attack and in assessing the patients with nondiagnostic electrocardiograms. Quantum dot based probes are receiving great attention for optical imaging of cells and in bioassays as an alternative to conventional organic fluorophores due to their unique size-dependent chemical and physical properties. In the current study quantum dot based fluorescence immunoassay was developed for simultaneous detection of the cardiac biomarkers troponin T and troponin I. A sandwich immunoassay was performed with capture antibodies immobilized on a 96-well plate. After binding targeted biomarkers to capture antibodies, detection antibodies conjugated to CdSe/ZnS quantum dots were then bound to the specific biomarkers forming a sandwich complex. The results of the assay showed a clear dependence of concentrations for both troponin T and I on the fluorescence emission of quantum dots that were bound to the detection antibodies. The detection limit for both troponin T and troponin I was 0.1 pg/mL. No significant cross reactivity was seen between the antibodies and the antigens. The multiplex detection method for screening of biomarkers is expected to yield a high throughput diagnostic tool for heart attack.

4.2 Introduction

Myocardial infarction (MI) or heart attack is the leading cause of death in both men and women worldwide.[1] Although long step have been taken to reduce the number of deaths, the number of patients is still increasing.[2, 3] Over several decades, the diagnosis of MI has been based on the "two out of three" criteria as defined by World Health Organization, including typical chest pain that lasts for more than 20 minutes, changes in electrocardiogram, and increase in the serum level of creatine kinase-MB.[4] The criteria for diagnosis was redefined recently, that gave more importance to cardiac biomarkers especially troponins as they are more superior to conventional measurement of CK-MB.[5, 6] Troponin is a complex of three regulatory muscle proteins troponin T (TnT), troponin I (TnI), and troponin C (TnC) that play crucial role in muscle contraction. Cardiac and skeletal muscles contain both troponin T and I, however the amino acid sequences of the proteins are different.[7] Troponin C is shared by cardiac and skeletal muscles and therefore do not exhibit cardiac specificity and is not used in the diagnosis of cardiac injury. Under normal conditions troponin T and I levels are very low, but immediately after heart attack the concentrations rise rapidly. The release kinetics is within 4-13 hour for both TnT and TnI following myocardial damage.[8, 9]

For the first time in 1989 Katus *et al* described an enzyme immunoassay to detect troponin T in human serum.[10] The troponin T was bound to the solid phase by an affinity-purified polyclonal antibody and detected by peroxidase labeled monoclonal antibody using one-step sandwich assay. Later the same group developed a much more sensitive enzyme immunoassay, using two troponin T-specific monoclonal antibodies with streptavidin-coated polystyrene tubes as the solid phase.[11] Recently Mayilo *et al* developed a homogenous immunoassay with gold nanoparticles as fluorescence quenchers, using this method a detection limit of 0.7 ng/mL for

cTnT was achieved.[12] The first assay that demonstrated the potential diagnostic specificity of troponin I quantification for myocardial infarction was developed by Cummins *et al* in 1983.[13] Currently, several immunoassay methods are available commercially for the detection of troponin I and troponin T separately, most of them are based on UV and some of them are based on fluorescence.[14-16] However, the current detection limits of troponin assays do not allow demonstration of normal cardiac troponin levels in healthy controls.[17] Thus lower detection limits with improved assay sensitivity and precision are required to improve risk assessment.

Colloidal semiconductor nanoparticles or quantum dots (QDs) have emerged as a new generation fluorescent labels in the two decades for optical imaging of cells, tissues and in bioassays as alternatives to conventional organic fluorophores due to their unique optical properties.[18-25] QDs offer advantages like brightness, greater photostability, and broad excitation wavelength range, size-tunable narrow and symmetric emission spectrum. More importantly, regardless of the excitation wavelength QDs can be excited efficiently at any wavelength shorter than the emission peak that will emit the same narrow, symmetric characteristic spectrum. This unique property makes it possible to simultaneously detect different emission peaks when different sizes of QDs are excited with a single wavelength. QDs have been used as fluorescent labels in several applications including multicolor imaging of tissues[26] and detection of toxins.[27] The applications of QDs have also been extended for microorganism detection using multicolor detection based immunoassay formats.[28, 29] Previously it was shown that QDs has exhibited superior photostability than traditional organic dyes in detection and has allowed dual color for *Cryptosporidium parvum* and *Giardia lamblia*.[30]

In the current study a new method of CdSe/ZnS quantum dot based fluorescence immunoassay has been developed for simultaneous detection of the cardiac biomarkers troponin

T and troponin I. In the immunoassay the capture antibodies were immobilized on a 96-well plate that were later bound to targeted biomarkers. A sandwich complex was formed after detection antibodies conjugated to CdSe/ZnS quantum dots were bound to their specific biomarkers. The results of the assay showed a clear dependence of troponins concentration on the fluorescence emission of quantum dots attached to the detection antibodies. Detecting the two biomarkers simultaneously is aimed to yield a high throughput diagnostic tool for heart attack.

4.3 Experimental Methods

4.3.1 Materials and reagents. Technical grade (90%) trioctylphosphine oxide (TOPO), technical grade (90%) trioctylphosphine (TOP), cadmium oxide (99.99%), selenium powder (99.5%), lauric acid (98%), technical grade (90%) hexadecylamine (HDA), diethyl zinc ($Zn(Et)_2$) solution 1.0 M in heptane, hexamethyldisilathiane ($(TMS)_2S$), methanol anhydrous (99.8%), chloroform (99.5%), 16-mercaptohexadecanoic acid (MHDA), tetramethylammonium hydroxide pentahydrate, Tween 20, 1-ethyl-3-(3-dimethylaminopropyl) carbodiimide hydrochloride (EDC), sulfo-*N*-hydroxysulfosuccunimide (sulfo-NHS), and bovine serum albumin (BSA) were purchased from Sigma Aldrich. Amine reactive maleic anhydride activated 96 well plates, and super block blocking buffer were purchased from Thermo Scientific. Mouse monoclonal cardiac troponin T antibody (1C11), mouse monoclonal cardiac troponin I antibody (M18), cardiac troponin T protein, cardiac troponin I protein, and creatine kinase-MB protein were purchased from Abcam. Mouse monoclonal cardiac troponin T antibody (7e7), and mouse monoclonal cardiac troponin I antibody (MF4) were purchased from Santa Cruz biotechnology.

4.3.2 Synthesis of TOPO capped luminescent quantum dots. TOPO-capped CdSe/ZnS quantum dots were prepared following a method first proposed by Peng *et al*[31] with a slight

modification.[32] Briefly, 12-13 mg of cadmium oxide and 160-180 mg of lauric acid were mixed under nitrogen atmosphere. The mixture was heated in a 100 mL three neck flask to slightly above 180°C to fully dissolve the cadmium oxide (clear solution). Then, 2 g of TOPO and 2 g HDA were added to the solution with constant stirring. Temperature was raised to 280°C before being cooled down slowly. Upon reaching the desirable temperature 80 mg selenium powder dissolved in 2 mL solution of TOP was rapidly injected into the solution under vigorous stirring. For shell coating, a 2 mL TOP solution containing 250 μL $(TMS)_2S$ and 1 mL $Zn(Et)_2$ was injected drop-wise into the solution. The reaction mixture was kept at 180°C for one hour before it was cooled to room temperature and washed three times with methanol, centrifuged at 4000 rpm for 10 minutes each, and redispersed in chloroform. The concentration of this solution was found to be 1 μM. The solution was stored at room temperature.

4.3.3 Synthesis of mercaptohexadecanoic acid (MHDA) coated quantum dots. 16-mercaptohexadecanoic acid coated quantum dots were prepared following a modified procedure developed by Bawendi[33] for the synthesis of lipoic acid capped CdSe/ZnS core-shell quantum dots. 25 mg of MHDA was heated up to 70-80°C to dissolve and 3 mL of 1 μM TOPO coated quantum dots and 3 mL of chloroform were added and stirred for 2-3 hours at 50-60°C. Then 6 mL of DI water containing tetramethylammonium hydroxide pentahydrate was added to the mixture and stirred for another half hour at room temperature and then allowed to settle down for few minutes. This resulted in a two-phase mixture with the aqueous MHDA coated quantum dots layer above the organic chloroform layer. The aqueous layer was collected and centrifuged several times to remove TOP/TOPO until clear solution was seen. Then the clear suspensions were collected and spin dialyzed two times with a cutoff molecular weight of 30000 Da to remove the excess MHDA. In each spin dialysis cycle, the sample was centrifuged at 3000 rpm

for 20 minutes and washed with DI water. MHDA coated quantum dots were kept at 4°C in DI water until used.

4.3.4 Conjugation of MHDA coated quantum dots with detection antibodies. Conjugation of antibodies onto MHDA coated CdSe/ZnS quantum dots was achieved using the classic EDC coupling reaction of COOH groups on the surfaces of the MHDA coated quantum dots and NH_2 groups of the antibody. Typically, 0.1 mL of MHDA coated CdSe/ZnS quantum dots, 20 μL of 30 mg/mL EDC and 20 μL of 30 mg/mL sulfo-NHS were added into a 1.5 mL tube. The mixture was vortexed for 15-20 min at room temperature to fully activate free carboxylic acid groups on the quantum dots. In this step, semi stable amine-reactive NHS-ester could be synthesized by the esterification of the activated carboxylic acid groups on the QDs and hydroxyl groups on the sulfo-NHS. 100 μL of detection antibodies was added into the system and was vortexed for at least 2 h. The unreacted antibody molecules were removed from the media by centrifugal concentrators (cutoff molecular weight: 100 kD). Quantum dots and antibodies were connected through strong covalent bonds. The final products were recollected into 10 mM PBS pH 7.4 buffer containing 0.1% BSA and kept at 4°C. The purified quantum dot-antibody conjugates were ready to be used to detect the target antigens.

4.3.5 Individual fluoroimmunoassays. Fluoroimmunoassays were essentially performed as previously described.[34, 35] Wells of clear microtiter plates were washed three times with 200 μL of wash buffer (PBS pH 8.0 buffer containing 0.05% Tween 20). Then, 100 μL of 25 μg/mL concentration of capturing antibodies dissolved in 10 mM PBS pH 7.4 buffer were added to the plate and incubated overnight at room temperature. The capture solution was discarded and the plates were blocked using 200 μL of super block blocking buffer and incubated for one hour at room temperature. This quenches the remaining reactive maleic anhydride groups and also

blocks left over open sites on the plate surface. The blocking buffer was discarded and the plate washed three times with wash buffer. Different concentrations of 100 μL, troponin T or troponin I antigens were added to plate wells and incubated for 1 hour at room temperature. Plate wells were washed three times with wash buffer to remove the unbound antigens. 100 μL of the detection antibodies conjugated to different colored quantum dots were added to the plate wells and incubated for one hour at room temperature and the unbound antibodies were removed by washing three times with the wash buffer.

4.3.6 Multiplexing fluoroimmunoassays. Wells of clear microtiter plates were washed three times with 200 μL of wash buffer (PBS pH 8.0 buffer containing 0.05% Tween 20). Then, 50 μL each of 50 μg/mL concentration of capturing antibodies dissolved in 10 mM PBS pH 7.4 buffer were added to the plate and incubated overnight at room temperature. The capture solution was discarded and the plates were blocked using 200 μL of super block blocking buffer and incubated for one hour at room temperature. The blocking buffer was discarded and the plate washed three times with wash buffer. Different concentrations of 50 μL of troponin T and troponin I antigens were added to plate wells and incubated for 1 hour at room temperature. Plate wells were washed three times with wash buffer to remove the unbound antigens. 50 μL each of the detection antibodies conjugated to two different colored quantum dots were added to the plate wells and incubated for one hour at room temperature and the unbound antibodies were removed by washing three times with the wash buffer.

4.3.7 Fluorescence spectroscopy measurements. Excitation and emission spectra were measured using a spectrofluorometer (SpectraMax M2, Molecular Devices) equipped with a 75 W continuous xenon arc lamp as a light source. All the samples were excited at 400 nm. Emission scans were measured from 450-750 nm.

4.3.8 Digital fluorescence imaging microscopy. Luminescence images were obtained using a digital inverted fluorescence microscope (Olympus IX71) equipped with a 100 W mercury lamp as a light source. The fluorescence images were collected via a 20 X microscope objective with numerical aperture = 0.5. A filter cube containing a 380±20 nm band-pass excitation filter, a 425 nm dichroic mirror, and a 450 nm long pass emission filter was used to ensure spectral imaging purity. Digital point controller (DP72) was used for digital imaging. An exposure time of 100 ms was typically used to acquire the fluorescence images.

4.4 Results and Discussion

TOPO coating of the luminescent CdSe/ZnS quantum dots were first replaced with 16-mercaptohexadecanoic acid using ligand exchange method. The optical properties of the quantum dots were well preserved even after ligand exchange with MHDA. Antibody conjugated quantum dots are often used for biological labeling and staining.[36] Covalent conjugation of quantum dots with biomolecules is most commonly based on cross-linking reactions between amine and carboxylic acid groups, between amine and sulfhydryl groups, or between aldehyde and hydrazide functional groups. Among these methods the amine-carboxylic acid cross-linking method is the more prominent one as most proteins contain primary amine and carboxylic acid groups and do not need chemical modifications before conjugation. However, some instability of the QDs might occur with this technique when chemically modifying the QDs stabilizer cap and the cross-reaction of the QD-COOH groups with multiple amines on biomolecules.[37] To overcome this problem, Hu *et al* studied the key factors influencing the chemical stability of QDs and demonstrated a QD-based bioconjugating strategy.[38] In the current work EDC coupling of quantum dots with the different detection antibodies were achieved following their method.

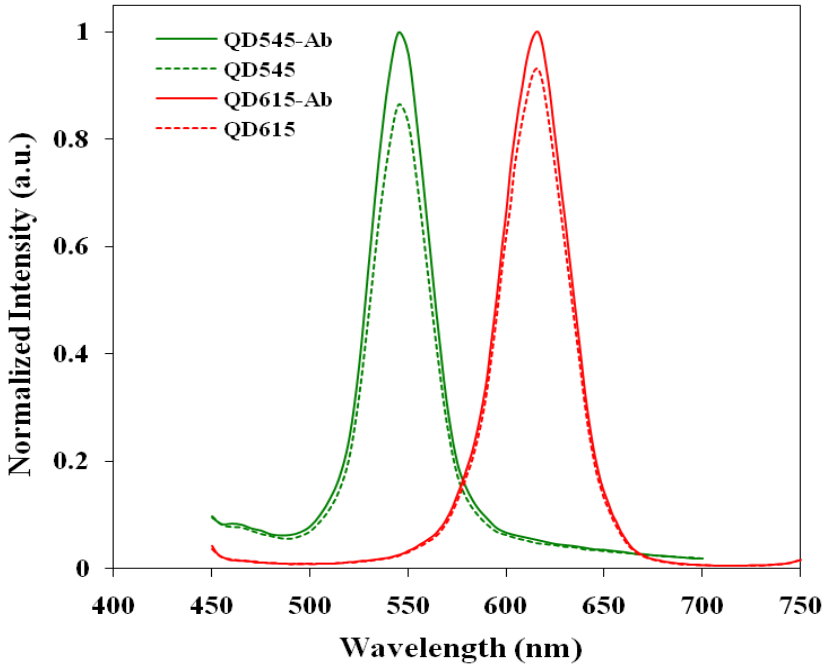

Figure 4.1 Fluorescence intensities of two different colored quantum dots (dotted lines) and QD-detection antibody conjugates (continuous lines) at the same concentration of QDs.

Figure 4.1 shows the emission spectra of 545 and 615 nm quantum dots before and after conjugation with the detection antibodies of troponin T and troponin I respectively. Quantum dot-antibody conjugates have shown slight enhancement in the emission intensity of the QDs while retaining optical properties of the quantum dots. This enhancement in intensity might be due to presence of antibodies layer on the surface of quantum dots. The stability of the QD-antibody conjugates stored at 4°C temperature was studied over a period of 28 days. The QD-antibody conjugates have shown very good stability when stored in 10 mM PBS pH 7.4 buffer containing 0.1% BSA demonstrated by 5% decrease in the initial fluorescence intensity (Figure 4.2).

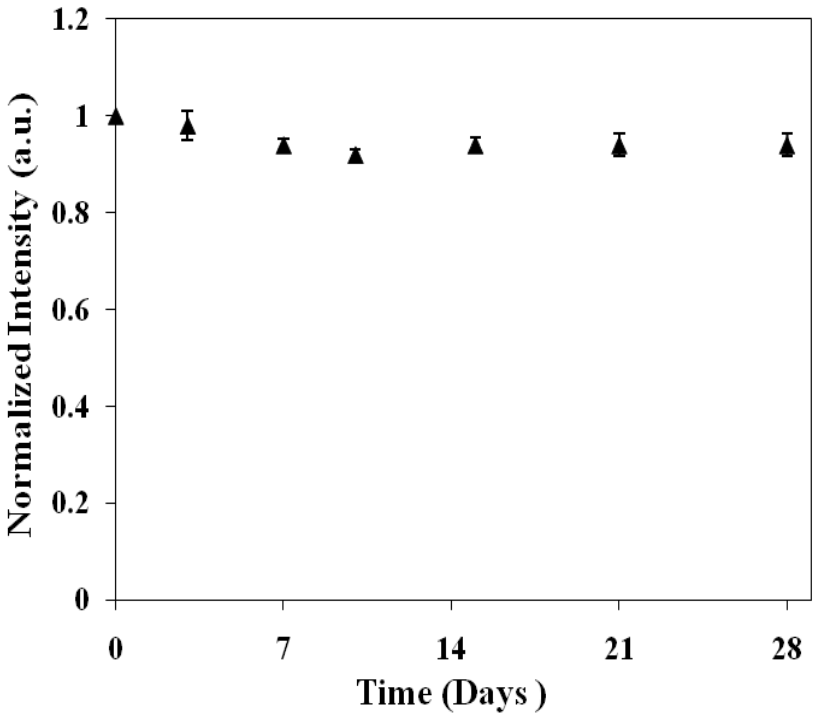

Figure 4.2 Normalized fluorescence intensity of QD-antibody conjugates at different days.

The immunoreaction was performed using sandwich type procedure. Scheme 4.1 shows the quantum dot based fluoroimmunoassay protocol used in this work. At first the capture antibodies were immobilized on the well plate followed by the addition of blocking buffer to block the nonspecific binding sites. The antigens, troponin T or/and troponin I were added that bind to their corresponding capture antibodies. The unbound antigens were removed by washing. Finally the detection antibodies conjugated to 545 or/and 615 nm quantum dots were added that bind to the corresponding antigens forming a sandwich immunocomplex. The fluorescence intensities of the quantum dots attached to the immunocomplex were measured for the quantification of the antigens troponin T and troponin I.

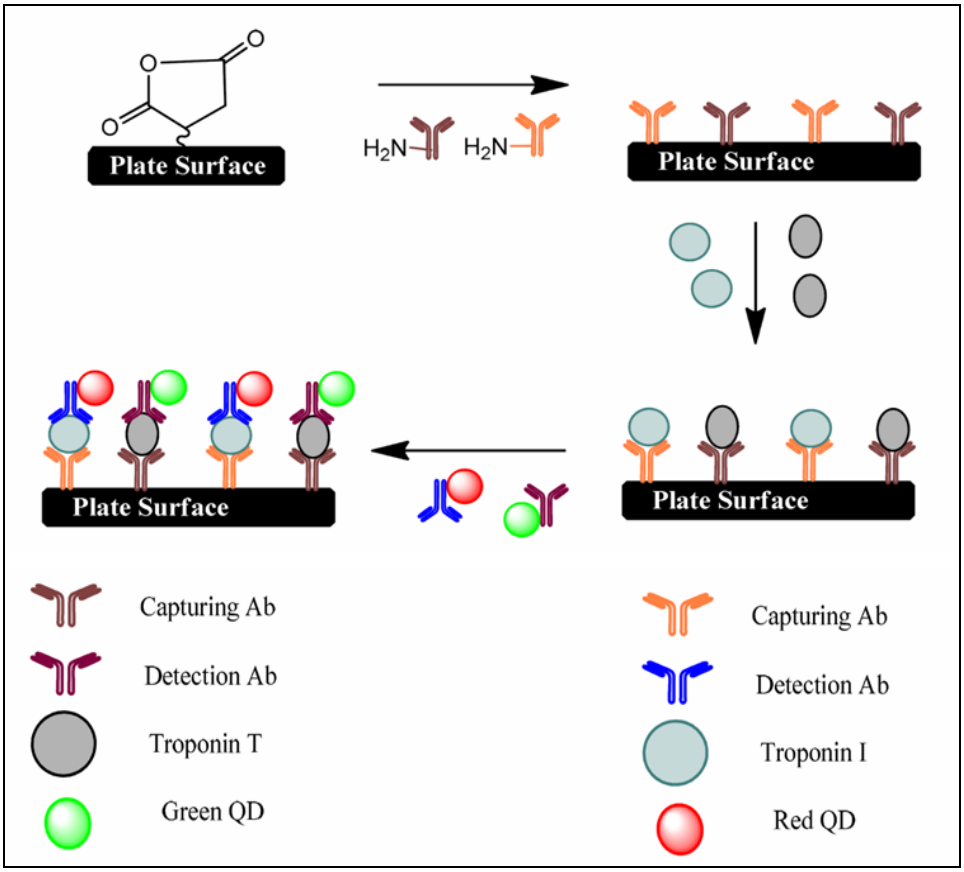

Scheme 4.1 Schematic representation of QD based fluoroimmunoassay principle.

4.4.1 Optimization of experimental conditions. The immobilization of the capturing antibody on well plate is crucial since it is the first step in the immunoassay system. The concentration of capture antibody solution in the immobilization determines the amount of antibody immobilized on the well plate. Serial concentrations of antibody solution were tested in order to investigate the maximum loading of the capturing antibody. The fluorescence intensity of the quantum dots present in the immunocomplex was increased with the capture antibody concentrations from 0 to 25 µg/mL. Further increase of antibody concentration in the immobilization did not improve the results (Figure 4.3).

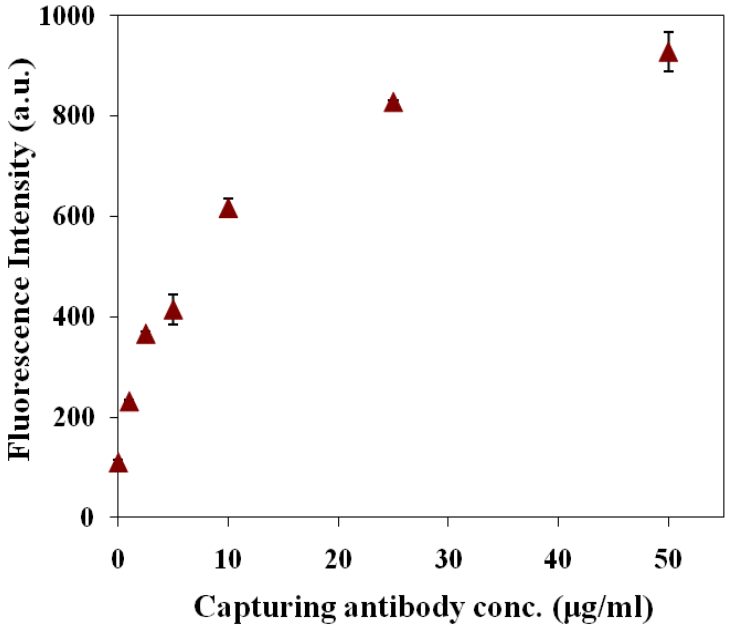

Figure 4.3 Immobilization of capturing antibody (anti-TnT) on 96-well plate at 10 ng/mL of troponin T protein and 60 minutes of incubation time. λ_{ex}: 400 nm.

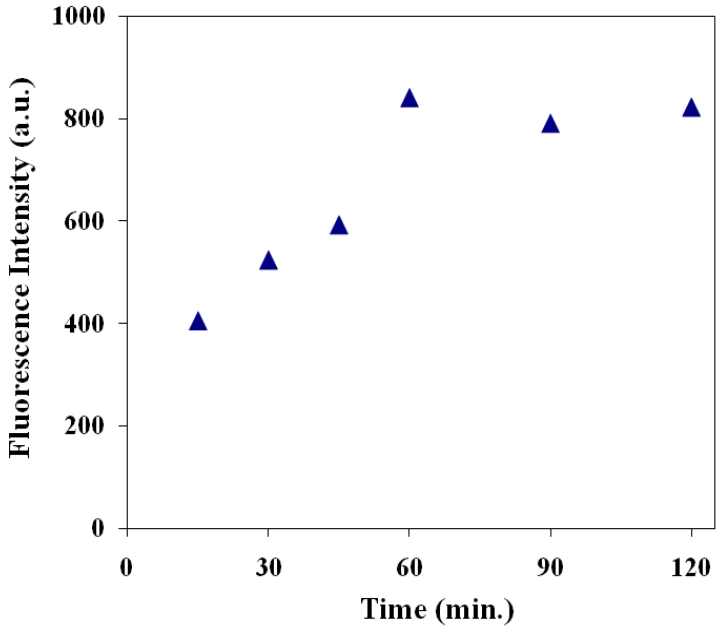

Figure 4.4 Effect of incubation time on capture of antigen on 96-well plate at 25 µg/mL of capture antibody and 10 ng/mL of troponin T protein concentration. λ_{ex}: 400 nm

Next, the effect of incubation time for capturing antigen by the capturing antibody on the plate was also optimized. As shown in Figure 4.4 the fluorescence intensity was increased with increasing the incubation time up to 60 minutes and further increasing in time did not show any increase in the emission intensity indicating that 60 minutes incubation time is optimal. Further incubation with longer time may destroy the activity of the antigen and might exert an effect on the reorganization of quantum dot conjugated detection antibodies with antigen.

4.4.2 Individual Assays. For each of the two antigens single analyte assays were performed initially to ensure the usefulness of QD-antibody pairs in a multicolor multianalyte study. In these assays, only the appropriate capture antibody and individual antigens were applied to wells, and the emission intensities of single colored QDs that are conjugated to detection antibodies will be measured for quantification.

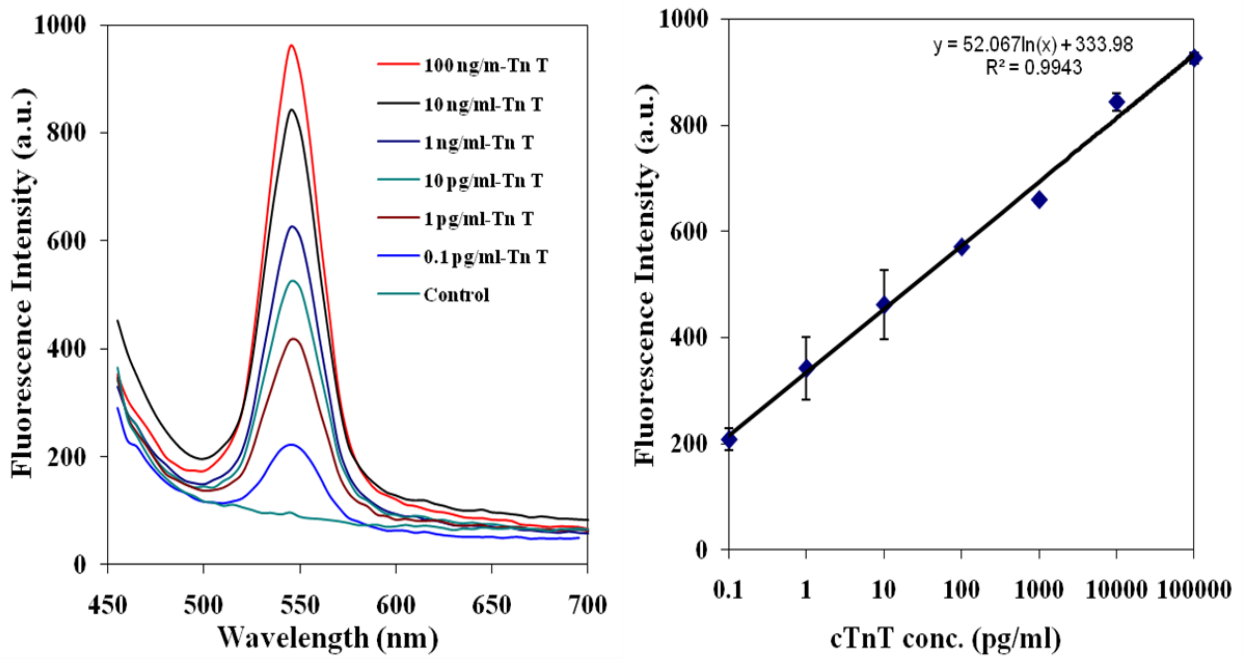

Figure 4.5 a) Emission spectra of 545 nm emitting QDs in the immunocomplex at different concentrations of troponin T b) relationship between troponin T concentration and the fluorescence intensity of the QDs.

Figure 4.5a shows the fluorescence emission spectra of 545 nm emitting quantum dots that are conjugated to anti-TnT antibodies. The emission intensity increased with increasing concentration of troponin T from 0 to 10 ng/mL. There is a linear-log relationship between the enhanced intensity of quantum dots and the concentration of troponin T (Figure 4.5b). The detection limit is as low as 0.1 pg/mL for the troponin T which is the best detection limit achieved so far that allows the demonstration of the troponin T levels even in the healthy normal controls.

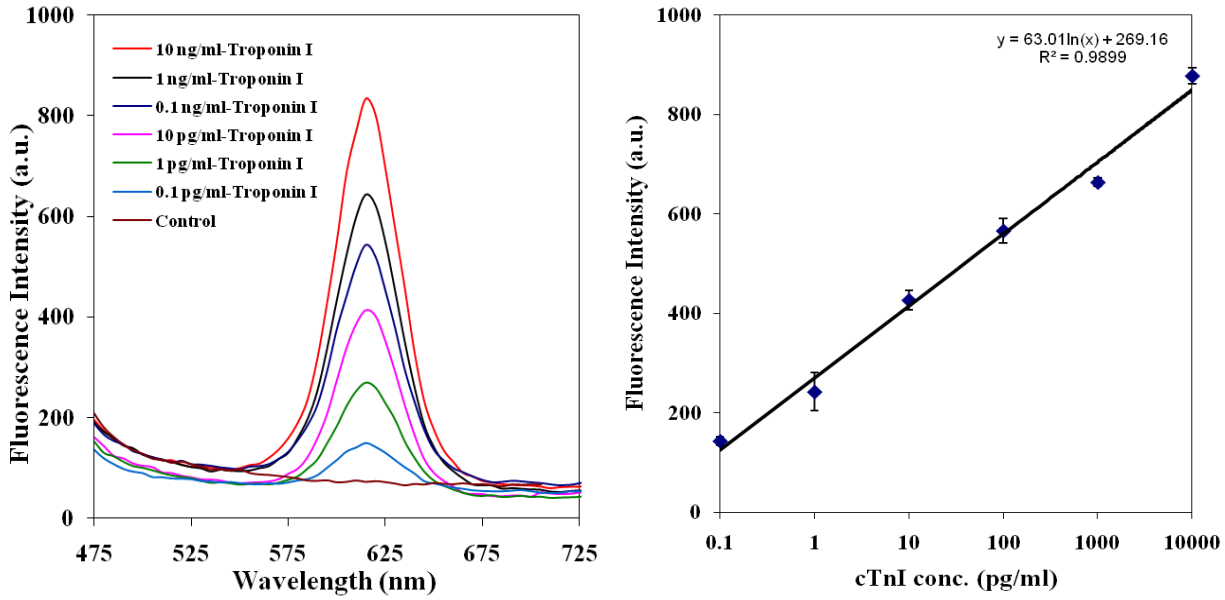

Figure 4.6 a) Emission spectra of 615 nm emitting QDs in the immunocomplex at different concentrations of troponin I b) relationship between troponin I concentration and the fluorescence intensity of the QDs.

Similarly Figure 4.6a is the fluorescence emission spectra of 615 nm emitting quantum dots that are conjugated to anti-TnI antibodies. Similar to troponin T the emission intensity increased with increasing concentrations of troponin I. Figure 4.6b shows the concentration dependence of the emission intensity of the quantum dots. Similar to troponin T the detection limit was as low as 0.1 pg/mL for the troponin I.

In principle, the specificity of the method depends mainly upon the specificity of the monoclonal antibodies. Nevertheless, the selectivity of the method is also affected by the non-specific binding on well plate, the properties of the proteins, and the nature of the fluorescence labels. The specificity of the method was studied to check for any cross reactivity between the antigens and antibodies. The experiments involved the addition of anti-troponin T capturing antibody to the well plate followed by the addition of four different antigens 1% BSA, troponin T, CK-MB, and Troponin I. The anti-troponin T detection antibodies conjugated to 545 nm emitting QDs were added to the well plate. The signals of the quantum dots for this experiment are represented as green bars in figure 4.7. Similar procedure was performed for troponin I and the signals from the 615 nm emitting QDs are represented as red bars in the figure 4.7. Greater signal intensities were observed for the specific antigen-antibody conjugates while there is no cross reactivity of the antibodies with the other antigens demonstrating the specificity of the method.

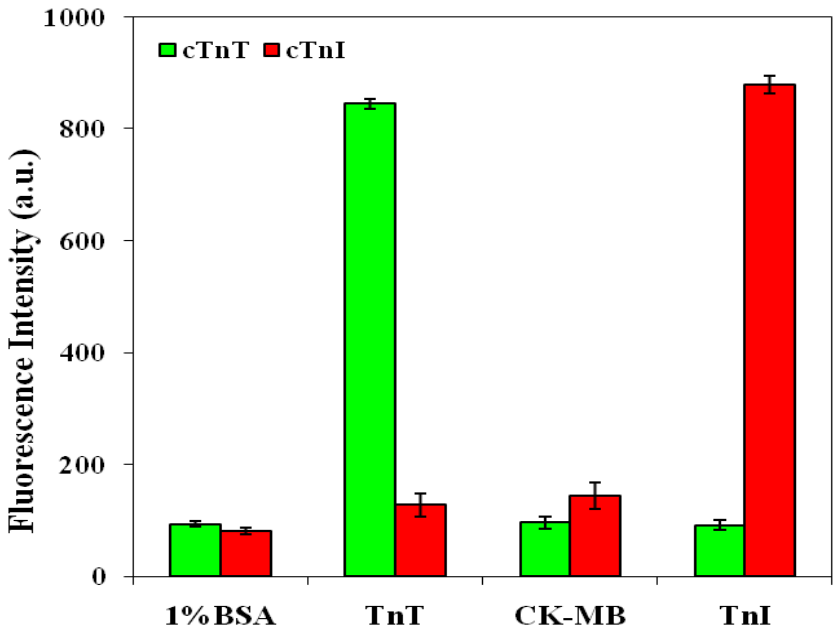

Figure 4.7 The selectivity of the quantum dot based fluoroimmunoassay method.

4.4.3 Multiplexing Assay. A mixture of troponin T and I capture antibodies were coated on the plate. After binding of troponin T and I antigens to capture antibodies, the detection antibodies conjugated to CdSe/ZnS quantum dots were then bound to the specific biomarkers. The emission spectra of both 545 nm and 615 nm QDs are showed in figure 4.8. The fluorescence intensities increased with increasing concentrations of troponin T and troponin I indicating dependence of the QDs signals on the concentrations of the corresponding antigens.

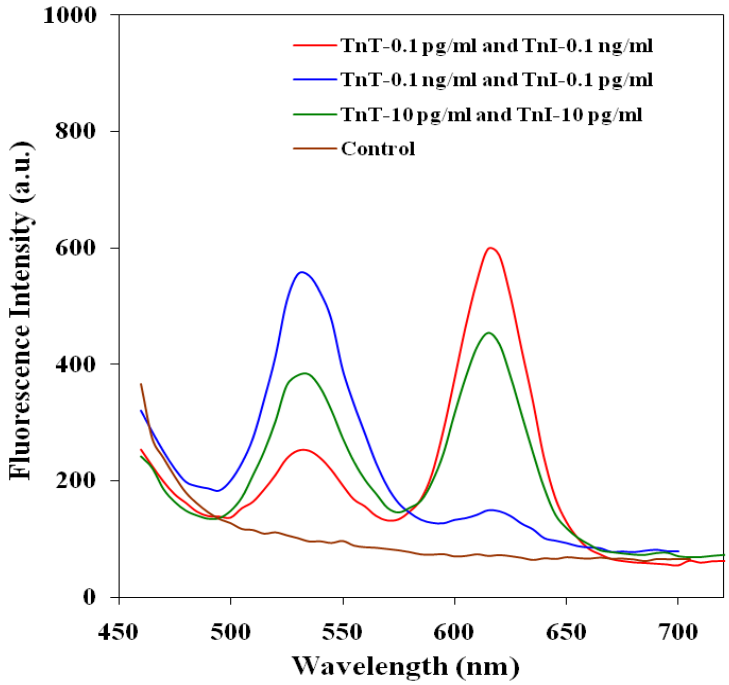

Figure 4.8 Emission spectra of 545 nm and 615 nm emitting QDs that are bound to different concentrations of troponin T and troponin I respectively.

4.5 Conclusions

In summary a new protocol has been developed for quantum dot based fluoroimmunoassay for simultaneous detection of troponin T and troponin I. MHDA coated quantum dots conjugated to detection antibodies have demonstrated greater stability for extended period. The experimental conditions optimized to perform individual assays for the detection of

troponin T and troponin I have achieved a detection limit of 0.1 pg/mL. The detection limits allow the diagnosis of troponin levels in healthy controls. The method was highly specific for the biomarkers troponin T and I with no observed cross reactivity. The multiplex assay was successful in detection of two biomarkers simultaneously. The experimental results support the success of the method in controlled aqueous (buffer) solution. Therefore to further establish the applicability of the method in real samples the method has to be verified in PBS buffer with high salt concentrations and eventually in serum samples. Despite success in developing new method for diagnosis of biomarkers the method also needs improvement in terms of fast response time as increased times for onsite analysis of the biomarkers will delay the patient diagnosis and treatment. The QD based fluoroimmunoassay developed will thus yield a high throughput diagnostic tool for heart attack.

4.6 References

(1) Robert, B. *The World Health Report 2004–Changing History.* **2004**, 120–124.

(2) Braunwald, E. E. In Heart Disease 5th Ed.; Saunders, W. B. Eds.; Philadelphia, PA, **1997**, p 1290.

(3) Braunwald, E. E. In Heart Disease 5th Ed.; Saunders, W. B. Eds.; Philadelphia, PA, **1997**, p 1126.

(4) World Health Organization task force on standardization of clinical nomenclature. *Circulation* **1979**, 59, 607-609.

(5) Babuin L, Jaffe A. S. *CMAJ* **2005,** 173, 1191–1202.

(6) Jaffe A. S. *Clin. Chim. Acta* **2007,** 381, 9–13.

(7) Alpert, J. S.; Thygesen, K.; Antman, E.; Bassand, J. P. *J Am Coll Cardiol* **2000**, 36(3), 959–969.

(8) Filatov, V. L.; Katrukha, A. G.; Bulargina, T. V.; Gusev, N. B. *Biochemistry* **1999**, 64, 969-985.

(9) Bertinchant, J. P.; Larue, C.; Pernel, I.; Ledermann, B.; Fabbro-Peray, P.; Beck, L.; Calzolari, C.; Trinquier, S.; Nigond, J.; Pau, B. *Clin. Biochem.* **1996**, 29, 587–594.

(10) Hugo, A. K.; Remppis, A.; Looser, S.; Hallermeier, K.; Scheffold, T.; Kubler, W. *J Mol Cell Cardiol* **1989,** 21, 1349-1353.

(11) Hugo, A. K.; Siegfried, L.; Klaus, H.; Andrew, R.; Thomas, S.; Anneliese, B.; Ulrich, E.; Ursula, G. *Clinical Chemistry* **1992**, 38(3), 386-393.

(12) Sergiy, M.; Meike, A. K.; Michael, W.; Andrey, L.; Thomas, A. K.; Alfons, N.; Konrad, K.; Fernando, D. S.; Jochen, F. *Nano Lett.* **2009**, 9(12), 4558-4563.

(13) Cummins, B.; Auckland, M. L.; Cummins, P. *Am. Hear. J.* **1987,** 113, 1333-1344.

(14) Sheila, A. G.; Darcy, J. L.; Mary, E. P.; Lisa, B.; Orthan, S. *Sensor Lett.* **2004**, 2(1), 58-63.

(15) Stacy, E. F.; Melanson, M. J.; Tanasijevic.; Petr, J. *Circulation* **2007**, 116, e501-e504.

(16) Angelo, C.; Elisabetta, D.; Francesco, R.; Domenico, D. B.; Fosco, P.; Valter, S.; Vittorio, C. *Clinical Chemistry* **2009**, 55(1), 196-198.

(17) Morrow, D. A.; Antman, E. M. *Clinical Chemistry* **2009,** 55(1), 5-8.

(18) Michalet, X.; Pinaud, F.; Bentolila, L. A.; Tsay, J. M.; Doose, S.; Li, J. J.; Sundaresan, G.; Wu, A. M.; Gambhir, S. S.; Weiss, S. *Science* **2005**, 307, 538-44.

(19) Jaiswal, J. K.; Simon, S. M. *Trends Cell Biol.* **2004**, 14, 497-504.

(20) Bruchez Jr, M.; Moronne, M.; Gin, P.; Weiss, S.; Alivisatos, A. P. *Science* **1998**, 281, 2013-2016.

(21) Chan, W. C.; Nie, S. *Science* **1998**, 281, 2016-2018.

(22) Peng, X. G.; Manna, L.; Yang, W. D.; Wickham, J.; Scher, E.; Kadavanich, A.; Alivisatos, A. P. *Nature* **2000**, 404, 59-61.

(23) Peng, Z. A.; Peng, X. G. *J. Am. Chem. Soc.* **2001**, 123, 183-184.

(24) Qu, L. H.; Peng, X. G. *J. Am. Chem. Soc.* **2002**, 124, 2049-2055.

(25) Medintz, I. L.; Uyeda, H. T.; Goldman, E. R.; Mattoussi, H. *Nat. Mater.* **2005**, 4, 435-446.

(26) Jaiswal, J. K.; Mattoussi, H.; Mauro, J. M.; Simon, S. M. *Nat. Biotechnol.* **2003**, 21, 47–51.

(27) Bhunia, A. K.; Banada, P.; Banerjee, P.; Valadez, A.; Hirleman, E. D. *J. Rapid Methods Autom. Microbiol.* **2007**, 15, 121–145.

(28) Su, X. L.; Li, Y. *Anal. Chem.* **2004**, 76, 4806–4810.

(29) Hahn, M. A.; Tabb, J. S.; Krauss, T. D. *Anal. Chem.* **2005**, 77, 4861–4869.

(30) Zhu, L.; Ang, S.; Liu, W. T. *Appl. Environ. Microbiol.* **2004**, 70, 597–578.

(31) Peng, Z. A.; Peng, X. G. *J. Am. Chem. Soc.* **2001**, 123, 183-184.

(32) Wang, D.; He, J.; Rosenzweig, N.; Rosenzweig, Z. *Nano Lett.* **2004**, 4, 409-413.

(33) Mattoussi, H.; Mauro, J. M.; Goldman, E. R.; Anderson, G. P.; Sundar, V. C.; Mikulec, F. V.; Bawendi, M. G. *J. Am. Chem. Soc.* **2000**, 122, 12142–12150

(34) Goldman, E. R.; Balighian, E. D.; Mattoussi, H.; Kuno, M. K.; Mauro, J. M.; Tran, P. T.; Anderson, G. P. *J. Am. Chem. Soc.* **2002**, 124, 6378-6382.

(35) Goldman, E. R.; Anderson, G. P.; Tran, P. T.; Mattoussi, H.; Charles, P. T.; Mauro, J. M. *Anal. Chem.* **2002**, 74, 841-847.

(36) Xing, Y.; Chaudry, Q.; Shen, C.; Kong, K. Y.; Zhau, H. E.; WChung, L.; Petros, J. A.; O'Regan, R. M.; Yezhelyev, M. V.; Simons, J. W.; Wang, M. D.; Nie, S. *Nat. Protoc.* **2007**, 2, 1152–1165.

(37) Medintz, I. L.; Uyeda, H. T.; Goldman, E. R.; Mattoussi, H. *Nat. Mater*. **2005**, *4*, 435–446.

(38) Mei, Hu.; Juan, Yan.; Yao, He.; Haoting, Lu.; Lixing, Weng.; Shiping, Song.; Chunhai, Fan.; Lianhui,Wang. *ACS Nano* **2010**, 4(1), 488–494.

Chapter 5

Detection of atherosclerosis biomarkers using a CdSe/ZnS quantum dot based fluorescence immunoassay

5.1 Abstract

Atherosclerosis is a chronic inflammatory vascular disease that involves several events at each step from early fatty streak lesions to highly dangerous rupture-prone plaque. Plaque rupture can lead to debilitating or deadly events such as heart attack and stroke. Simultaneous detection of plasma markers of inflammation and plaque instability will improve assessment of risk for vascular events. The current study is aimed to develop a QD based fluorescence immunoassay for simultaneous detection of plasma markers monocyte chemoattractant protein-1, interleukin 15, and interleukin 18 involved in fatty streak and plaque instability. As preliminary work experimental conditions were optimized for detection of MCP-1 and IL-15 achieving detection limits of 100 pg/mL and 10 pg/mL respectively. The detection limits are comparable to currently reported methods. Further a new approach was proposed to incorporate QDs into silica beads before binding to the detection antibodies to further improve the detection limits. The future prospects for this work are optimization of experimental conditions for third biomarker IL-18 and multiplexing the three biomarkers for simultaneous detection. This study thus provides preliminary results to yield a reliable method for simultaneous and rapid detection of multiple atherosclerosis biomarkers for early diagnosis.

5.2 Introduction

Atherosclerosis is a chronic inflammatory vascular disease that involves several events at each step from early fatty streak lesions to highly dangerous rupture-prone plaque.[1] The principal mechanisms of myocardial and cerebral infarctions involve disruption of atherosclerotic plaques and the subsequent formation of thrombus or blood clot.[2] Atherosclerotic plaques are classified into two types, stable and susceptible, of which the latter one is more vulnerable to rupture.[3] A vulnerable plaque is characterized by a large lipid-rich core, a thin fibrous cap, and penetration by inflammatory cells, such as macrophages.[4] Thus, to provide the information for early treatment and risk assessment the detection of vulnerable plaques becomes clinically important. Detection of vulnerable atherosclerotic plaques involved several imaging techniques including conventional X-ray contrast angiography, to detect morphological characteristics such as stenosis. However, X-ray contrast angiography was not successful in determining whether a plaque is stable or vulnerable as both types of plaques cause stenosis.[5] In addition to conventional methods other approaches involving the use of magnetic resonance imaging (MRI) have also been developed. These approaches have been successful in discriminating lipid cores, fibrous caps, and hemorrhaged lesions.[6-10] To directly image an atheroma intravascular ultra sonography technique are also currently being used.[11-13] Computed tomography,[14] and positron emission tomography[15] are the other new techniques used for diagnosis. However all these new approaches do not provide information about presence of inflammation which is indicative of a vulnerable plaque though the images provide morphological characteristics of the atheroma.

Recent research have repeatedly shown the use of biomarkers in different stages of atherosclerosis like molecular proinflammatory biomarkers, plaque destabilization and plaque rupture biomarkers to predict future cardiovascular prevalence not only in healthy individuals,

but also in patients with acute coronary syndrome.[16] Therefore testing patients for several of these biomarkers will provide important information useful for predicting future incidence of atherosclerosis. In the previous chapter quantum dots based fluoroimmunoassay method has been developed for simultaneous detection of heart attack biomarkers, troponin T and troponin I that achieved a detection limit of 0.1 pg/mL. The multiplex assay was able to detect two biomarkers simultaneously that will yield a high throughput diagnostic tool for heart attack.

The current study aims at development of QD based fluorescence immunoassay for simultaneous detection of three atherosclerosis markers monocyte chemoattractant protein-1 (MCP-1), interleukin 15 (IL-15), and interleukin 18 (IL-18) that play significant role in two important stages of atherosclerosis, fatty streaks and plaque destabilization. MCP-1 is an important chemokine whose expression increases in atherosclerotic lesions, particularly in macrophage-rich areas.[17, 18] Interleukin 15 is a biomarker associated with atherosclerosis whose expression is found exclusively in fibrolipid and lipid-rich plaques in complex foam cells.[19, 20] IL-18, is another biomarker and increased expression of IL-18 is seen in lesions prone to rupture, and is localized mainly in plaque macrophages.[21, 22] Simultaneous detection of plasma markers of inflammation and plaque instability will improve risk assessment for vascular events.

5.3 Experimental Methods

5.3.1 Materials and reagents. Technical grade (90%) trioctylphosphine oxide (TOPO), technical grade (90%) trioctylphosphine (TOP), cadmium oxide (99.99%), selenium powder (99.5%), lauric acid (98%), technical grade (90%) hexadecylamine (HDA), diethyl zinc ($Zn(Et)_2$) solution 1.0 M in heptane, hexamethyldisilathiane ($(TMS)_2S$), methanol anhydrous (99.8%), chloroform (99.5%), 16-mercaptohexadecanoic acid (MHDA), tetramethylammonium hydroxide pentahydrate, Tween 20, 1-ethyl-3-(3-dimethylaminopropyl) carbodiimide hydrochloride (EDC),

sulfo-*N*-hydroxysulfosuccunimide (sulfo-NHS), and bovine serum albumin were purchased from Sigma Aldrich. Amine reactive maleic anhydride activated 96 well plates, and super block blocking buffer were purchased from Thermo Scientific. Mouse monoclonal IL-15 antibody, rabbit polyclonal IL-15 antibody, IL-15 protein, mouse monoclonal MCP-1 antibody, rabbit polyclonal MCP-1 antibody, MCP-1 protein were purchased from Abcam.

5.3.2 Synthesis of TOPO capped luminescent quantum dots. TOPO-capped CdSe/ZnS quantum dots were prepared following a method first proposed by Peng *et al*[23] with a slight modification.[24] Briefly, 12-13 mg of cadmium oxide and 160-180 mg of lauric acid were mixed under nitrogen atmosphere. The mixture was heated in a 100 mL three neck flask to slightly above 180°C to fully dissolve the cadmium oxide (clear solution). Then, 2 g of TOPO and 2 g HDA were added to the solution with constant stirring. Temperature was raised to 280°C before being cooled down slowly. Upon reaching the desirable temperature 80 mg selenium powder dissolved in 2 mL solution of TOP was rapidly injected into the solution under vigorous stirring. For shell coating, a 2 mL TOP solution containing 250 μL $(TMS)_2S$ and 1 mL $Zn(Et)_2$ was injected drop-wise into the solution. The reaction mixture was kept at 180°C for one hour before it was cooled to room temperature, washed three times with methanol, centrifuged at 4000 rpm for 10 minutes each, and redispersed in chloroform. The concentration of this solution was found to be 1 μM. The solution was stored at room temperature.

5.3.3 Synthesis of mercaptohexadecanoic acid (MHDA) coated quantum dots. 16-mercaptohexadecanoic acid coated quantum dots were prepared following a modified procedure developed by Bawendi[25] for the synthesis of lipoic acid capped CdSe/ZnS core-shell quantum dots. 25 mg of MHDA was heated up to 70-80°C to dissolve and 3 mL of 1 μM TOPO coated quantum dots and 3 mL of chloroform were added and stirred for 2-3 hours at 50-60°C. Then 6

mL of DI water containing tetramethylammonium hydroxide pentahydrate was added to the mixture and stirred for another half hour at room temperature and then allowed to settle down for few minutes. This resulted in a two-phase mixture with the aqueous MHDA coated quantum dots layer above the organic chloroform layer. The aqueous layer was collected and centrifuged several times to remove TOP/TOPO until clear solution was seen. Then the clear suspensions were collected and spin dialyzed two times with a cutoff molecular weight of 30000 Da to remove the excess MHDA. In each spin dialysis cycle, the sample was centrifuged at 3000 rpm for 20 minutes and washed with DI water. MHDA coated quantum dots were kept at 4°C in DI water until used.

5.3.4 Conjugation of MHDA coated quantum dots with detection antibodies. Conjugation of antibodies onto MHDA coated CdSe/ZnS quantum dots was achieved using the classic EDC coupling reaction of COOH groups on the surfaces of the MHDA coated quantum dots and NH_2 groups of the antibody. Typically, 0.1 mL of MHDA coated CdSe/ZnS quantum dots, 20 μL of 30 mg/mL EDC and 20 μL of 30 mg/mL sulfo-NHS were added into a 1.5 mL tube. The mixture was vortexed for 15-20 min at room temperature to fully activate free carboxylic acid groups on the quantum dots. In this step, semi stable amine-reactive NHS-ester could be synthesized by the esterification of the activated carboxylic acid groups on the QDs and hydroxyl groups on the sulfo-NHS. 100 μL of detection antibodies was added into the system and was vortexed for at least 2 h. The unreacted antibody molecules were removed from the media by centrifugal concentrators (cutoff molecular weight: 100 kD). Quantum dots and antibodies were connected through strong covalent bonds. The final products were recollected into 10 mM PBS pH 7.4 buffer containing 0.1% BSA and kept at 4°C. The purified quantum dot-antibody conjugates were ready to be used to detect the target antigens.

5.3.5 Individual fluoroimmunoassays. Fluoroimmunoassays were essentially performed as previously described. [26, 27] Wells of clear microtiter plates were washed three times with 200 μL of wash buffer (PBS pH 8.0 buffer containing 0.05% Tween 20). Then, 50 μL of different concentration of capturing antibodies dissolved in 10 mM PBS pH 7.4 buffer were added to the plate and incubated overnight at room temperature. The capture solution was discarded and the plates were blocked using 200 μL of super block blocking buffer and incubated for one hour at room temperature. This quenches the remaining reactive maleic anhydride groups and also blocks left over open sites on the plate surface. The blocking buffer was discarded and the plate washed three times with wash buffer. Different concentrations of 50 μL of IL-15 or MCP-1 antigens were added to plate wells and incubated for 1 hour at room temperature. Plate wells were washed three times with wash buffer to remove the unbound antigens. 50 μL of the detection antibodies conjugated to different colored quantum dots were added to the plate wells and incubated for one hour at room temperature and the unbound antibodies were removed by washing three times with the wash buffer.

5.3.6 Fluorescence spectroscopy measurements. Excitation and emission spectra were measured using a spectrofluorometer (SpectraMax M2, Molecular Devices) equipped with a 75 W continuous xenon arc lamp as a light source. All the samples were excited at 400 nm. Emission scans were measured from 450-750 nm.

5.3.7 Digital fluorescence imaging microscopy. Luminescence images were obtained using a digital inverted fluorescence microscope (Olympus IX71) equipped with a 100 W mercury lamp as a light source. The fluorescence images were collected via a 20 X microscope objective with numerical aperture = 0.5. A filter cube containing a 380±20 nm band-pass excitation filter, a 425 nm dichroic mirror, and a 450 nm long pass emission filter was used to ensure spectral imaging

purity. Digital point controller (DP72) was used for digital imaging. An exposure time of 100 ms was typically used to acquire the fluorescence images.

5.4 Results and Discussion

A similar method developed in chapter 4 was used to detect atherosclerosis biomarkers. 16-mercaptohexadecanoic acid was used to replace TOPO coating of the luminescent CdSe/ZnS quantum dots to make them water soluble and biocompatible. Figure 5.1 shows the emission spectra and normalized emission spectra of TOPO coated quantum dots and MHDA coated quantum dots respectively. The optical properties of the quantum dots were well preserved even after ligand exchange with MHDA as shown in Figure 5.1b.

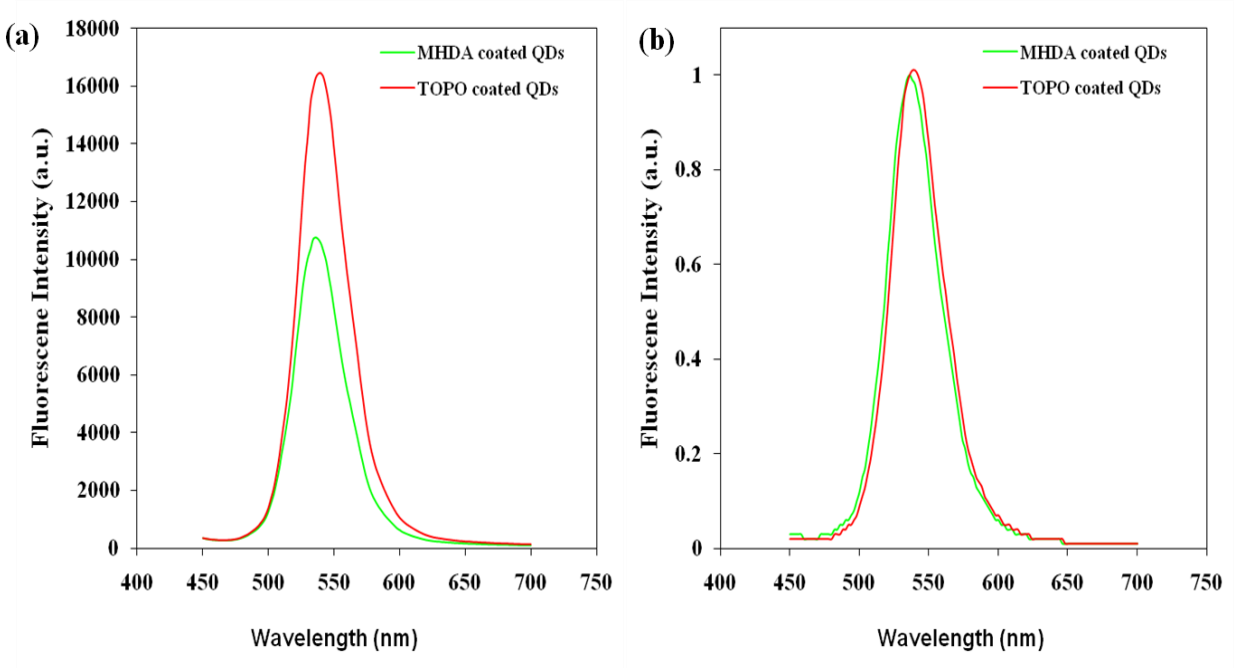

Figure 5.1 (a) Emission and (b) normalized emission spectra of TOPO coated quantum dots (red line) and MHDA coated quantum dots (green line) at same concentration of quantum dots.

Antibody conjugated quantum dots are often used for biological labeling and staining.[28] The EDC coupling reaction between a carboxylic group and an amine group is the classic reaction for bioconjugation of biomolecules (Scheme 5.1). EDC reacts with the carboxylic

groups on the MHDA coated QDs and forms an amine reactive O-acylisourea intermediate. This intermediate is very susceptible to hydrolysis and hence is unstable and short lived. The desired coupling cannot occur if the targeted amine does not find the active carboxylate before hydrolysis and this is overcome by adding the sulfo-NHS. The advantage of addition of sulfo-NHS to the EDC reaction was to increase the stability of the active intermediate by converting it to amine reactive sulfo-NHS ester intermediate which reacts with the attacking amine from the antibodies. Excess reagent and isourea are formed as byproducts of the cross-linking reaction that are water-soluble and can be easily removed by dialysis or filtration.[29] The QD-antibody bioconjugates were found to be stable and their brightness remained the same for a long time when stored in a refrigerator at 4°C in the PBS pH 7.4 buffer solution containing 0.1% BSA.

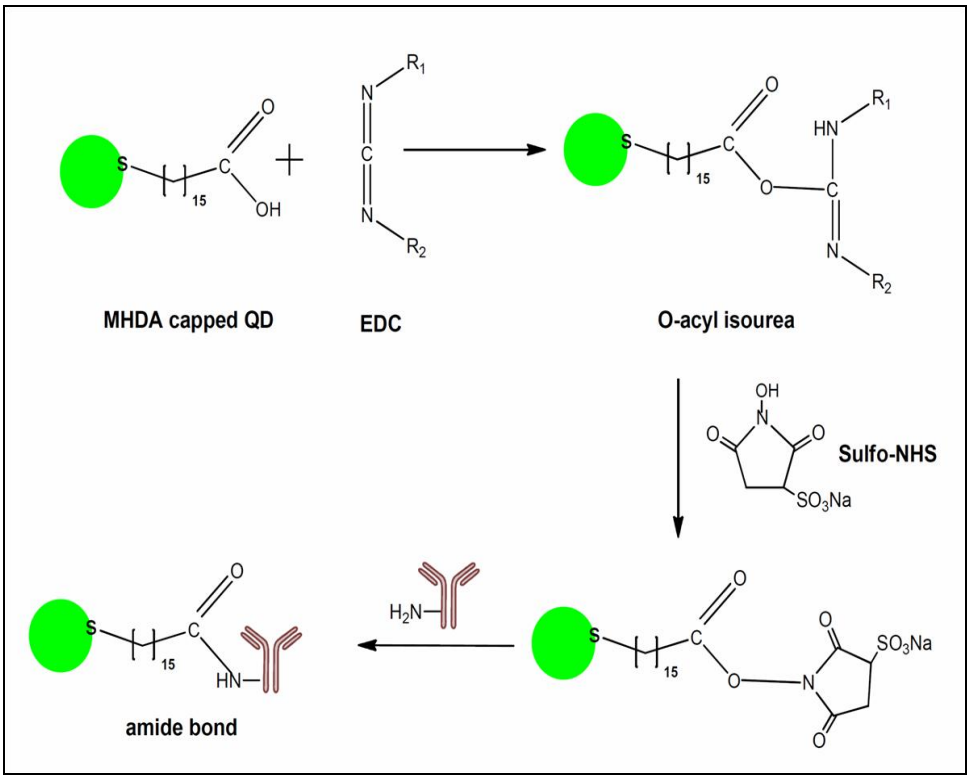

Scheme 5.1 Schematic representation of EDC/NHS coupling chemistry.

The immunoreaction was performed using sandwich assay. The workflow of quantum dot based fluoroimmunoassay is depicted in scheme 5.1. First the capture antibodies were immobilized on the well plate followed by blocking buffer to block the nonspecific binding. The antigens IL-15 or/and MCP-1 were added that bind to the corresponding capture antibodies and the unbound antigens were removed by washing. Finally the detection antibodies conjugated to 545nm or/and 615 nm quantum dots were added that bind to the corresponding antigens forming a sandwich immunocomplex. The fluorescence intensities of the quantum dots attached to the immunocomplex were measured for the quantification of the antigens IL-15 and MCP-1.

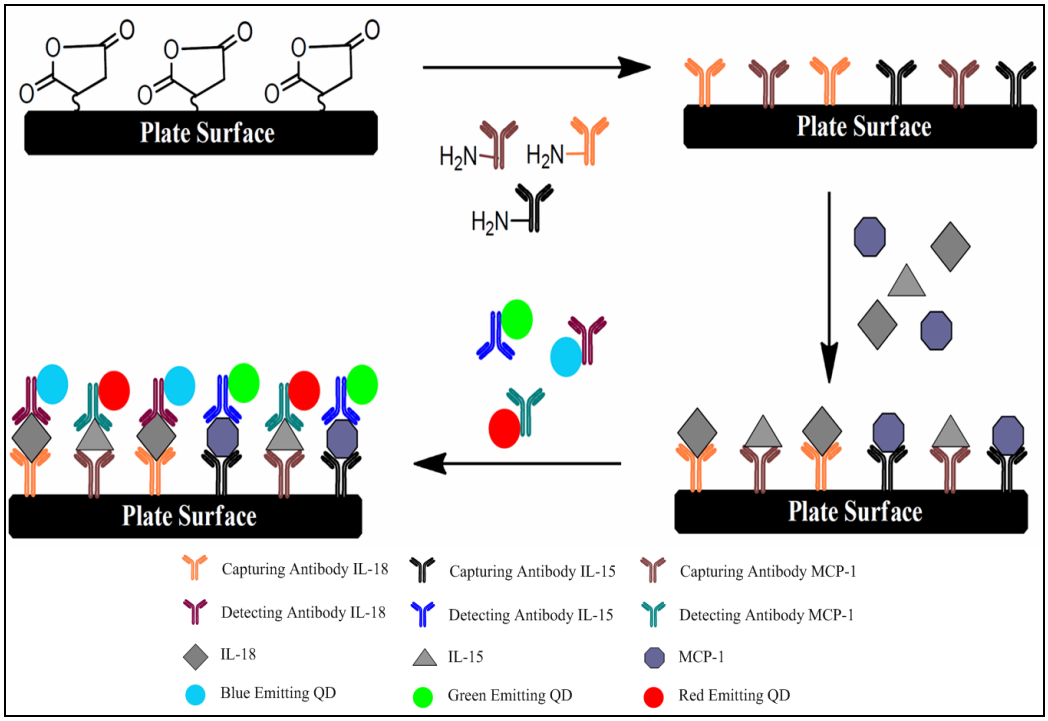

Scheme 5.2 Schematic representation of QD based fluoroimmunoassay principle.

The experimental conditions were initially optimized for the detection of two biomarkers IL-15 and MCP-1. The effect of incubation time was optimized for capturing antigen by the capturing antibody on the plate. The antigens were added at a concentration of 1 ng/mL and incubated at 37^{o}C for different time intervals. The fluorescence intensity increased with

increasing the incubation time for up to 2 hours and further increasing in time did not show any increase in the emission intensity suggesting 2 hours as optimal incubation time at 37^{o}C. Further incubation for longer periods may destroy the activity of the antigen and effect reorganization of quantum dots conjugated detection antibodies with antigen.

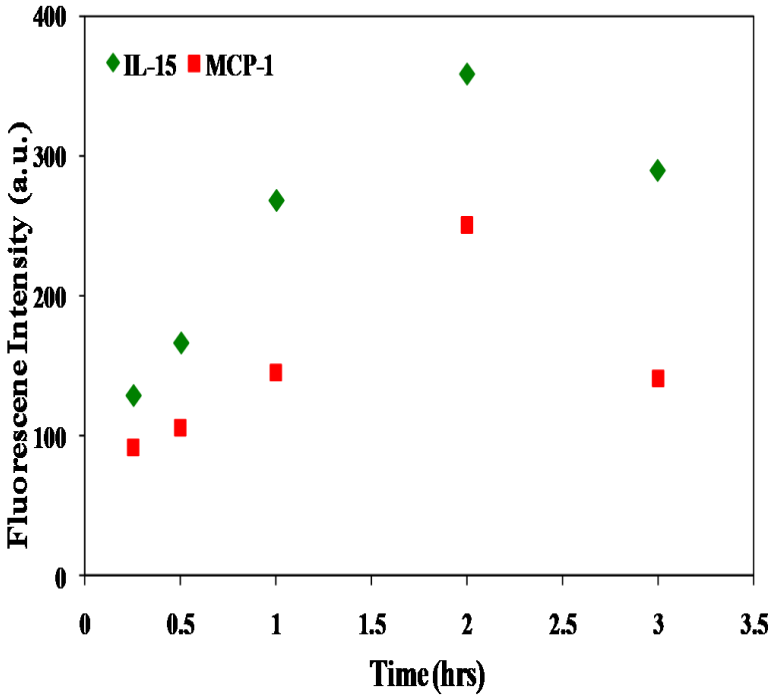

Figure 5.2 Effect of incubation time on capture of antigen on 96-well plate at 25 µg/mL of capture antibodies and 1 ng/mL of IL-15 (green) and MCP-1 protein (red) concentration. λ_{ex}: 400nm.

The immobilization of the capturing antibody on well plate is crucial since it is the first step in the immunoassay. The concentration of capture antibody solution in the immobilization determines the amount of antibody immobilized on the well plate. Serial concentrations of antibody solution from 0 to 50 µg/mL were tested in order to investigate the maximum loading of the capturing antibody. The fluorescence intensity of the quantum dots present in the immunocomplex increased with the capture antibody concentrations from 0 to 50 µg/mL for IL-

15 and from 0 to 10 µg/mL for MCP-1. Further increase in antibody concentration for the immobilization did not improve the previously observed fluorescence intensities (Figure 5.3).

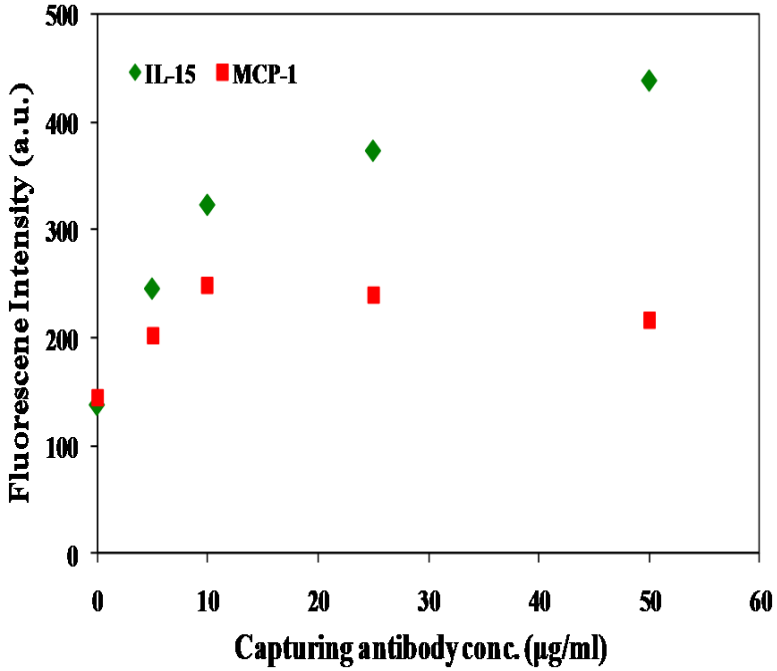

Figure 5.3 Immobilization of capturing antibodies on 96-well plate at 1 ng/mL of IL-15 (green) and MCP-1 protein (red) and 60 minutes of incubation time. λ_{ex}: 400 nm.

Individual analyte assays were done for each of the two antigens, IL-15 and MCP-1 to ensure the use of QD-antibody pairs in a multicolor multianalyte study. In these assays, the appropriate capture antibody and individual antigens were applied to wells, and the emission intensities of single colored QDs that are conjugated to detection antibodies were measured for quantification. Figure 5.4a shows the fluorescence emission spectra of 545 nm emitting quantum dots that are conjugated to anti-IL15 antibodies. The emission intensity increased with increasing concentrations of troponin T from 0 to 10 ng/mL. There is a linear-log relationship between the enhanced intensity of quantum dots and the concentrations of IL-15 (Figure 5.4b). It was possible to detect as low as 10 pg/mL for IL-15.

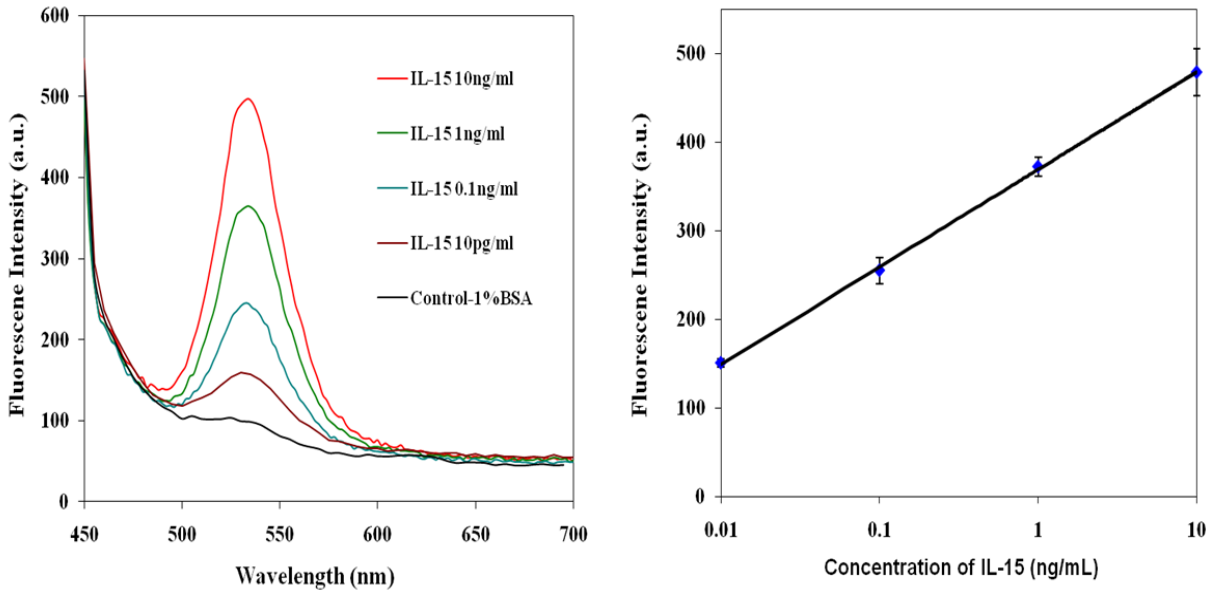

Figure 5.4 a) Emission spectra of 545 nm emitting QDs in the immunocomplex at different concentrations of IL-15 protein b) relationship between IL-15 concentration and the fluorescence intensity of the QDs.

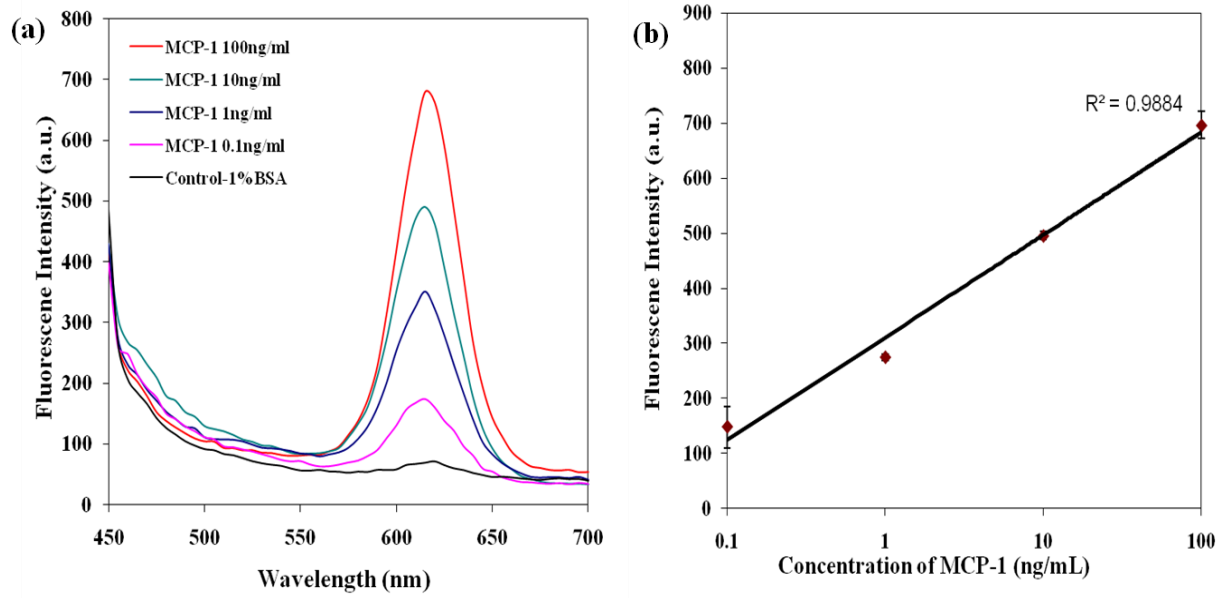

Figure 5.5 a) Emission spectra of 615 nm emitting QDs in the immunocomplex at different concentrations of MCP-1 b) relationship between MCP-1 concentration and the fluorescence intensity of the QDs.

Similarly, Figure 5.5a is the fluorescence emission spectra of 615 nm emitting quantum dots that are conjugated to anti-MCP-1 antibodies. Similar to IL-15 the emission intensity increased with increasing concentrations of troponin I. Figure 5.5b shows the concentration dependence of the emission intensity of the quantum dots. The detection limit was found to be 100 pg/mL for the MCP-1. The specificity of the method was studied to check for any cross reactivity between the antigens and antibodies. The experiments involved the addition of anti-IL15 capturing antibody to the well plate followed by the addition of different antigens 1% bovine serum albumin (BSA), IL-15, and MCP-1. The anti-IL15 detection antibodies conjugated to 545 nm emitting QDs were added to the well plate. The signals of the quantum dots for this experiment are represented as green bars in Figure 5.6. Similar procedure was performed for MCP-1 and the signals from the 615 nm emitting QDs are represented as red bars in the Figure 5.6. Greater signal intensities were observed for the specific antigen-antibody conjugates while there is no significant cross reactivity of the antibodies with the other antigens demonstrating the specificity of the method.

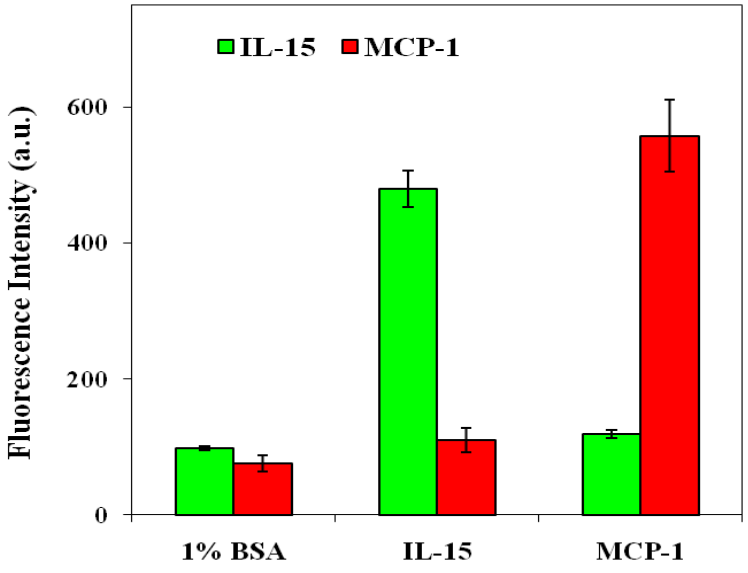

Figure 5.6 The selectivity of the quantum dot based fluoroimmunoassay method.

The detection limits achieved in this work for the biomarkers of atherosclerosis though were not the best but are comparable to the currently available methods. This can be attributed to the low binding affinity of antigen-antibody pairs used in this method. Therefore a new approach was proposed to improve the detection limits by incorporating TOPO coated QDs into silica beads before binding to the detection antibodies (Scheme 5.3). Incorporation of large number of QDs into a single silica bead will not only improve signal intensity but also will help improve results even with low binding affinity antigen-antibody pairs. Furthermore, to complete the study optimization of IL-18 and multiplexing of the assay have to be done for simultaneous detection of the biomarkers. Also the applicability of the method in real samples collected from patients has to be established.

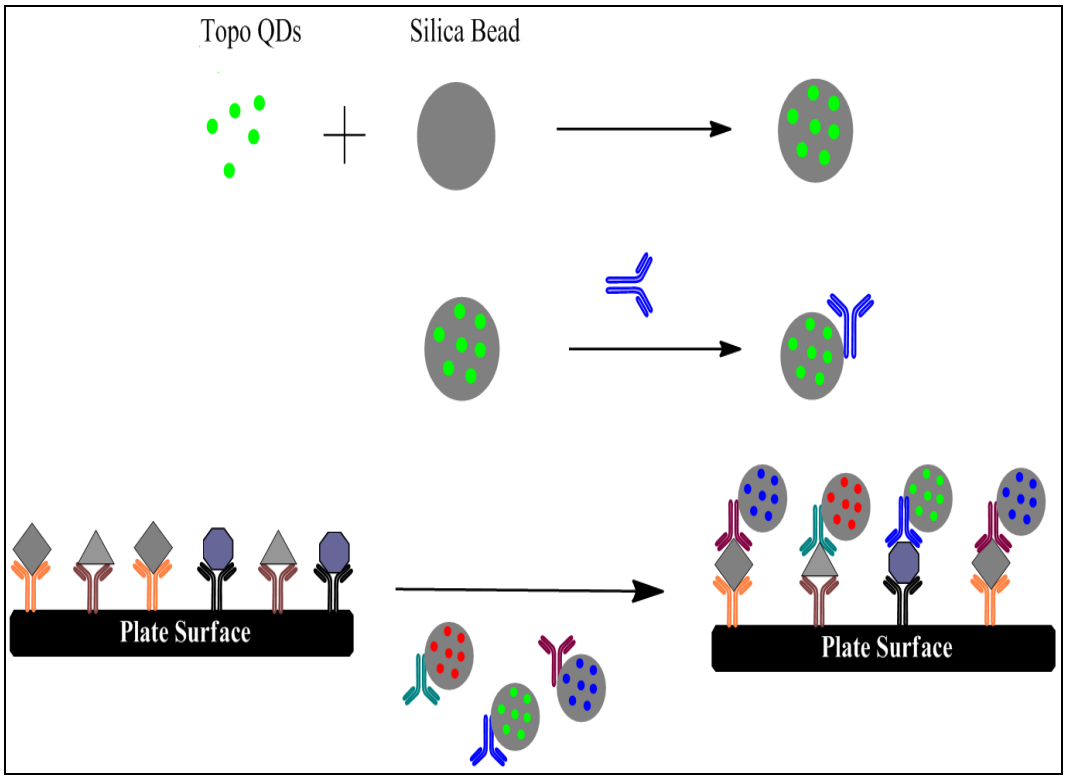

Scheme 5.3 Schematic representation of QDs incorporated silica bead based fluoroimmunoassay principle.

5.5 Conclusions

The overall goal of the current study is to develop quantum dot based fluoroimmunoassay for simultaneous detection of three plasma markers MCP-1, IL-15, and IL-18. Current work only shows the optimized experimental conditions to perform individual assays for the detection of MCP-1 and IL-15. The methods achieved a detection limit of 10 pg/mL for IL-15 and 100 pg/mL for MCP-1 respectively. The inability to achieve better detection limits was attributed to low binding affinity between the antigen-antibody pairs used in this method. Furthermore, to complete the study optimization of IL-18 needs to be done to multiplex the assay for simultaneous detection of these biomarkers. In addition a new approach was proposed to improve the detection limits of MCP-1, IL-15 including IL-18 utilizing incorporation of quantum dots into silica beads that is expected to increase the sensitivity of the method. The multiplex assay able to detect three biomarkers simultaneously will be a high throughput diagnostic tool for atherosclerosis. Also the applicability of the method in real samples collected from patients has to be established. Despite the limitations the preliminary results are encouraging to develop reliable method that will see light in the diagnose of atherosclerosis.

5.6 References

(1) Ross, R. *Nature* **1993**, 362(6423), 801-809.

(2) Fuster V. Circulation **1994**, 90, 2126-2146.

(3) Ross, R. *New England Journal of medicine* **1999**, 340(2), 115-126.

(4) Virmani, R.; Burke, A. P.; Farb, A.; Kolodgie, F.D. *Prog Cardiovusc Dis* **2002**, 44, 349-356.

(5) Libby, P. *Circulation* **1995**, 91, 2844-2850.

(6) Wasserman, B. A.; Smith, W. I.; Trout, H. H.; Cannon, R. O. III; Balaban, R. S.; Arai, A. E. *Radiology*. **2002**, 223, 566 –573.

(7) Kramer, C. M.; Cerilli, L. A.; Hagspiel, K.; DiMaria, J. M.; Epstein, F. H.; Kern, J. A. *Circulation*. **2004**, 109, 1016 –1021.

(8) Kerwin, W.; Hooker, A.; Spilker, M.; Vicini, P.; Ferguson, M.; Hatsukami, T.; Yuan, C. *Circulation*. **2003**, 107, 851–856.

(9) Lin, W.; Abendschein, D. R.; Haacke, E. M. *J Magn Reson Imaging*. **1997**, 7, 183–190

(10) Kerwin, W. S.; O'Brien, K. D.; Ferguson, M. S.; Polissar, N.; Hatsukami, T. S.; Yuan, C. *Radiology*. **2006**, 241, 459–468.

(11) Losordo, D. W.; Rosenfield, K.; Kaufman, J.; Pieczek, A.; Isner, J. M. *Circulation* **1994**, 89, 2570 –2577.

(12) Schoenhagen, P.; Ziada, K. M.; Kapadia, S. R.; Crowe, T. D.; Nissen, S. E.; Tuzcu, E. M.*Circulation* **2000**, 101, 598–603.

(13) Von Birgelen, C.; Klinkhart, W.; Mintz, G. S.; Papatheodorou, A.; Herrmann, J.; Baumgart, D.; Haude, M.; Wieneke, H.; Ge, J.; Erbel, R. *J Am Coll Cardiol*. **2001**, 37, 1864 – 1870.

(14) Motoyama, S.; Kondo, T.; Sarai, M.; Sugiura, A.; Harigaya, H.; Sato, T.; Inoue, K.; Okumura, M.; Ishii, J.; Anno, H.; Virmani, R.; Ozaki, Y.; Hishida, H.; Narula, J. *J Am Coll Cardiol.* **2007**, 50, 319 –326.

(15) Rudd, J. H. F.; Warburton, E. A.; Fryer, T. D.; Jones, H. A.; Clark, J. C.; Antoun, N.; Johnstrom, P.; Davenport, A. P.; Kirkpatrick, P. J. *Circulation*. **2002**, 105, 2708 –2711.

(16) Stary, H. C.; Chandler, A. B.; Dinsmore, R. E.; Fuster, V.; Glagov, S.; Insull, W.; Rosenfeld, M. E.; Schwartz, C. J.; Wagner, W. D.; Wissler, R. W. *Circulation* **1995**, 92, 1355– 1374.

(17) Mach, F. *Curr. Atheroscler. Rep*. **2001**, 3, 243–251.

(18) Yamamoto, T.; Eckes, B.; Mauch, C.; Hartmann, K.; Krieg, T. *J Immunol*. **2000**, 164, 6174–6179.

(19) Elhage, R.; Jawien, J.; Rudling, M.; Ljunggren, H. G.; Takeda, K.; Akira, S.; Bayard, F.; Hansson, G. K. *Cardiovasc Res.* **2003**, 59, 234–240.

(20) Wuttge, D. M.; Eriksson, P.; Sirsjö, A.; Hansson, G. K.; Stemme, S. *Am. J. Pathol.* **2001**, 159, 417-23.

(21) Ishida, Y.; Migita, K.; Izumi, Y.; Nakao, K.; Ida, H.; Kawakami, A.; Abiru, S.; Ishibashi, H.; Eguchi, K.; Ishii, N. *FEBS Lett.* **2004**, 69, 156 –160.

(22) Mallat, Z.; Corbaz, A.; Scoazec, A.; Besnard, S.; Leseche, G.; Chvatchko, Y.; Tedgui, A. *Circulation* **2001**, 104, 1598 –1603.

(23) Peng, Z. A.; Peng, X. G. *J. Am. Chem. Soc.* **2001**, 123, 183-184.

(24) Wang, D.; He, J.; Rosenzweig, N.; Rosenzweig, Z. *Nano Lett.* **2004**, 4, 409-413.

(25) Mattoussi, H.; Mauro, J. M.; Goldman, E. R.; Anderson, G. P.; Sundar, V. C.; Mikulec, F. V.; Bawendi, M. G. *J. Am. Chem. Soc.*, **2000**, 122, 12142–12150

(26) Goldman, E. R.; Balighian, E. D.; Mattoussi, H.; Kuno, M. K.; Mauro, J. M.; Tran, P. T.; Anderson, G. P. *J. Am. Chem. Soc*. **2002**, 124, 6378-6382.

(27) Goldman, E. R.; Anderson, G. P.; Tran, P. T.; Mattoussi, H.; Charles, P. T.; Mauro, J. M. *Anal. Chem.* **2002**, 74, 841-847.

(28) Xing, Y.; Chaudry, Q.; Shen, C.; Kong, K. Y.; Zhau, H. E.; WChung, L.; Petros, J. A.; O'Regan, R. M.; Yezhelyev, M. V.; Simons, J. W.; Wang, M. D.; Nie, S. *Nat. Protoc.* **2007**, 2, 1152–1165.

(29) Hermanson, G. T. *Bioconjugate Techniques*; Academic Press Inc.: San Diego, CA, **1996**.

Chapter 6

Summary and Conclusions

Luminescent quantum dots (QDs) have emerged as alternative fluorescent probes over the last two decades in several biological and biomedical fields. They exhibit unique photo-physical properties, such as broad absorption spectra with narrow and symmetrical emission peaks, high quantum yield, high photostability, and size dependent luminescence. This dissertation focused on development of quantum dot based bioassays for real time monitoring of enzyme activity and simultaneous detection of several biomarkers.

Recently many research labs have developed quantum dot based fluorescence resonance energy transfer (FRET)-based assays.[1-3] Chang *et al* developed solution based FRET assays using QDs as donors and gold nanoparticles (AuNPs) as acceptors for proteolytic activity measurements.[4] Shi *et al* from our lab have covalently linked molecular fluorescent acceptors to the surface of single quantum dots and used the FRET probes for real-time monitoring of protease activity in solution.[3] Most of the developed quantum dot based FRET assays have measured the proteolytic activity. In this study, a quantum dot based FRET assay was employed for lipase activity measurements. The liposome encapsulated quantum dot based fluorescence resonance energy transfer probes were synthesized and characterized to monitor the enzymatic activity of phospholipase A_2. The unique feature of this work is the platform, quantum dot containing liposomes that can be prepared using commercially available substrates. Since the quantum dots are not attached covalently to the phospholipids they do not affect the enzyme activity of phospholipase A_2. The phospholipid bilayer in QD-liposomes was also labeled with

acyl NBD fluorophores. The application of molecular fluorophores as acceptors allows ratiometric measurement to monitor FRET that results in real time changes in quantum dot and fluorescent acceptor emission peaks. The addition of phospholipase A_2 to QD-liposomes showed changes in FRET signals due to cleavage of SN2-acyl bond and release of NBD fluorophores from the membrane. The NBD molecules are hydrophilic in nature and move away from the hydrophobic bilayers following PLA_2 enzyme cleavage. The changes in FRET signals were found to be phospholipase A_2 concentration dependent. The QD based FRET probes were able to detect the enzyme activity as low as 0.0075 U/ml (PLA_2 = 1500 U/mg) in 30 min at room temperature which is the best detection limit attained so far in comparison to commercially available kits with detection limits up to 0.05 U/mL. Further the FRET probes were also used to screen the inhibition efficiencies of two phospholipase A_2 inhibitors 1-hexadecyl-3-(trifluoroethyl)-sn-glycero-2-phosphomethanol and 3(4octadecyl)benzoylacrylic acid. QD based FRET probes allow for multiplexing and screening large number of inhibitors simultaneously. The method is also suitable for both kinetic analysis and large-scale screening using automated readers for 96-well plates.

Despite several advantages offered by CdSe/ZnS QDs, replacement of organic fluorophores is limited due to cytotoxicity associated with the individual ions present in the quantum dots.[5, 6] Recently, focus has been shifted to the synthesis of cadmium free quantum dots. InP quantum dots are more appropriate because they are less cytotoxic and have a wide emission range from the UV to near infra red region of the electromagnetic spectrum, which makes them ideal candidates for *in vivo* applications as opposed to CdSe quantum dots. However, the quantum yield of III-V quantum dots is less than 1% due to surface traps, dangling bonds in the crystal lattice and high activation barrier for de-trapping as compared to II-VI

semiconductors.[7] Recently Peng *et al* reported InP/ZnS core–shell quantum dot synthesis using a fatty amine; for this method the quantum yields reached up to 40%.[8] A one step and one pot method for the synthesis of highly luminescent InP with QYs of up to 30% and InP/ZnS QDs with QYs of up to 60% was reported by Nann *et al*.[9] More recently, Reiss *et al* synthesized InP/ZnS QDs in a single step with quantum yield up to 70%.[10] In the current work, InP/ZnS quantum dots were incorporated for the first time into liposomes, making the InP/ZnS quantum dots water soluble and biocompatible. The structural characterization of InP/ZnS quantum dots demonstrated well preserved integrity of liposomes even after incorporation of InP/ZnS quantum dots. The photostability studies of InP/ZnS QD-liposomes compared with the MHDA capped quantum dots and InP/ZnS quantum dots showed that encapsulation with liposomes enhanced the photostability of the InP/ZnS quantum dots. The effect of pH on the optical properties of InP/ZnS quantum dots showed only less than 10% variation in the PL intensity of InP as opposed to 35% variation in PL intensity of InP/ZnS coated with mercaptosuccinic acid reported previously by Yong *et al*.[11] The results demonstrated advantages of InP/ZnS QD-liposomes over InP/ZnS quantum dots. The InP/ZnS QD-liposome complexes thus synthesized will find a wide range of biological applications such as bioimaging, bioassays, and immunoassays.

Among several unique characteristics one of the most popular features of quantum dots is their ability to multiplex. This unique property makes it possible to simultaneously detect different emission peaks when different sizes of QDs are excited with a single wavelength. Quantum dots have been used in multiplexed assays by several studies by different research groups to detect biomolecules such as multiple DNA targets to specific neurotoxins. In the current study a new method of CdSe/ZnS quantum dot based fluorescence immunoassay has been developed for simultaneous detection of the cardiac biomarkers troponin T and troponin I.

Currently, several immunoassay methods are available commercially for the detection of troponin I and troponin T separately, most of them are based on UV absorbance, and some of them are based on fluorescence.[12-14] However, the detection limits of current troponin assays do not allow detection of normal cardiac troponin levels in healthy controls.[15] Thus lower detection limits with improved assay sensitivity and precision are required to improve assessment of risk. A sandwich immunoassay was performed with capture antibodies immobilized on a 96-well plate. After binding targeted biomarkers to capture antibodies, detection antibodies conjugated to CdSe/ZnS quantum dots were then bound to the specific biomarkers forming a sandwich complex. The experimental conditions optimized to perform individual assays for the detection of troponin T and troponin I have achieved a detection limit of 0.1 pg/mL compare to current detection limits of 10 pg/mL for troponin T and 22 pg/mL of troponin I. The detection limits allows the diagnosis of troponin levels in healthy controls. The method was highly specific for the biomarkers troponin T and I with no observed cross reactivity with different antigens troponin T, troponin I, 1% bovine serum albumin (BSA), and creatine kinase (CK-MB). The multiplex assay was able to detect two biomarkers simultaneously that will yield a high throughput diagnostic tool for heart attack. The experimental results support the success of the method in controlled aqueous (buffer) solution. Therefore to further establish the applicability of the method in real samples the method has to be verified in PBS buffer with high salt concentrations and eventually in serum samples. In addition the method also needs improvement in terms of fast response time for onsite analysis of the biomarkers that will expedite patient's diagnosis and treatment procedures.

According to recent United States statistics, the first symptom of atherosclerosis is heart attack or sudden cardiac death among the majority of men and women with this disease. This

situation is indicative of the lack of diagnostic methods in early stages of atherosclerosis. Recent research has shown the presence of biomarkers at different stages of atherosclerosis, such as molecular proinflammatory biomarkers, plaque destabilization and plaque rupture biomarkers. These markers can help predict future cardiovascular disease not only in healthy individuals, but also in patients with acute coronary syndrome. The method described above for the detection of heart attack markers was extended to detect atherosclerosis biomarkers. Thus this study aims at development of QD based fluorescence immunoassay for simultaneous detection of three atherosclerosis markers MCP-1, IL-15, and IL-18 that play significant roles in two important stages of atherosclerosis, fatty streaks and plaque destabilization. Current work only shows the optimized experimental conditions to perform individual assays for the detection of MCP-1 and IL-15. The method was able to detect as low as 100 pg/mL of MCP-1 and 10 pg/mL of IL-15. The inability to achieve better detection limits was attributed to low affinity between the antigen-antibody pairs used in this method. Therefore a new approach was proposed to improve the detection limits by incorporating QDs into silica beads before binding to the detection antibodies. Incorporation of large number of QDs into a single silica bead will not only improve signal intensity but also will help improve results with low affinity antigen-antibody pairs. Furthermore, to complete the study optimization of IL-18 and multiplexing of the assay have to be done for simultaneous detection of the biomarkers. Also the applicability of the method in real samples collected from patients has to be established. Despite the limitations the preliminary results support the development of multiplex assay to detect three biomarkers simultaneously that will yield reliable, sensitive, efficient methods for diagnosis of atherosclerosis.

6.1 Limitations and Future Studies

Quantum dots have several advantages over organic dyes as fluorescence probes however they pose cytotoxicity that limits their applications especially for *in vivo* studies. Hence there is greater inclination of research towards the synthesis of cadmium free QDs in which InP/ZnS QDs emerged as highly potential candidates. InP/ZnS QDs were first time incorporated into liposomes in this dissertation which not only makes them biocompatible but also have shown to exhibit several advantages in comparison to InP/ZnS QDs. In future studies InP/ZnS QD-liposomes cytotoxicity needs to be verified. Also cellular internalization studies of the QD-liposomes would be helpful in demonstrating their potential use in cellular applications. Finally with their emissions in wide range of wavelengths from blue to near infra red region their applicability can be extended to various areas including cellular labeling, microbiology labeling, bioassays, and in NIR imaging.

Quantum dot based immunoassays are promising tools in simultaneous detection of several biomarkers that will need improvement for their implementation in clinical diagnostics. The first one being no reliable method for the estimation of number of antibodies attached to one quantum dot which might lead to failure in discrimination of different samples especially at lower concentration ranges. Second one is cytotoxicity; though not a major obstacle in using the QDs for *in vitro* applications may have negative consequences on the lab personnel working with QDs in comparison to commercially available immunoassay kits. Replacing the CdSe QDs with InP QDs would greatly minimize these negative consequences. Finally the time and labor might also be a limiting factor in the QD based fluoroimmunoassays as it involves several bioconjugation steps. Taking these into account and the methods developed in this dissertation

with further improvisation, the applicability has to be verified in future with serum samples collected from the patients for clinical applications.

6.2 References

(1) Medintz, I. L.; Clapp, A. R.; Mattoussi, H.; Goldman, E. R.; Fisher, B.; Mauro, J. R. *Nat. Mater.* **2003**, 2, 630-639.

(2) Clapp, A. R.; Medintz, I. L.; Mauro, J. M.; Fisher, B. R.; Bawendi, M. G.; Mattoussi, H. *J. Am. Chem. Soc.* **2004**, 126, 301-310.

(3) Shi, L.; De Paoli, V.; Rosenzweig, N.; Rosenzweig, Z. J. *Am. Chem. Soc.* **2006**, 128, 10378-10379.

(4) Chang, E.; Miller, J. S.; Sun, J.; Yu, W. W.; Colvin, V. L.; Drezek, R.; West, J. W. L. *Biochem. Biophys. Res. Commun.* **2005**, 334, 1317–1321.

(5) Hoshino, A.; Fujioka, K.; Oku, T.; Suga, M.; Sasaki, Y. F.; Ohta, T.; Yasuhara, M.; Suzuki, K.; Yamamoto, K. *Nano Lett.* **2004**, 4, 2163-2169.

(6) Kirchner, C.; Liedl, T.; Kudera, S.; Pellegrino, T.; Javier, A. M.; Gaub, H. E.; Stolzle, S.; Fertig, N.; Parak, W. J. *Nano Lett.* **2005**, 5, 331-338.

(7) Kim, S. H.; Wolters, R. H.; Heath, J. R. *J. Chem. Phys.* **1996**, 105, 7957-7963.

(8) Xie, R. G.; Battaglia, D.; Peng, X. G. *J. Am. Chem. Soc.* **2007**, 129, 15432-15433.

(9) Xu, S.; Ziegler, J.; Nann, T. *J. Mater. Chem.* **2008**, 18, 2653–2656.

(10) Li, L.; Reiss, P. *J. Am. Chem. Soc.* **2008**, 130, 11588–11589.

(11) Yong, K; Ding, H; Roy, I; Law, W; Bergey, E.J.; Maitra, A.; Prasad, P.N. *ACS Nano* **2009**, 3 (3), 502-510.

(12) Sheila, A. G.; Darcy, J. L.; Mary, E. P.; Lisa, B.; Orthan, S. *Sensor Lett.* **2004**, 2(1), 58-63.

(13) Stacy, E. F.; Melanson, M. J.; Tanasijevic.; Petr, J. *Circulation* **2007**, 116, e501-e504.

(14) Angelo, C.; Elisabetta, D.; Francesco, R.; Domenico, D. B.; Fosco, P.; Valter, S.; Vittorio, C. *Clinical Chemistry* **2009**, 55(1), 196-198.

(15) Morrow, D. A.; Antman, E. M. *Clinical Chemistry* **2009,** 55(1), 5-8.

Vita

The author was born in Bhimavaram, Andhra Pradesh, India. He obtained his Bachelor's and Master's degree in chemistry from Andhra University in 2000 and 2002 respectively. Then he worked in an USFDA approved pharmaceutical company, Dr. Reddy's Laboratories for three years in India. To pursue a PhD in analytical chemistry, he joined the University of New Orleans chemistry graduate program and became a member of Dr. Zeev Rosenzweig's research group in 2006 and Dr. Matthew A. Tarr's research group in 2007.